ECOSYSTEM RESPONSES TO SEASONAL SNOWPACK VARIATION IN THE WESTERN UNITED STATES

by

Gregory E. Maurer

A dissertation submitted to the faculty of
The University of Utah
in partial fulfillment of the requirements for the degree of

Doctor of Philosophy

Department of Biology

The University of Utah

May 2014

THE UNIVERSITY OF UTAH GRADUATE SCHOOL

STATEMENT OF DISSERTATION APPROVAL

The dissertation of Gregory E. Maurer has been approved by the following supervisory committee members:

David R. Bowling , Chair	20 December, 2013
	Date Approved
Thure E. Cerling , Member	20 December, 2013
	Date Approved
James R. Ehleringer , Member	20 December, 2013
	Date Approved
Thomas H. Painter , Member	29 March, 2014
	Date Approved
John S. Sperry , Member	20 December, 2013
	Date Approved

and by Neil J. Vickers , Chair of the Department of Biology and by David B. Kieda, Dean of the Graduate School.

ABSTRACT

Snow cover directly influences soil temperature (T_{soil}) and water content (θ), two primary drivers of ecosystem processes such as primary production and soil biogeochemical cycling. Variations in seasonal snowpack size, duration, and other characteristics therefore have the potential to significantly impact ecosystem structure and function. In the mountain ranges of the interior western United States, a region with abundant snowfall and complex topography, there is great temporal and spatial variability in snowpack characteristics. Interactions between snow and ecosystems are poorly quantified here, and with significant hydroclimatic (and snowpack) change occurring in the western U.S., it is increasingly critical to understand how this regional snowpack variability influences ecosystem structure and function. In three complementary research projects I tested the hypothesis that seasonal snowpack characteristics influence ecohydrological and biogeochemical processes in the montane ecosystems of this region.

Using data from a large network of automated snowpack monitoring stations (252 sites), I quantified interannual and spatial patterns in T_{soil} and θ, and their dependence on regional snowpack variation over an 11 year period. Below-snowpack and warm season T_{soil} and θ were significantly related to snowpack size, melt date, and early season snow accumulation. In a 3-year manipulative experiment I compared the impacts of aeolian dust deposition, canopy structure, and interannual snowfall variability on snowpack ablation and ecosystem processes in a subalpine conifer forest. Canopy structure had a larger impact (through interception and shading) on snow accumulation and ablation than dust addition treatments. Dust and canopy structure effects on T_{soil}, θ, and ecosystem processes were small compared to the effects of interannual variability in snowpack size and melt timing. In a study of 21 conifer forests in the Wasatch and Uinta ranges of Utah, I tested whether climatic drivers, including snowpack characteristics, explained spatial patterns in soil and detrital organic matter stock size and isotopic composition (^{13}C and ^{15}N). The climate of these sites explained only a small portion of variability in stock sizes and isotope ratios, suggesting that site-specific factors (disturbance, species, soil texture) are predominant controllers of the production and decomposition of forest organic matter stocks.

for Laurel, Hazel, and Margaret

CONTENTS

CHAPTER 1

INTRODUCTION

Seasonal snowpacks are a defining and highly variable climatic feature of the Earth's temperate zones. In the northern hemisphere, two-thirds of the North American and Eurasian continents are classified as "snow transient regions" that experience frequent snow cover events between December and March. The mountainous regions of these continents experience snow cover events during even longer portions of each year (Groisman et al. 1994, Frei and Robinson 1999, Edwards et al. 2007). There is growing appreciation that significant biological activity occurs below seasonal snowpacks and that variation in snowpack depth, duration, and other characteristics impacts ecosystem processes in winter and the warm season. For example, studies in snow-dominated ecosystems have demonstrated that a significant fraction of total annual ecosystem carbon assimilation occurs in early spring when snowmelt water is most available (Monson et al. 2002, Schimel et al. 2002, Hu et al. 2010), and that a substantial proportion of total annual soil respiration occurs beneath snow (reviewed in Liptzin et al. 2009). In some ecosystems, in fact, more than half of all carbon assimilated during the growing season may be respired away during winter (Grogan et al. 2001, Monson et al. 2005, 2006a, Nobrega and Grogan 2007). Given the broad extent of seasonally snow-covered ecosystems, research addressing the impact of snowpack variability on ecosystems and ecosystem processes is surprisingly limited.

Seasonal snowpacks strongly alter the energy and water budgets of soils. Snow has a high shortwave albedo and a low thermal conductivity, making it highly effective at insulating soil from the radiative and thermal environment at the snow surface (Zhang 2005). Under persistent winter snow cover, this results in long periods of stable soil temperature while soils are decoupled from winter cooling or spring warming above the snowpack. This is followed by a rise in temperature once the snowpack melts (Sturm et al. 1997, Lundquist and Lott 2008). In cold regions where winter thaw events are uncommon and winter evapotranspiration rates are low, snow accumulation is the primary winter hydrological process. In spring, this is followed by a peak in soil water content, ground water recharge, and streamflow that coincides with the timing of snow melt (Bales et al. 2006, 2011, Hamlet et al. 2007, Stewart 2009). During the melt period, soil water content is generally high and is driven by the snow melt process, topography, and soil texture (McNamara et al. 2005, Litaor et al. 2008, Seyfried et al. 2009). As the warm season progresses,

however, the soil hydrological regime transitions to one dominated by rain events and evapotranspiration (Loik et al. 2004, Williams et al. 2009). Seasonally snow-covered ecosystems, therefore, experience distinct soil thermal and hydrological states (Grayson et al. 1997, Western et al. 2004, Bartlett et al. 2004) tied to the seasonal transit of snow.

Soil temperature and water content are primary drivers of many ecosystem processes. Primary production and evapotranspiration are highly dependent on soil water content (Schneider and Childers 1941, Havranek and Benecke 1978, Oren and Pataki 2001). The processes that occur within soil, including soil respiration, organic matter decomposition, nutrient cycling, nitrogen transformations, and many others, are the direct or indirect result of metabolism by plant roots and the soil microbial community. As such, the rates of these processes scale with temperature (Clarke and Fraser 2004). Metabolism by roots and microbes also requires hydration of the organisms themselves and accessibility of substrates via liquid water (Borken and Matzner 2009). Many field and laboratory studies have demonstrated the temperature and moisture dependence of soil respiration, for instance (Orchard and Cook 1983, Lloyd and Taylor 1994). Additionally, when soils are near 0 °C, as soils often are beneath snow, soil respiration is known to become more sensitive to temperature changes (Kirschbaum 1995, Fang and Moncrieff 2001) Thus, much of the seasonal variation in soil respiration rates and potentially other ecosystem processes, is determined by the temperature and water content of soils.

1.1 The study region and its climate

The mountain ranges of the interior western U.S., which lie between the eastern slopes of the Sierra Nevada and Cascade Ranges and the eastern edge of the Rockies, have hydrological systems that are dominated by seasonal snow cover. This region has a continental climate with a large seasonal temperature range. Beginning in November, storms originating in the North Pacific deliver snowfall to much of the western U.S. until well into the spring (Mock 1996, Sheppard et al. 2002). This snow is the dominant precipitation input to mountain watersheds of the region, making up 39–67% of annual precipitation (Serreze et al. 1999). In many areas snowpacks persist into the summer months, meaning that soils may be snow-covered for greater than half the year. Melting snowpacks generate the bulk of annual streamflow (50–80%), soil moisture recharge, and water for human uses such as irrigation, municipal water, and hydroelectric power (Stewart et al. 2004, Barnett et al. 2005, Hamlet et al. 2007, Bales et al. 2011). May and June tend to be dry months, but during July and August the North American Monsoon draws moisture north from the Gulfs of California and Mexico (Higgins et al. 1997), depositing significant summer rain across Northwest Mexico, Arizona, New Mexico, and smaller amounts of rain into southern Utah and Colorado (Adams and Comrie 1997, Sheppard et al. 2002). The hydrological importance of snow in the interior western U.S. makes it a well-suited locale for the study of snowpack influence on ecosystems and ecosystem processes.

The land surface of the interior western U.S. is characterized by complex topography and heterogeneous vegetation cover. Consequently, air temperature, precipitation, and evapotranspiration vary considerably over short distances here (Flerchinger et al. 1998, Lundquist and Cayan 2007, Daly et al. 2008, Goulden et al. 2012). Varied topography and vegetation also give rise to spatial variation in snow accumulation, surface energy balance, and snowpack ablation (Marks and Dozier 1992, Link and Marks 1999a, Marks and Winstral 2001, Bales et al. 2006, Musselman et al. 2008, Molotch et al. 2009, Clark et al. 2011). Currently, spatial patterns in soil temperature and water content are not well quantified in this region, but are most likely related to this climate, snow, and ecohydrological process variation. Given their prevalence, seasonal snowpacks may provide a large amount of thermal and hydrological control over the soil environment and associated ecosystem processes of the interior western U.S.

A large body of research has determined that the snowpacks of the western United States are diminishing in size (Hamlet et al. 2005, Mote et al. 2005, Mote 2006, Dyer and Mote 2007, Clow 2010, Nayak et al. 2010, Harpold et al. 2012) and melting earlier (Dettinger and Cayan 1995, McCabe and Clark 2005, Regonda et al. 2005, Stewart et al. 2005, Hamlet et al. 2007). Particularly since the 1980s, there have been consistent declines in snowpack across the Northern Rocky Mountains that appear to be a response to increasing surface temperature, particularly during spring (Clow 2010, Pederson et al. 2011, 2013, Kapnick and Hall 2012). Much of this change, which is discussed in further detail in the chapters ahead, has been attributed to anthropogenic climate change (Barnett et al. 2008, Pierce et al. 2008, Pederson et al. 2013). Greater dust emission from low-lying areas may also play a role in regional snowpack change (Neff et al. 2008, Painter et al. 2010). In view of current snowpack trends, elucidating the mechanisms and future trajectory of ecosystem responses to seasonal snowpack variability in the western U.S. should be a research priority.

1.2 Research questions

I undertook this study to better understand the influence that seasonal snowpacks have on soil temperature (T_{soil}), soil moisture (θ), and ecosystem processes in mountainous regions. Where persistent snowpacks accumulate, it is reasonable to expect that the size, duration, melt timing, or other snowpack characteristics have effects on T_{soil} and θ that, in turn, influence ecosystem process rates. I expected that these changes would be measurable either between sites or between years with different snowpacks. Moreover, I expected that ecosystem development over the long term would be influenced by prevailing snowpack conditions. Specifically, the chapters ahead address three research questions:

1. How does variability in seasonal snowpack characteristics (size, melt timing, early season accumulation) influence the soil environment at one location or among multiple locations?
2. Do differences in snowpack characteristics lead to differences in ecosystem process rates, particularly in soils?

3. Are snow-dominated ecosystems structured by their prevailing snowpack characteristics?

To answer these questions, I collected and analyzed climate, soil, and ecosystem data at both regional and individual ecosystem scales. These data came from interior western U.S. sites that ranged in seasonal snowpack size, melt timing, or other characteristics due to either experimental snowpack manipulations or natural regional variability. The resulting analyses and interpretations explain linkages between seasonal snowpacks, the soil environment, and ecosystem structure and function. Though this research took place under the current climate and snowpack regime of the interior western United States, my hope is that it provides a foundational understanding from which other researchers may anticipate and study ecosystem responses to the climate and snowpacks of the future.

1.3 The chapters

Chapter 2 presents an examination of multiple hypotheses predicting how seasonal snowpack characteristics, including snowpack size, early season accumulation, and melt timing, influence T_{soil} and θ in the mountains of the interior western U.S. This analysis relied on snowpack and soil data from a network of automated snowpack and meteorological monitoring stations operated by the USDA National Resources Conservation Service (the SNOTEL network). I collected and analyzed the full available T_{soil} and θ dataset (6.3 years of continuous data, on average) from 252 SNOTEL stations in 8 states. At these sites, below-snowpack T_{soil} remained near 0 °C and snowpacks insulated soil from winter temperature fluctuations at the snow surface. Interannual (within a site) and across-site (all 252 sites) variation in T_{soil}, however, were significantly related to differences in snowpack size and onset timing and were large enough to impact biogeochemical processes. Between the start of snowpack accumulation and the beginning of spring snowpack ablation, θ remained low at many sites and was unresponsive to precipitation events. Warm season θ was only weakly influenced by snowpack size or melt timing.

Chapter 3 describes a snowpack manipulation experiment designed to test whether differences in snowpack duration and melt timing would impact soil carbon cycle processes and water availability for vegetation. I added dust to the surface of the snowpack in three subalpine forest plots to accelerate the rate of snowpack ablation. In these plots and three control plots I measured soil respiration and plant litter mass loss in winter and the warm season and xylem water potential during the warm season. This study forest had a heterogeneous and relatively open canopy structure, and I quantified this structure using hemispherical photographs. The 3 years of the experiment also experienced more than a twofold range in snowfall amount and a 50 day range in snowpack melt timing. This interannual variability added an additional covariate to the experiment. These data were used to examine the relative size of dust, canopy, and interannual variability effects on snow accumulation, snow ablation, and ecosystem processes. Dust addition had a smaller effect on snowpack ablation rate than did the effect of snow interception and shading by the overstory canopy. Interannual variability in snowpack size and melt

timing had the greatest effect on T_{soil}, θ, and ecohydrological processes.

Chapter 4 presents a study of soil and detrital organic matter stock size and isotopic composition at 21 conifer forests in the Wasatch and Uinta mountains of Utah. These forests were in locations adjacent to SNOTEL stations that were chosen to span the range of snowpack size and elevation present in the SNOTEL network. After extensive sampling of forest floor and soil organic matter pools at each forest, I calculated the biomass of each pool. Subsamples of each pool were analyzed for percent carbon, percent nitrogen, and the stable isotope ratios of carbon and nitrogen. I then quantified the relationships between climate, including mean snowpack characteristics, and carbon stock sizes and isotopic composition. Carbon stock size in the various organic matter pools did not increase with elevation, as has been observed in similar studies. This indicates that forest litter production declined more rapidly with elevation than did the rate of decomposition. Trends in stable isotope composition indicated that forests were drought limited even at sites with later-melting snowpacks, and that soil microbial activity declined with elevation in spite of the thermal and hydrological effects of snow cover.

CHAPTER 2

SEASONAL SNOWPACK CHARACTERISTICS INFLUENCE SOIL TEMPERATURE AND WATER CONTENT AT MULTIPLE SCALES IN INTERIOR WESTERN U.S. MOUNTAIN ECOSYSTEMS

2.1 Abstract

Mountain snowpacks directly and indirectly influence soil temperature (T_{soil}) and water content (θ). Vegetation, soil organisms, and associated biogeochemical processes certainly respond to snowpack-related variability in the soil biophysical environment, but there is currently a poor understanding of how snow-soil interactions vary in time and across the mountain landscape. Using data from a network of automated snowpack monitoring stations in the interior western U.S., we quantified seasonal and landscape patterns in T_{soil} and θ, and their dependence on snowpack characteristics over an eleven year period. Elevation gradients in T_{soil} were absent beneath winter snowpacks, despite large gradients in air temperature (T_{air}). Winter T_{soil} was warmer and less variable than T_{air}, but interannual and across-site variation in T_{soil} was likely large enough to impact biogeochemical processes. Winter soil θ varied between years and across sites, but during a given winter at a site it changed little between the start of snowpack accumulation and the initiation of spring snow melt. Winter T_{soil} and θ were both higher when early-winter snow accumulation was greater. Summer soil θ was lower when summer T_{air} was high. Depending on the site and the year examined, summer soil θ was higher when there was greater summer precipitation, a larger snowpack, later snowpack melt, or a combination of these factors. We found that snowpack-related variability in the soil environment was of sufficient magnitude to influence biogeochemical processes in snow-dominated ecosystems.

2.2 Introduction

Snowfall is the dominant hydrologic input to the mountain watersheds of the western U.S., making up 40–70% of annual precipitation (Serreze et al. 1999). Winter snowpacks persist for a large portion of each year and are primary controllers of the energy and water balance of soils in the region. Snowpack effects on soil temperature and water content directly and indirectly influence vegetation, soil microbial communities, and associated biogeochemical processes during the cold season and the warm season (Lipson et al. 2002, Monson et al. 2006b, Litaor et al. 2008). The western U.S. experiences high interannual and spatial variability in snowpack size, duration, and melt timing, but at present, there is no comprehensive understanding of how this variability influences the soil environment.

The rates of many biogeochemical processes vary with temperature and moisture. Studies of soil carbon cycling across elevation gradients, for example, have found that changes in soil respiration, rates of organic matter decomposition, and the storage of soil carbon are linked to soil temperature and moisture (Amundson et al. 1989, Trumbore et al. 1996, Conant et al. 2000, Kueppers and Harte 2005). Despite colder temperature, these and other ecologically important processes occur beneath winter snowpacks. Below-snowpack soil respiration accounts for anywhere from ~12% to 50% of the annual carbon dioxide loss in ecosystems with persistent winter snowpacks (Liptzin et al. 2009). In addition, decomposition (Hobbie and Chapin 1996, Williams et al. 1998, Kueppers and Harte 2005, Baptist et al. 2009), nitrogen mineralization and immobilization by microbial communities (Brooks and Williams 1999, Schimel et al. 2004, Grogan et al. 2004, Kielland et al. 2006), and the production and consumption of greenhouse gasses such as methane and nitrous oxide (Sommerfeld et al. 1993, Mast et al. 1998, Schurmann et al. 2002, Groffman et al. 2006, Filippa et al. 2009) all occur beneath seasonal snowpacks. Winter snowpack characteristics can influence soil temperature in ways that alter soil carbon cycling during the warm season (Nowinski et al. 2010). It is unknown how much these biogeochemical processes vary in time and space due to a poor understanding of how snowpacks influence the temperature and moisture environment of soils.

The energy and water balance of the soil surface changes dramatically beneath a snowpack. Because snow has high shortwave albedo and low thermal conductivity, snowpacks decouple soil energy exchange from the radiative and thermal environment at the snowpack surface (Sturm et al. 1997, Grundstein et al. 2005). During winter, this slows cooling of soil through radiative, sensible, and latent heat exchange, and when energy availability increases in the spring, it slows warming of the soil by the same processes (Bartlett et al. 2004, Zhang 2005). Snowpacks temporarily store water, thereby isolating soil from winter precipitation until sufficient energy is available to melt snow and deliver water to soils, streams, or the subsurface (McNamara et al. 2005, Hamlet et al. 2007, Williams et al. 2009, Bales et al. 2011). Winter precipitation can be lost through sublimation or redistributed by wind, vegetation interception,

topographic effects, and lateral water movement through the snowpack (Daly et al. 1994, Clark et al. 2011, Ohara et al. 2011, Eiriksson et al. 2013). The impact of these processes on soil temperature and moisture varies depending on snowpack size, distribution, duration, and other snowpack and climate characteristics. Because the interannual and spatial variability in snowpack characteristics and climate are high in the western U.S., it is likely that soil temperature, soil moisture, and associated biogeochemical processes will be highly variable in response.

Numerous studies have identified declining trends in snowcover extent, duration, and snowpack size in the western U.S. (Hamlet et al. 2005, Mote et al. 2005, Mote 2006, Dyer and Mote 2007). Model projections tend to agree that these trends will continue and intensify in the coming century (Brown and Mote 2009, Seager and Vecchi 2010). Although observed changes have been most pronounced for maritime climates, snowpack changes have also been reported in the interior western U.S. (Clow 2010, Nayak et al. 2010, Harpold et al. 2012). Researchers have found trends toward earlier spring runoff timing (Dettinger and Cayan 1995, McCabe and Clark 2005, Stewart et al. 2005, Hamlet et al. 2007) and a larger proportion of precipitation falling as rain instead of snow (Hamlet et al. 2005, Regonda et al. 2005, Knowles et al. 2006, Gillies et al. 2012). Climatic phenomena that influence snowpack size, distribution, and duration are linked to perturbations of ecosystems and human communities in this area, such as widespread increases in wildfire (Westerling et al. 2006), drought (Cayan et al. 2010), tree mortality (Anderegg et al. 2011), and insect outbreaks (Logan et al. 2010). Understanding the relationships between climate, snowpack variability, and the soil environment is critical to predicting how ecosystems and biogeochemical processes will respond to future changes in climate.

Here we examine the extant variability in soil temperature and water content in the mountains of the interior western United States and how it is influenced by seasonal snowpack size, environmental conditions during snowpack accumulation, and melt timing. Our study area has a continental climate with cold winters, a seasonal precipitation pattern, and variable winter snowpacks. Sites with maritime climates, which are warmer and have more frequent late winter/early spring snowpack melt and rain-on-snow events (Mote 2006, Knowles et al. 2006, Kapnick and Hall 2012), were deliberately excluded from our analysis because we expect them to have different snowpack, soil temperature, and soil moisture dynamics. This study takes advantage of a long-term dataset collected by the USDA Natural Resources Conservation Service (NRCS) Snowpack Telemetry (SNOTEL) network. We examine the following hypotheses:

1. There are no elevation gradients in soil temperature when seasonal snowpacks are present.
2. Soil temperature is dependent on snowpack characteristics such as snowpack size and the timing of accumulation.
3. Winter soil moisture a) changes minimally between the start of snowpack accumulation and the

initiation of snowpack melt and b) is dependent on fall and early-winter conditions.

4. Warm season soil moisture is dependent on snowpack size and the timing of snowpack melt.

We show that snowpack-related variability in soil temperature and moisture is of sufficient magnitude to influence soil biological activity, and we discuss the relevance of this complex biophysical environment for ecosystems and biogeochemical processes.

2.3 Methods

2.3.1 Study area and sites description

The SNOTEL network (http://www.wcc.nrcs.usda.gov/snow/) is composed of automated stations located in middle to upper elevation basins throughout the western U.S. This network's purpose is to forecast water supply in regions where snowfall makes up a significant portion of annual precipitation. Our study area includes all sites in Arizona, Colorado, Idaho, Montana, Nevada, New Mexico, Utah, and Wyoming (574 stations—which we refer to as all sites). We excluded all SNOTEL stations in coastal states (CA, OR, WA) because they include mountain ranges with a maritime climatic influence that is distinct from the climate of the interior western U.S. Typically, SNOTEL stations are located in natural or artificial clearings within forested areas and do not span the entire topographic range of the watersheds in which they are operated. Our results, therefore, do not fully represent watershed-scale hydrological processes.

The standard set of SNOTEL measurements includes snow water equivalent (SWE, snow pillow), accumulated precipitation (storage gauge), snow depth (ultrasonic depth sensor), and air temperature (T_{air}, naturally ventilated extended range thermistor). Instrument specifications for these measurements are documented in the NRCS Snow Survey and Water Supply Forecasting National Engineering Handbook (Natural Resources Conservation Service 2010). In our 8-state study area, a subset of 252 stations (which we refer to as soil sites) were equipped with sensors (Stevens Hydraprobe I and II, Stevens Water Monitoring Systems, Inc., Portland, OR, USA) that monitor vertical profiles of soil temperature (T_{soil}) using integrated thermistors, and soil volumetric water content (θ) using a calibrated measurement of soil dielectric permittivity. The calibration equations used to determine T_{soil} and θ are the same for all sensors and soil types (Seyfried et al. 2005) and are not updated after sensors are installed (Tony Tolsdorf, NRCS, personal communication). The instrument uncertainties for temperature and water content measurements are specified at ± 0.26 °C and 3.4%, respectively (Seyfried et al. 2005, Bellingham and Fleming n.d.). Because the dielectric properties of ice and liquid water are different, measurements of θ decline sharply as soil water enters the solid phase (Spaans and Baker 1996). We did not correct for this effect. The number and placement of soil sensors varied among the soil sites, so we used only data from sensors at 5, 20, and 50 cm below the top of the mineral soil horizon for consistency. Soil sensor profiles were typically located within 20 m of the location of the standard SNOTEL instrumentation.

Our study sites spanned a range in elevation from 875 to 3542 m (Fig. 2.1a), in mean annual temperature from -2.8 to 11.3 °C (Fig. 2.1b), and in latitude from 32.9 to 49.0 °N (data not shown). For the period from 2001 to 2011 (inclusive), these sites had a broad range in snowpack size, snowpack start day, snow-free day, and other climatic variables (defined below, see Fig. 2.1). Statistics for snowpack characteristics and selected climatic variables for our study sites during the 2001 to 2011 period are shown in Table 2.1.

2.3.2 Data processing

We examined hourly T_{soil} and θ data for all available years through 2011 from the soil sites. On average, there were 6.3 full years of soil sensor data at these sites. We also examined daily measurements of SWE, precipitation, and air temperature at all sites for the years 2001 to 2011, or for longer periods in cases where the soil sensor record extended to before 2001 (mean = 10.1 years). Files with less than a complete water year (Oct 1–Sept 30) were excluded, and all data were plotted and visually screened to remove problematic data. When T_{soil}, θ, SWE, or T_{air} data were more than three standard deviations from the moving-window mean (24h window for hourly data, 10d for daily data) of a time series, they were classified as outliers and removed. Because soils have a broad range of textural and hydraulic properties, soil θ measurements were not directly comparable between individual sensors. To facilitate comparison across all sensors, θ data for each sensor were normalized linearly according to its full observed range of values (lowest = 0, highest = 1).

Following the quality control steps above, we calculated a number of statistics from each time series. The mean and standard deviation of T_{air}, SWE, T_{soil}, and θ were calculated for months and quarters (3-month means of OND, JFM, AMJ, and JAS) at all sites. We calculated accumulated precipitation for each warm season month (MJJAS), and for the summer quarter (JAS). Time series of SWE were used to calculate several snowpack metrics. Peak SWE was calculated as the maximum SWE during a water year. Snowpack start day was the first day of persistent snow cover (> 5mm of SWE lasting 2 or more days) after Oct 1. Snow-free day was the first snow-free day following the day that peak SWE occurred. Total snow-covered days was the number of days with > 5mm of SWE. For the below-snow period between the snowpack start and snow-free days, we calculated the mean and standard deviation of T_{soil}, θ, and T_{air}. Finally, we calculated presnowpack T_{soil}, θ, and T_{air} for each water year, defined as the mean of each quantity during the 2-week period immediately prior to snowpack start day. When calculating any of the values above from these time series, time periods missing more than 5% of data (15.9% of all calculations) were excluded.

2.3.3 Hypothesis testing

We examined both interannual and intersite variability in the quantities described above, and used both types of variability to test our hypotheses. Interannual variability refers to variation in a measured quantity over multiple years at one site. To test a hypothesis using interannual variability, we performed least-squares linear regression using all years of data from a site. We then repeated the same test for every site and summed the number of sites with significant relationships ($p < 0.05$). To test whether the slopes of these relationships were significant in the aggregate, we fit a multilevel linear model to data from all sites using site as a random variable.

Intersite variability refers to variation in a measured quantity across sites during one or multiple years. When a hypothesis involved clear two-variable relationships across sites, we used simple linear regression (e.g., temperature-elevation gradients or across-site relationships between soil θ at two time periods). Hypotheses involving intersite relationships between more than one explanatory variable were tested using a combination of principal component analysis (PCA) and multiple regression.

As is common with environmental data, many of our explanatory variables were correlated, which makes interpretation of multiple regression results unreliable. To overcome this limitation, we performed two PCAs, one for the below-snow period and one for the warm season. These used our calculated snowpack, soil, and climate statistics (see section 2.2 for a description) as explanatory variables to produce a number of new, uncorrelated principal component axes. All observations in our dataset then received a score for each axis. We used these scores as explanatory variables in multiple regression analysis of observations from all years together and subsets of individual year observations (2007, 2009, and 2011). These tests added statistical support for some hypotheses beyond that found using linear regression. A brief summary of the PCA results and our interpretation of the axes will be given in section 3.6. A detailed description of PCA and multiple regression methods and results is presented in the appendix (Appendix A).

2.3.3.1 Hypothesis 1

We examined elevation gradients in T_{soil} and T_{air} using simple linear regression with data from all soil sites. To minimize the influence of latitude or continental location, we also performed the analysis with a geographically constrained subset of sites (Utah). The elevation gradients (slopes of the regressions) were examined for January and July.

2.3.3.2 Hypothesis 2

Interannual relationships between mean below-snow T_{soil} and several explanatory variables, including snowpack characteristics (Table 2.2), were examined using simple linear regression at each individual site, and a multilevel linear model to test slope significance for all sites together. We tested the signifi-

cance of intersite relationships between these variables using multiple regression, with mean below-snow T_{soil} (in individual years, and all years together) as the dependent variable and below-snow principal component axes as explanatory variables.

2.3.3.3 Hypothesis 3a

We examined within-year variation in below-snow soil θ using two metrics. First, we quantified the month-to-month changes in mean soil θ from October to May at every soil site, in every available year. Second, we calculated the cumulative change between presnowpack soil θ and mean monthly θ in October through May.

2.3.3.4 Hypothesis 3b

To test this hypothesis we used simple linear regression between mean winter quarter (JFM) θ and the same explanatory variables used for Hypothesis 2 (Table 2.2) at each site. We used a multilevel linear model to test slope significance for all sites together. We also used multiple regression with below-snow principal component axes (Table 2.3) as explanatory variables.

2.3.3.5 Hypothesis 4

e tested this hypothesis using simple linear regression of summer quarter (JAS) θ versus a number of warm season variables and snowpack characteristics (see Table 2.4) at each site. We used a multilevel linear model to test slope significance for all sites together. We also used multiple regression with warm season principal component axes (Table 2.3) as explanatory variables. As an additional test for intersite differences in summer quarter θ, we compared groups of sites with high and low elevation (a proxy for air temperature), SWE, and summer rainfall. Sites in high summer rainfall groups received greater than 20% of total annual precipitation during the summer quarter (JAS). High and low thresholds for SWE and elevation were selected above and below the mean for all sites, at a value that allowed greater than seven sites in each group.

2.4 Results

2.4.1 Snowpack and the soil environment at one site

To illustrate the relationships between snowpack characteristics, T_{soil}, and θ, we highlight multiple years of observations at Currant Creek, Utah. In Fig. 2.2a, ten consecutive 1-year time series of SWE are plotted on a common time axis. Despite similarities in the shape of the SWE hydrographs, there were large interannual differences. Total snow-covered days ranged between 133 and 185 days. Snowpack start day ranged between 22 October and 1 December, and snow-free day ranged between 1 April and 11 May (both varied by ~40 days). Peak SWE ranged between 96 and 400 mm. The data in Fig. 2.2b illustrate the

interannual variability and within-year stability of below-snow T_{soil}. Mean below-snow T_{soil} across years ranged between -0.5 and 2.3 °C. Below-snow T_{soil} varied little within any given year even though T_{air} consistently dropped far below 0 °C in December through February (data not shown). During the coldest year in the record (2010), T_{soil} dropped to almost -5 °C during December and remained well below 0 °C for most of the remainder of winter. The transition to springtime warming of the soil began at the snow-free date, and in some years this occurred after mean T_{air} had climbed above 0 °C. The beginning of spring soil warming varied between years by ~40 days (Fig. 2.2b). Below-snow θ changed little until the spring melt began, even as large amounts of precipitation accumulated in the snowpack (Fig. 2.2c). There are exceptions to this, however. In 2010 below-snowpack θ dropped to near zero during the cold soil event described above. This and similar events may indicate the freezing of soil water. Winter quarter θ at the site had high interannual variability, ranging between 3 and 23% (θ not normalized here). In a given year, peak θ coincided roughly with the snow-free date and then declined over the next 2 months. The timing of peak θ varied between years by ~40 days.

2.4.2 Change in temperature with elevation

In the warm season (July), both T_{soil} and T_{air} declined with elevation across all sites, but in January the T_{soil} elevation gradient was absent (Fig. 2.3a, b). Results were similar when sites were geographically restricted (Utah, Fig. 2.3c, d). The Utah sites had a July T_{soil} (20 cm depth) elevation gradient of -4.2 °C/km (Fig. 2.3c, $p < 0.001$), which was slightly smaller than the July T_{air} gradient (Fig. 2.3d, -5.0 °C, $p < 0.001$). In January the T_{soil} elevation gradient for the Utah sites was minimal, but statistically distinguishable from no relationship (-0.7 °C/km, $p < 0.001$), while a gradient in T_{air} remained (-2.9 °C/km, $p < 0.001$). The difference between T_{soil} and T_{air} ($T_{soil} - T_{air}$) during January increased with elevation (2.0 °C/km, $p < 0.01$) in both groups of sites (data not shown).

2.4.3 Stability of winter soil moisture

Once a snowpack accumulated, there were only small month-to-month changes in normalized soil θ (averaged across all sites) until the snowpack began to melt (Fig. 2.4). Between October and November, monthly mean θ increased by ~0.1 (normalized units, dimensionless). There was a slight decline in θ of surface soils (5 and 20 cm depths) between November and December, followed by little month-to-month change from December to February. There was an increase in θ again in March (Fig. 2.4a). Cumulative changes in mean winter month θ were small (Fig. 2.4b), increasing, on average across all sites, by less than 0.25 (normalized units) between the presnowpack period and March.

2.4.4 Interannual variability in below-snow soil temperature

Interannual variability in below-snow T_{soil} was related to snowpack characteristics. During water year 2005 at the Mosby Mountain site (Utah, Fig. 2.5), for example, a large snowpack accumulated early and T_{soil} never dropped below 0 °C. In contrast, during water year 2010, the snowpack accumulated slowly and was thin during the early-winter. This allowed the soil to cool, and T_{soil} remained well below 0 °C for most of the winter. Similar occurrences of low below-snow T_{soil} (< 0 °C) during years with small early-winter snowpacks were widespread in our study area (Fig. 2.6).

Mean below-snow T_{soil} was warmer in years when mean November, December, and January SWE were higher (Fig. 2.7a, one site for December; Table 2.2, all significant results, January data not shown), and when mean T_{air} during the below-snow period was higher (Table 2.2). These relationships, however, were only significant at 23–39 sites, depending on soil depth (Table 2.2). At some sites, T_{soil} was positively correlated with snowpack start day and below-snow period T_{air} (12–15 sites, Table 2.2), meaning later snowpack accumulation or warmer winter weather was associated with warmer T_{soil} at those sites. The multilevel linear model (Table 2.2) and multiple regression (section 3.6) provided additional statistical support for some of these relationships.

2.4.5 Interannual variability in soil water content

Interannual variability in winter quarter soil θ was dependent on fall and early-winter snowpack conditions. At 17–48 sites (depending on soil depth), mean winter quarter θ was higher in years when mean November, December, or January SWE were higher (Fig. 2.7b, one site for December; Table 2.2, all significant results, January data not shown). Some sites had higher winter quarter θ in years with a later snowpack start day (10–15 sites, Table 2.2). Winter quarter θ was also positively related to winter T_{air} at around 9–13 sites and to peak SWE at around 6–19 sites (depending on depth of θ measurements, Table 2.2).

Interannual variability in summer quarter θ was dependent on summer precipitation, snowpack characteristics, and summer air temperature. At 6–26 sites (depending on soil depth), mean summer quarter θ was higher in years with greater summer quarter precipitation. (One site shown in Fig. 2.7c; Table 2.4, all significant results). This relationship was significant most often at the 5 cm measurement depth (26 sites). Summer quarter θ was also higher in years with greater peak SWE at 13–22 sites (depending on soil depth), but this relationship was significant more often at the 50 cm measurement depth (22 sites, Table 2.4). At some sites (8–17 sites, soil depth dependent), summer quarter θ was higher in years with a later snow-free date or warmer winter T_{soil}, and lower in years with warmer summer T_{air} (Table 2.4). Again, multilevel linear models and multiple regression added statistical support to some of these relationships (Tables 2.2 and 2.4, section 3.6).

2.4.6 Intersite variability in soil temperature and water content

There was high intersite variability in below-snow T_{soil}, winter quarter soil θ, and summer quarter soil θ in our study area. Mean January T_{soil}, for example, had a range of 11 °C across the soil sites, about half the range in mean January T_{air} (Fig. 2.8). To test whether intersite differences in these variables were related to snowpack and other climatic variables across our study sites, we used multiple regression analysis with PCA scores as the explanatory variables. Detailed PCA and multiple regression results are presented in Appendix A, but we summarize these results here and in Table 2.3.

The first four principal component axes from our below-snow PCA were significant as explanatory variables for mean below-snow T_{soil} and winter quarter θ (20 cm depths) in multiple regression analyses (Table 2.3). Based on their explanatory variable loadings (Table A.2), we interpreted these axes as the spring snowmelt axis (PC1), the winter temperature axis (PC2), the snowpack start temperature axis (PC3), and the fall snow/soil axis (PC4). Mean below-snow T_{soil} was significantly higher at sites with warmer winter T_{air} (PC2) and warmer presnowpack T_{soil} and T_{air} (PC3). Sites with warmer presnowpack temperatures tended to be those with an early snowpack start day (Table A.2). Below-snow T_{soil} was also significantly warmer at sites with higher early-winter SWE accumulation (PC1 and 4). Mean winter quarter θ was significantly higher at sites with warmer winter T_{air} (PC2), but unlike T_{soil}, it was lower at sites with warm presnowpack T_{soil} and T_{air}. Winter quarter θ was significantly higher at sites with greater October and November SWE and sites with higher presnowpack θ (PC4). Some of these axes were not significant when individual years of data were tested with these multiple regression models.

The first three principal component axes from our warm season PCA were significant explanatory variables for mean summer quarter θ (20 cm, Table 2.3). We interpreted these axes (Table A.6) as the summer T_{air} axis (PC1), the spring snowmelt/summer precip axis (PC2), and the winter T_{soil} axis (PC3). Mean summer quarter θ was significantly lower at sites with warmer summer T_{air} (PC1). Summer quarter θ was significantly higher at sites with greater warm season precipitation, higher peak SWE, and later snow-free date (PC2 and 3). Again, the significance of some of these axes changed when individual years of data were used in the model. Some explanatory variable loadings for the warm season PCA changed between individual years (Table A.6).

Examination of summer quarter soil θ distributions revealed differences between groups of sites with high and low elevation, SWE, and summer rainfall (Fig. 2.9). We found that the high summer rainfall sites had, on average, higher summer quarter θ than low summer rainfall sites. Groups with high peak SWE and high elevation had higher summer quarter θ when compared to groups with lower peak SWE or elevation.

2.5 Discussion

2.5.1 Soil temperature variation below seasonal snowpacks

Temperature in the bulk atmosphere and near surface air declines with elevation (Fig. 2.3). Hence, one might expect T_{soil} to also decline with elevation. Soil temperature showed little dependence on elevation when a snowpack was present, despite large gradients in T_{air} in our study area (Fig. 2.3). The moist adiabatic lapse rate is generally between 3 and 7 °C/km (Whiteman 2000) and we observed July T_{air} and T_{soil} elevation gradients similar to this across our sites. Elevation gradients in T_{soil} were much smaller than T_{air} gradients when a snowpack was present (Fig. 2.3). These data support our first hypothesis that seasonal snowpacks remove elevation gradients in T_{soil} and are evidence that insulation by snow dramatically reduces energy exchange at the soil surface.

Insulation by snowpacks kept soils warmer than air during the winter. Across all sites, we found mean below-snow T_{soil} values of 0.3, 0.7, and 1.3 °C at 5, 20, and 50 cm depths, respectively, all of which were warmer than mean T_{air} during the same period (-1.8 °C, Fig. 2.3 and 2.8). Other studies have shown similar T_{soil} patterns, with below-snowpack T_{soil} exceeding T_{air} when a snowpack is present (Brooks et al. 1995, Van Miegroet et al. 2000, Hardy et al. 2001, Seyfried et al. 2001, Körner and Paulsen 2004, Monson et al. 2006a, Lundquist and Lott 2008, Sutinen et al. 2009, Masbruch et al. 2012, Schmid et al. 2012, Raleigh et al. 2013), but to our knowledge, these landscape-scale changes in T_{soil} gradients have not been demonstrated.

Despite insulation by snowpacks, there was considerable variability in T_{soil} during winter. We found interannual and intersite ranges in below-snow T_{soil} as large as 7 (mean = 1 °C) and 11 °C (mean = 6 °C), respectively, in our study area (Fig. 2.8). To our knowledge, interannual variability in winter T_{soil} has only been quantified in a few isolated studies in western U.S. mountains. At Niwot Ridge, Colorado, for example, there was a 1.5 °C range in below-snowpack T_{soil} over a 6-year period (Monson et al. 2006b). Comparable studies that have considered spatial variability in T_{soil} over snow-dominated mountainous areas are few (Körner and Paulsen 2004, Scherrer and Körner 2010).

Much of the observed variability in below-snow T_{soil} was related to fall and early-winter conditions, including snowpack size, presnowpack T_{air} and T_{soil}, and snowpack start day. Snowpack thermal resistance increases with depth, and at greater snow depths soil temperature stops responding to seasonal surface temperature fluctuations (Sturm et al. 1997, Bartlett et al. 2004, Grundstein et al. 2005, Zhang 2005). We found that soils were frequently warmer when there was greater early-winter SWE accumulation (Table 2.2, Table 2.3, PC1 and PC4). Cold soils (mean monthly T_{soil} < 0 °C) during early winter months were more common at sites with small snowpacks, while sites with large snowpacks were generally above 0 °C (Fig. 2.6, only Dec. and Jan. shown). We estimated the SWE at which fitted T_{soil} was within 90% of its upper temperature bound to be 308 to 480 mm. At 30% snow density, this is

equivalent to a 1 to 1.6 meter snowpack. This is higher than the estimate of 0.4 m in Brooks and Williams (1999). The model of Bartlett et al. (2004) predicts that a snow depth of 1 meter insulates the ground from most seasonal T_{air} fluctuations and halts the early-winter decline in soil temperature. These results support our second hypothesis that winter soil temperature is dependent on snowpack characteristics. Below-snow T_{soil} was also warmer in years with later snowpack start days (Table 2.2) at some sites, which is inconsistent with our expectations. A number of sites had higher soil moisture in years with late snowpack start days, so it is possible that warmer T_{soil} in late accumulation years can be accounted for by the high heat capacity of water in the soil or by latent heat release during soil freezing (Brooks et al. 2011).

2.5.2 Soil moisture variation below seasonal snowpacks

Soil moisture below the snowpack was generally stable for several months within a given winter, providing support for our hypothesis (3a) that soil water content changes minimally between the start of snowpack accumulation and the initiation of snowpack melt. After November, there was little month-to-month or cumulative change in mean monthly θ, and below-snow θ remained similar to presnowpack θ until February (Fig. 2.4). Both are evidence that evapotranspiration was low, and little precipitation or snowmelt water infiltrated into soils for 3 winter months or more. In March and April, month-to-month and cumulative increases in θ were observed, suggesting that snowmelt began to reach the soil at this time (Fig. 2.4).

Winter quarter soil moisture was dependent on fall and early-winter snowpack and soil conditions. On average, mean winter quarter θ was around 0.4 (normalized) suggesting that, in general, soil moisture was not fully recharged in fall and early-winter months. Winter quarter θ was higher when there was greater early-winter SWE accumulation or greater presnowpack soil moisture (Table 2.2, Table 2.3, PC4). In some years, winter quarter θ was lower at sites where presnowpack T_{soil} and T_{air} were high (Table 2.3, PC3), indicating that higher evapotranspiration during this period may have dried soils. These observations, coupled with the stability of soil θ during the cold season (Fig. 2.4), provide support for our hypothesis (3b) that midwinter θ was determined by conditions in fall and early-winter. We also found, however, a positive relationship between winter quarter θ and winter T_{air} (Table 2.2, Table 2.3 – PC2), suggesting that winter melt events at warmer sites or in warm years may lead to some recharge of soil moisture.

The fall and early-winter period can be viewed as a transitional state between the relative stability of the warm and cold seasons. During this transition, the soil environment is highly sensitive to variability in temperature and precipitation (Grayson et al. 1997, McNamara et al. 2005). This is understandable because the phase (rain or snow) of precipitation, and the likelihood that snowfall will melt and recharge soil θ, are both highly sensitive to temperature fluctuations during this time. We did not use fall and

early-winter precipitation or snowmelt as explanatory variables in multiple regression analysis, and it is possible that these would have provided some additional information. Whatever the dominant drivers of θ are during this fall and early-winter transition period, it appears that winter θ is sometimes determined at this time.

2.5.3 Warm season soil moisture and snowpack variability

We found some evidence that summer quarter air temperature, rainfall, and prior spring snowpack characteristics influenced summer soil moisture. Summer quarter θ was lower during warmer years (Table 2.4), but only at 8–13 sites (depending on soil depth). Sites with warmer T_{air} (Table 2.3 – PC1) also had lower summer quarter θ. Low summer quarter θ may have been the result of high evapotranspiration rates in warm years that removed water from soil. Evapotranspiration is enhanced by warmer air temperature and associated higher evaporative demand. Soil water is primarily recharged by water pulses from snowmelt or summer rain events. Accordingly, we found higher summer quarter θ when there was greater summer precipitation, larger prior spring snowpacks, and later snow-free dates (Table 2.4, Table 2.3, PC2 and 3). These relationships were not significant at all sites or in all individual years tested, indicating that the importance of precipitation and snowpack varied in time and space. This provides limited support for our hypothesis (4) that warm season soil moisture is influenced by snowpack characteristics. Warm season air temperature, however, was a more consistent explanatory variable. In our comparison of sites grouped by summer rainfall, elevation, and snowpack size, the group with the highest mean summer quarter θ was the one with sites at high elevations (cooler), with large snowpacks, and large amounts of summer rainfall (Fig. 2.9). High summer rainfall sites were generally wetter than sites with less summer rainfall, and median summer soil moisture was lower at low elevation and low SWE groups. We also found evidence that warm season rainfall events primarily wet the upper layers of the soil profile, while snowmelt recharged θ at greater depth (Table 2.4).

These results, though complex, agree with other studies of soil water recharge at catchment (Seyfried 1998, McNamara et al., 2005; Williams et al. 2009) and regional scales in the western U.S. (Loik et al. 2004, Hamlet et al. 2007). Both Seyfried (1998) and Williams et al. (2009) found that spatial variability in snowpack size and melt timing explained spatial variability in θ early in the warm season. As soil moisture declined after the snowpack melted, however, those spatial patterns were replaced by soil moisture patterns determined by summer rain. Mountain soils are often shallow and have a small water storage capacity that limits soil moisture recharge by snowmelt water (Smith et al. 2011). A possible explanation for the weak relationships we observed between summer quarter θ and snowpack is that snowmelt-derived soil water was depleted prior to the summer quarter at many sites. This is consistent with recent observations in the region (Molotch et al. 2009). Local controls, such as soil texture, vegetation, and topography can also greatly influence soil water storage and the rate of θ drawdown

during the warm season (Litaor et al. 2008, Williams et al. 2009, Bales et al. 2011). These and other site-specific variables are undoubtedly important and highly variable in our study area.

2.5.4 Implications for ecosystems and biogeochemical processes

Soil microbial activity occurring near the freezing point of water is highly sensitive to temperature. This has been observed in laboratory (Fang and Moncrieff 2001, Mikan et al. 2002, Öquist et al. 2009) and field studies of soil biogeochemical processes (Brooks et al. 1996, Elberling and Brandt 2003, Monson et al. 2006b). Other than the effect of temperature on biochemical reaction kinetics, several explanations for this phenomenon have been made, including changes in the availability of liquid water (Mikan et al. 2002, Öquist et al. 2009) and organic carbon substrates (Brooks et al. 2005, Schimel and Mikan 2005, Davidson and Janssens 2006), and the exponential growth of soil microbial communities at low temperatures (Schmidt et al. 2009). Because of this temperature sensitivity, seemingly minor changes in winter soil temperature can have major effects on biogeochemical processes, even at the ecosystem level. In the study by Monson et al. (2006b), for example, an interannual range in below-snow T_{soil} from -1.5 to 0 °C was responsible for a 21% variation in cumulative annual net ecosystem CO_2 exchange at Niwot Ridge, Colorado. We found that below-snow T_{soil} averaged around 0 °C across our western U.S. study sites, but interannual and intersite ranges in below-snow T_{soil} were large enough to significantly impact rates of biological activity in soils (Fig. 2.8).

Soil frost events become less likely in temperate mountain ecosystems as the sizes of seasonal snowpacks increase. Frost formation damages root and microbial biomass and because some soil organisms are more cold-sensitive than others, soil community composition can change (DeLuca et al. 1992, Sutinen et al. 1999, Tierney et al., 2001; Feng et al. 2007, Comerford et al. 2013). Frost damage is thought to release labile carbon and nutrient rich cell contents into the soil (Matzner and Borken 2008), and a variety of effects on soil biogeochemical processes have been observed following freeze-thaw events. These include increases in soil respiration (Schimel and Clein 1996, Brooks et al. 1997, Feng et al. 2007), higher soil inorganic nitrogen concentration and N2O emission (DeLuca et al. 1992, Brooks et al. 1996, Groffman et al. 2001, 2006), and greater export of carbon, nitrogen, and other nutrients from soils in solution (Boutin and Robitaille 1995, Brooks et al. 1998, Fitzhugh et al. 2001, Haei et al. 2010). Some studies, however, have found that soil frost events have little net effect on, or reduce the rates of these same biogeochemical processes (Lipson et al. 2000, Grogan et al. 2004, Hentschel et al. 2009, Muhr et al. 2009, Groffman et al. 2011). We found indirect evidence of soil frost at one site (Fig. 2.2b and c), and extensive evidence that fall and early-winter conditions influenced whether soil temperature dropped below 0 °C during the winter (Fig. 2.6).

Soil moisture also has a well-recognized influence on soil biological activity and associated biogeochemical processes (Orchard and Cook 1983, Borken and Matzner 2009). Below-snow soil microbial

processes, such as those that emit carbon dioxide, methane, and nitrogen oxides during winter, respond to variations in soil moisture (Mast et al. 1998, Liptzin et al. 2009, Filippa et al. 2009, Aanderud et al. 2013). There is some evidence that the availability of soil water beneath melting spring snowpacks stimulates the upregulation of photosynthesis and transpiration in conifer forests in our study area (Monson et al. 2005, Zarter et al. 2006b). Within a given winter, we generally found stability in below-snow soil θ (Fig. 2.4), but considerable interannual and intersite variability was driven by fall and early-winter snow and temperature conditions.

Winter biological and biogeochemical activity can be substantial given the below-snow T_{soil} and moisture conditions found in our study area. Below-snow soil respiration, for example, has been shown to account for anywhere from ~12 to 50% of the annual respiration flux in seasonally snow-covered ecosystems (reviewed in Liptzin et al. 2009). Aside from some studies of soil processes along elevation transects in our region (Amundson et al. 1989, Trumbore et al. 1996, Kueppers and Harte 2005), there is little data on how biogeochemical processes vary spatially and temporally in seasonally snow-covered mountain ecosystems. There has been some effort to synthesize aspects of the interactions between snow, soil, and winter biogeochemical cycling into a conceptual model (Brooks and Williams 1999, Liptzin et al. 2009, Brooks et al. 2011). In this framework, snowpacks limit soil biological activity when they are shallow or transient enough to allow frozen soil for long periods or permanent enough to restrict warm-season primary production and thereby reduce the supply of carbon for soil heterotrophs. The majority of our study sites fall between these extremes. Short duration frost events occur, often in response to fall and early-winter snow and weather conditions. These may enhance nutrient availability via organic matter fragmentation (Hobbie and Chapin 1996) and turnover of microbial biomass (Schimel and Clein 1996, Brooks and Williams 1999). Typically, however, soils are thawed during winter, permitting the activity and growth of a large below-snowpack soil microbial community (Lipson et al. 1999, Schmidt et al. 2009). The decomposition of autumn plant litter inputs provides a carbon source for the growth of this community and fuels the winter biogeochemical activity discussed above (Taylor and Jones 1990, Hobbie and Chapin 1996, Schmidt and Lipson 2004).

The influence of winter snowpacks on the soil biophysical environment also extends to the warm season. Following the winter growth of large below-snow microbial communities, the spring melt is accompanied by a change in microbial community and a rapid decline in microbial biomass (Brooks et al. 1996, Lipson et al. 1999). The subsequent flush of nutrients can be lost in spring runoff (Hood et al. 2003) or exploited by plants during the warm season (Brooks et al. 1998, Jaeger III et al. 1999, Lipson et al. 1999). The spring snowmelt also marks the beginning of the growing season for most plant communities, and changes in the timing of melt can alter the timing of plant phenological events, such as greening and flowering, in alpine plant communities (Steltzer et al. 2009). Warm season activity by plant

and soil communities in snow-dominated ecosystems depends heavily on snowmelt water (Brown-Mitic et al. 2007, Litaor et al. 2008, Riveros-Iregui and McGlynn 2009), and differences in snowpack size and melt timing can have significant effects on forest productivity (Molotch et al. 2009, Tague et al. 2009, Hu et al. 2010). Our results support the idea that snowmelt enhances warm season soil moisture availability, but this effect is variable and dependent on snowpack size, melt timing, and summer air temperature for a particular site or year.

2.5.5 Limitations and future research

There are a number of limitations to this study, many of which provide opportunity for future investigation. We focused our study on elucidating the climatic drivers of T_{soil} and θ, and consequently ignored many site-specific variables that influence the soil biophysical environment. Soils vary widely in composition and texture, for example, which have significant effects on water retention and thermal or hydraulic conductivity (Campbell et al. 1994, Abu-Hamdeh and Reeder 2000, Haverkamp et al. 2005). Our study sites also vary in topographic position and vegetation cover, which may strongly influence precipitation accumulation, evapotranspiration rate, soil and groundwater flow, and soil surface energy balance. None of these site-specific variables, or other potential sources of uncertainty, are accounted for in our study. The statistical models we fit in this study explained only a small amount of the variance in T_{soil} and θ across our study sites (R^2 of 0.07–0.42, Table 2.3), and it is likely that inclusion of additional site-specific variables and uncertainties would have improved this analysis.

Another limitation stems from our use of artificial, rather than hydrologically defined, seasonal periods. Averaging data into quarterly or monthly values, which are arbitrary with respect to the annual hydrologic cycle, risks losing important information about hydrologic events and processes. In studies examining intersite or interannual variability, such as ours, it may be advantageous to compare hydrologically based events and seasons rather than artificially imposed ones. Such an approach has been successfully used to study interannual variability in forest ecohydrological processes (Thomas et al. 2009).

2.6 Conclusions

We found that seasonal snowpack characteristics had significant effects on the soil biophysical environment. First, snowpacks decoupled T_{soil} from T_{air}, reducing elevation gradients in T_{soil} across the landscape during the cold season. Second, below-snow T_{soil} was greatly influenced by the timing and magnitude of snow accumulation, and low early-winter snowpacks led to cooler soil and higher likelihood of freeze-thaw events. Third, soil θ changed little between the start of snowpack accumulation and the initiation of snowpack melt. Fourth, winter quarter soil θ was influenced by fall and early-winter precipitation or temperature. Finally, snowmelt-derived soil moisture was a limited resource, but availability

of this resource was more likely with large snowpacks and later melt timing.

The magnitudes of these effects suggest that changes in snowpack characteristics, particularly during fall, early-winter, and late spring, will impact soil biological activity and associated biogeochemical processes in the western U.S. Studies of current hydroclimate, and projected trends in this region indicate that snowpack and temperature changes during these seasons are underway and likely to intensify (Brown and Mote 2009, Seager and Vecchi 2010, Barichivich et al. 2012, Kapnick and Hall 2012). We therefore anticipate changes to the soil temperature and moisture environment of the region and a significant response from ecosystems and biogeochemical processes.

2.7 Acknowledgments

The authors wish to acknowledge Anne Nolin and two anonymous reviewers for their attentive comments, which greatly improved this manuscript. We also thank a number of staff and scientists of the NRCS Snow Survey program. Tim Bardsley, Jim Marron, Tony Tolsdorf, Karen Vaughan, and Randall Julander provided valuable information and/or helpful discussions on using and interpreting SNOTEL data. Undergraduate Richard Malyn and high-school student Davis Unruh donated time collecting SNOTEL data files. Greg Maurer was partially supported during this study by Office of Science (BER), U.S. Department of Energy, grant DE-SC0005236.

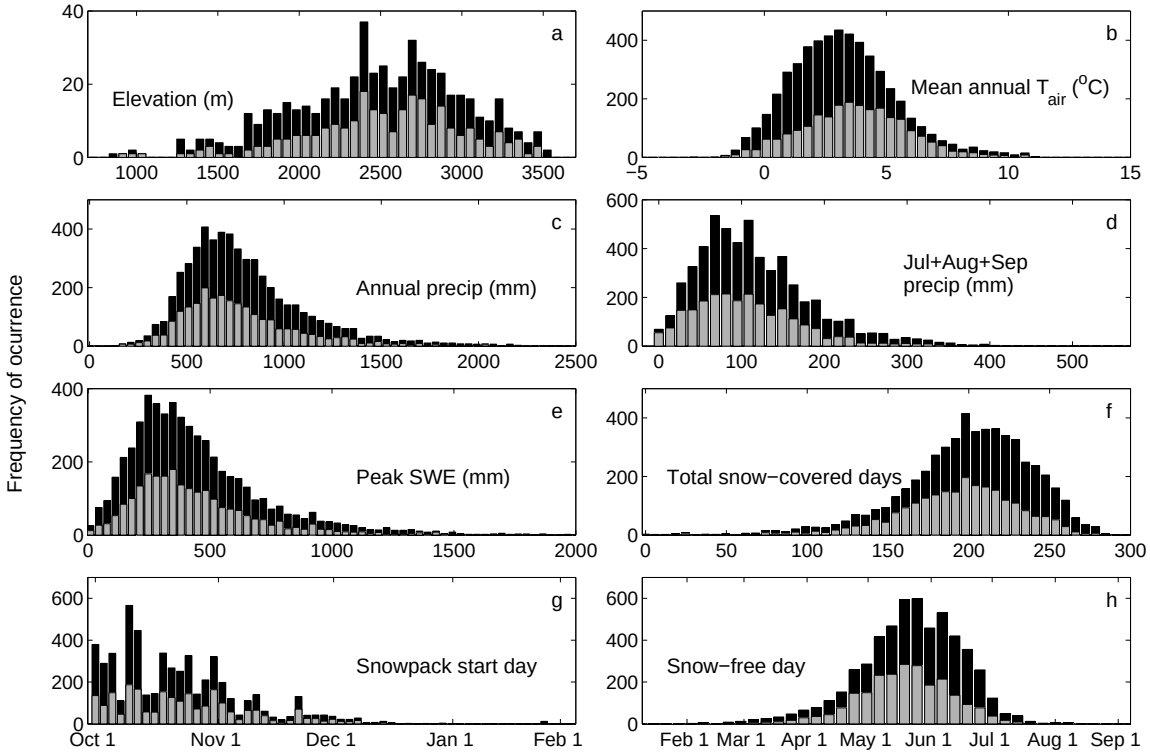

Figure 2.1. Frequency distributions for selected climate and snowpack characteristics during water years 2001 to 2011, inclusive. Distributions are shown for the full set of SNOTEL stations in the interior western U.S. (black bars, 574 sites in AZ, CO, ID, MT, NM, NV, UT, WY) and for the subset of those sites that have soil sensor profiles installed (gray bars, 252 sites).

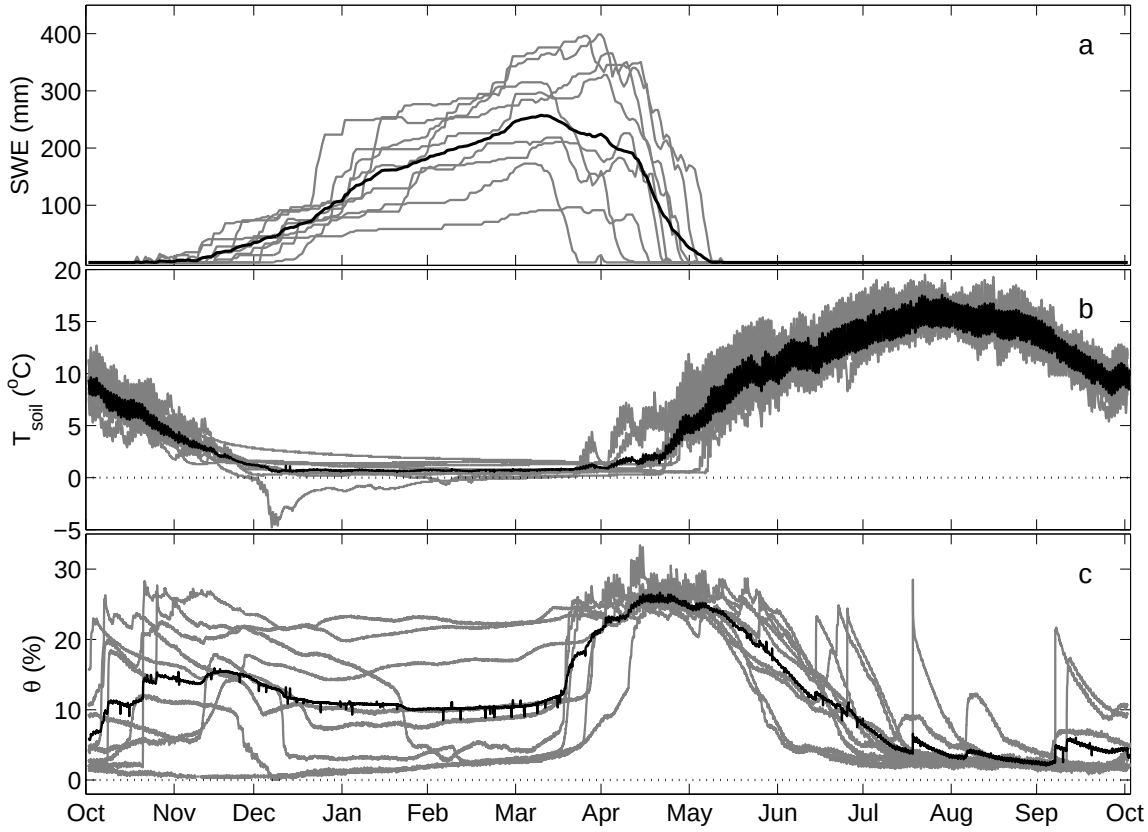

Figure 2.2. Time series of SWE (a), 20 cm T_{soil} (b), and 20 cm θ (c) from 2002–2011 at the Currant Creek site (UT). One time series for each individual year since installation of the soil sensors is plotted in gray, and the mean of all these years is plotted in black.

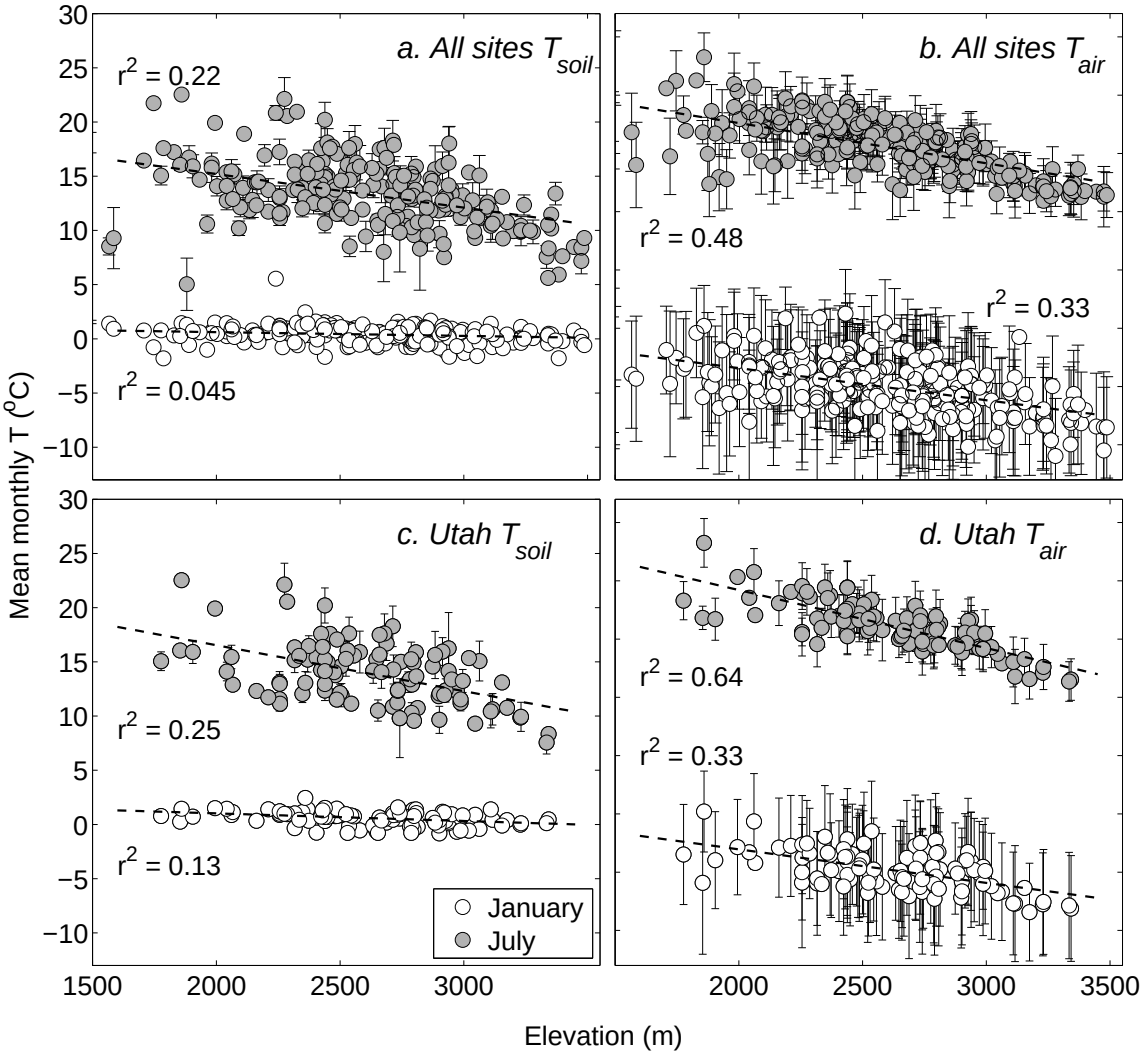

Figure 2.3. Elevation gradients in mean monthly T_{soil} (left panels) and T_{air} (right panels). January and July data at all soil sites (n = 252) are shown in panels (a) and (b), and at Utah soil sites (n = 102) in panels (c) and (d). All points are multiyear means of January or July measurements from all available water years, and error bars are 1 standard deviation (some are smaller than the symbols). Dashed lines are least-squares linear regressions. T_{soil} measurements are from 20 cm depth. Regression equations for panels (a) and (b): July mean T_{soil} = -3.1x + 21.41; January mean T_{soil} = -0.3x + 1.31; July mean T_{air} = -3.4x + 24.50; January mean T_{air} = -2.8x + 2.08. All slopes are significantly different than zero ($p < 0.01$). Utah regression coefficients are given in the text.

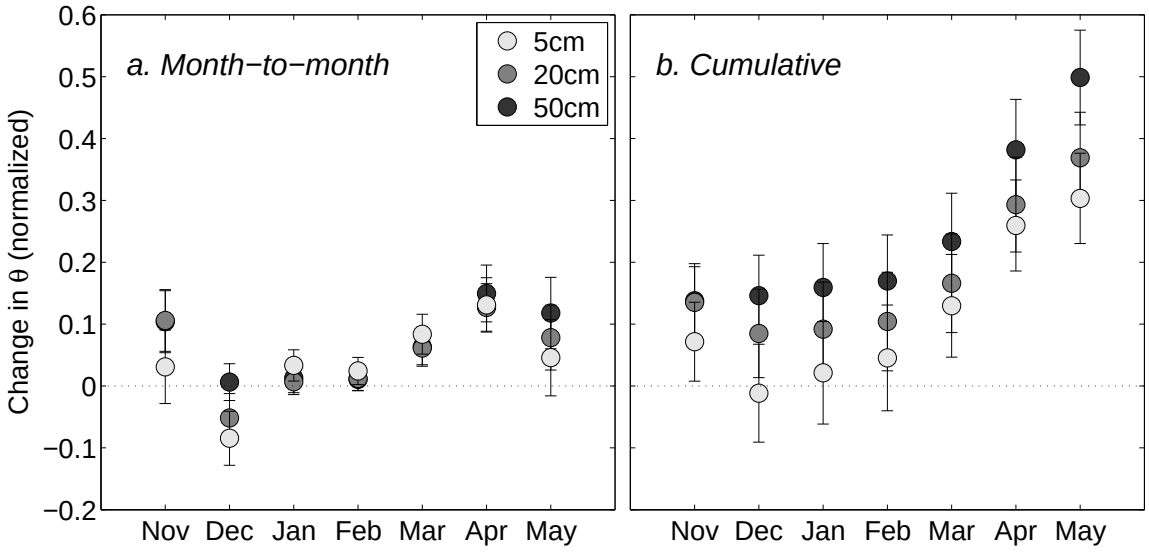

Figure 2.4. Monthly change in normalized soil θ (dimensionless) at three soil depths. Panel (a) shows one-month changes in mean θ (mean month θ – mean prior month θ). Panel (b) shows the cumulative change in soil θ since the presnowpack period as described in the text (mean month θ – presnowpack θ). Points represent the mean change for the soil sites (n = 252) at the indicated depth. Error bars are 1 standard error. A dotted line indicating no change in θ is plotted for reference.

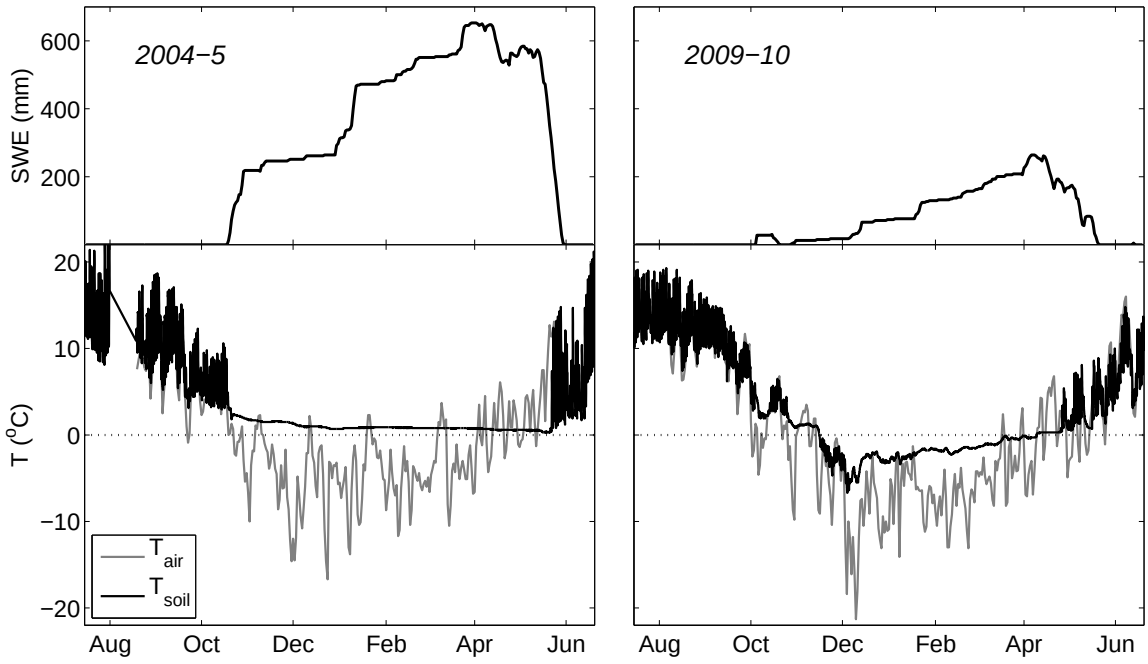

Figure 2.5. Daily T_{soil} (5 cm depth), T_{air}, and SWE at Mosby Mountain site (UT) during 2 contrasting years. In water year 2005, a large snowpack (SWE) accumulated early, leading to stable, above-zero T_{soil} during the entire below-snow period. In water year 2010, a small early-season snowpack led to subzero T_{soil} for much of the below-snow period.

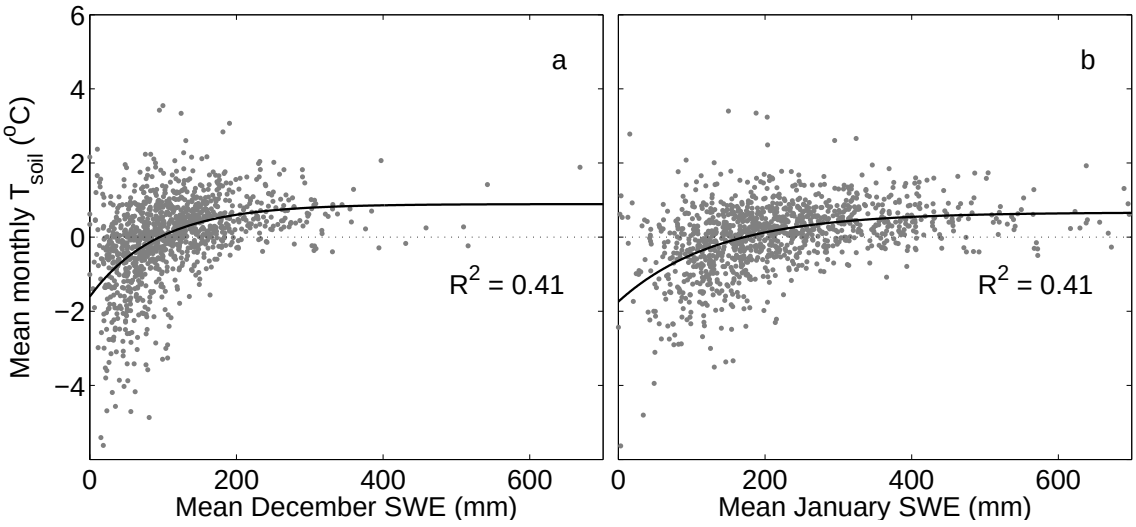

Figure 2.6. Mean monthly T_{soil} as a function of mean monthly SWE in early winter for all sites (n = 252). Each point represents the mean T_{soil} at 5 cm depth for 1 month at an individual site. The solid lines are the least-squares fit to a bounded exponential function ($y = a(1 - be^{-cx})$). The fitted values of the upper temperature bounds in December and January are 0.89 and 0.67 °C, respectively. The fitted values of SWE at 90% of these upper bounds are 308.6 and 480.3 mm, respectively. Data for December and January of all available water years are shown here, but similar patterns were present during February (R^2 = 0.35) and at other depths (not shown, 20 cm R^2 values = 0.34–37, 50 cm R^2 values = 0.27–0.31). Low early season T_{soil} occurred more frequently with a small snowpack.

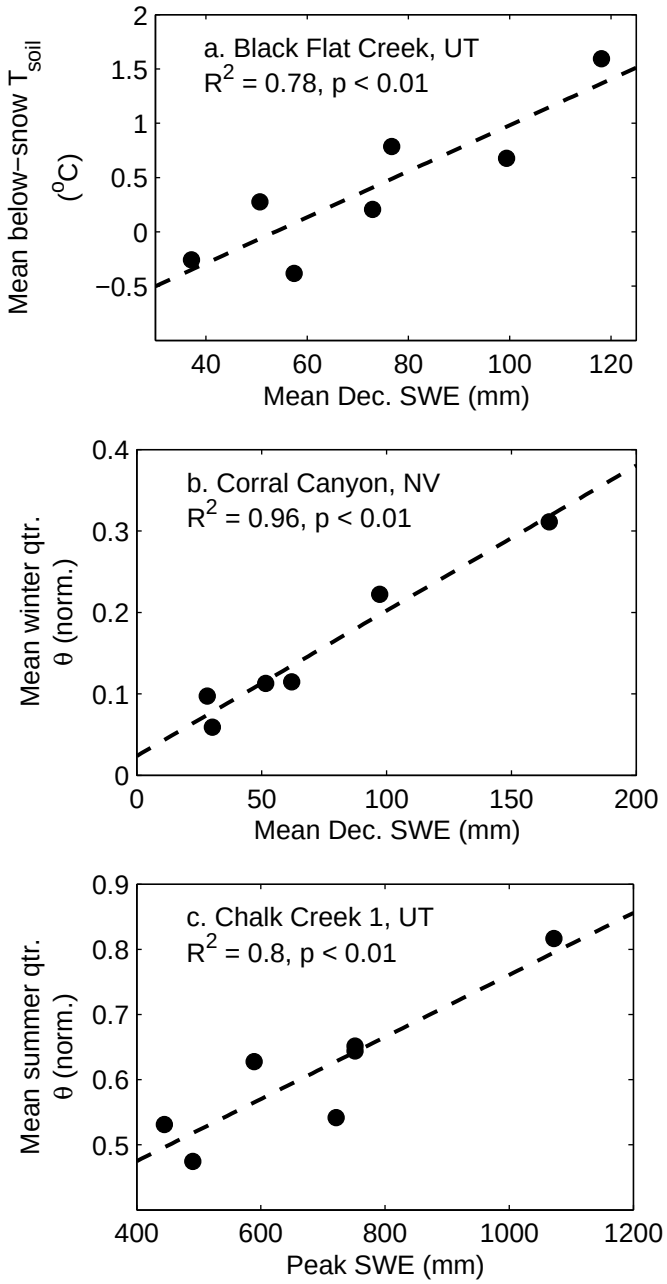

Figure 2.7. Simple linear regressions of (a) mean below-snow T_{soil} versus mean December SWE, (b) mean winter quarter (JFM) 20 cm θ versus December mean SWE, and (c) mean summer quarter (JAS) 50 cm θ versus peak SWE during different years (interannual variability) at individual SNOTEL sites. These are shown as examples of the regression results presented in Tables 2.2 and 2.4.

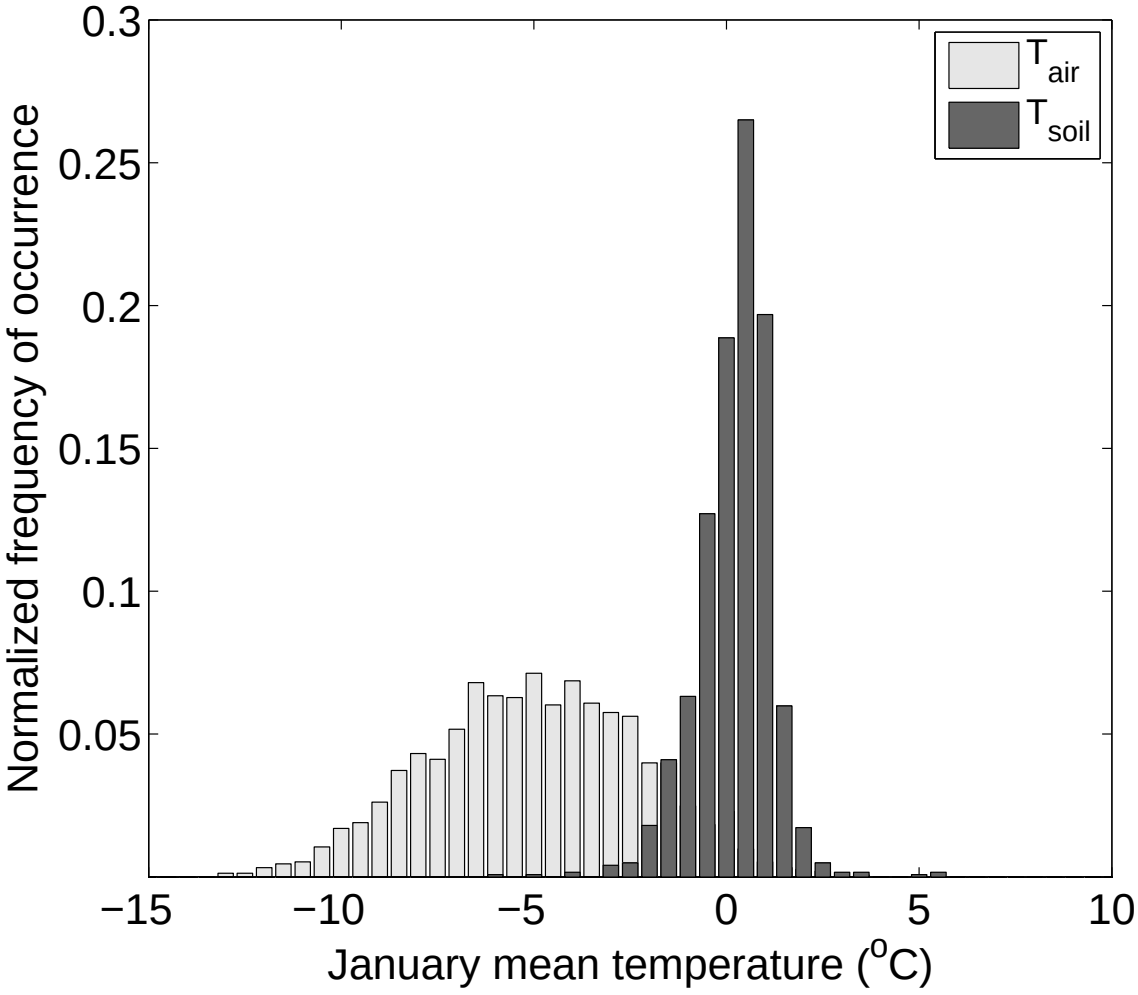

Figure 2.8. Frequency distributions of mean January soil (20 cm) and air temperature for all sites and all years of data (2001–2011). The histograms are standardized to show the fraction of data in each temperature bin.

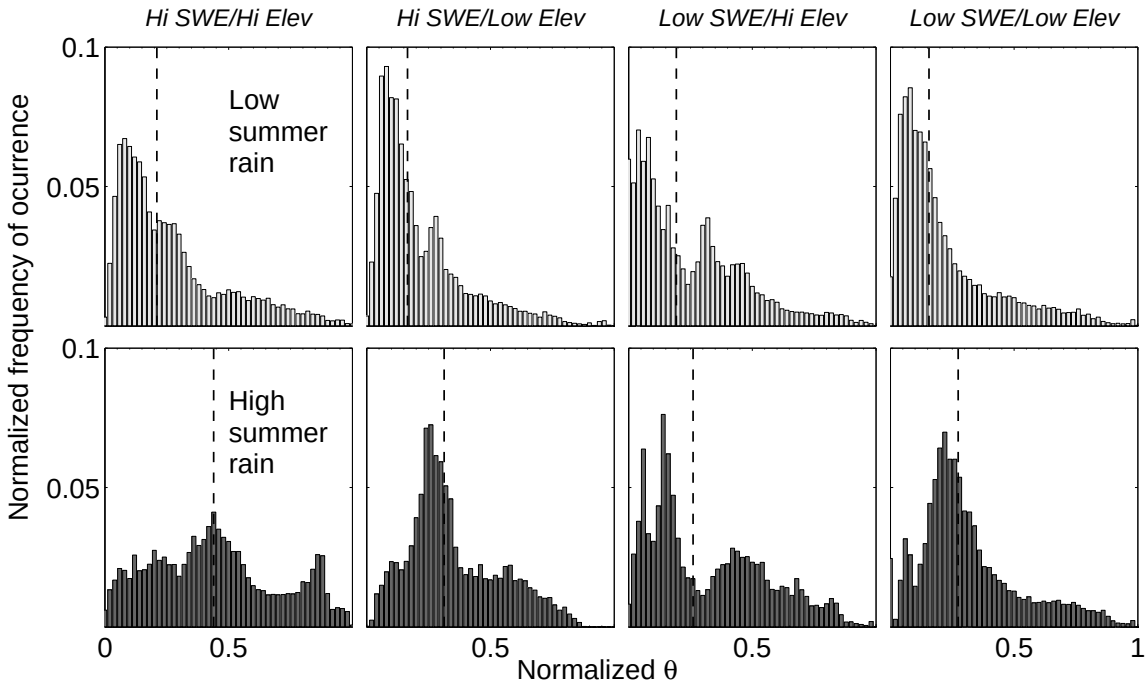

Figure 2.9. Frequency distributions of mean summer quarter θ (normalized 20 cm data for Jul., Aug., and Sep.) for subsets of soil sites with contrasting profiles of elevation, mean snowpack size, and summer precipitation. Sites in the top row received less than 20% of total annual precipitation in the 3 summer months. Sites in the lower row received greater than 20%. High and low elevation and SWE groups are defined in the text. The same 6 years of data, 2006–2011, are used in each group of sites. Median summer quarter soil θ for each group is plotted with a dashed vertical line.

Table 2.1. Mean and standard deviation of elevation, snowpack metrics, and selected climate variables for the years 2001 to 2011 (inclusive). Data for all sites (n = 574) and the soil sites (n = 252) are shown.

	All sites		Soil sites	
Variable	Mean	SD	Mean	SD
Elevation (m)	2511.4	513.5	2549.8	483.0
Mean annual T_{air} (°C)	3.4	2.1	3.9	2.2
Annual precip. (mm)	821.1	322.1	791.6	301.1
Summer quarter precip. (mm)	124.0	73.3	114.1	68.3
Peak SWE (mm)	463.6	285.9	456.9	268.4
Total snow-covered days (d)	204.1	39.6	197.8	37.6
Snowpack start day	Oct 24	17.8	Oct 26	17.5
Snow-free day	May 23	25.2	May 20	23.1

Table 2.2. Summarized results for linear regression of mean below-snow T_{soil} and mean winter quarter θ on a number of explanatory variables. Results from 5 cm, 20 cm, and 50 cm soil depths are shown (n = 252 sites). All regression coefficients (not shown) indicated positive relationships to the explanatory variable. For each variable, numbers represent the total number of sites in which simple linear regression was significant ($p < 0.05$). Asterisks denote the level of significance of the explanatory variable in a multilevel linear model using site as the random variable (*** for $p < 0.001$; ** for $p < 0.01$; * for $p < 0.05$).

	Below-snow T_{soil}			Winter quarter θ		
Explanatory variables	5cm	20cm	50cm	5cm	20cm	50cm
Peak SWE	12***	10***	10*	19***	12***	6***
Snowpack start day	13	15	12	15*	10	12
Pre-snowpack T_{air}	8***	9***	8*	8*	9**	7***
Below-snow period T_{air}	11***	14***	13***	13***	10**	9***
Snow-free day	5***	6*	5	10***	8***	7**
Mean Nov. SWE	23***	28***	30*	36***	19***	17***
Mean Dec. SWE	37***	39***	29***	48***	48***	27***

Table 2.3. Multiple regression results for three dependent variables. Mean below-snow T_{soil} and winter quarter θ were regressed against principal component scores from the below-snow PCA, and mean summer quarter θ was regressed against scores from the warm season PCA (see Appendix for PC axis details). Each multiple regression model was tested using data from all years together and data from each of three individual years. Regression coefficients for each PC axis and asterisks denoting their significance as explanatory variables in the model (*** for p < 0.001; ** for p < 0.01; * for p < 0.05) are shown.

Dependent variables	Explanatory variables	All years	2007	2009	2011
Below-snow T_{soil}	Spring snowmelt (PC 1)	-0.02 **	0.02	-0.02	0.03 **
	Winter temperature (PC 2)	0.14 ***	-0.09 ***	-0.15 ***	-0.11 ***
	Snowpack start temperature (PC 3)	-0.04 *	0.08 *	0.13 **	-0.07 **
	Fall snow/soil (PC 4)	0.12 ***	0.24 ***	-0.15 *	-0.02
	Model Adjusted R^2	*0.22*	*0.28*	*0.28*	*0.32*
Winter quarter θ	Spring snowmelt (PC 1)	0.00 *	0.00	0.01 *	0.02 ***
	Winter temperature (PC 2)	0.04 ***	-0.02 **	-0.05 ***	-0.04 ***
	Snowpack start temperature (PC 3)	0.02 ***	-0.05 ***	-0.02 .	0.01
	Fall snow/soil (PC 4)	0.04 ***	0.09 ***	-0.09 ***	-0.04 **
	Model Adjusted R^2	*0.23*	*0.38*	*0.42*	*0.32*
Summer quarter θ	Summer T_{air} (PC 1)	-0.02 ***	0.02 ***	-0.01 ***	-0.03 ***
	Spring snowmelt/summer precip (PC 2)	0.01 **	0.02 **	0.00	-0.01
	Winter T_{soil} (PC 3)	0.02 ***	0.00	-0.01	0.02 **
	Model Adjusted R^2	*0.16*	*0.26*	*0.07*	*0.18*

Table 2.4. Summarized results for linear regression of mean summer quarter θ on a number of explanatory variables. Results from 5 cm, 20 cm, and 50 cm soil depths are shown (n = 252 sites). Negative regression coefficients are indicated in parentheses, all others were positive. For each variable, numbers represent the total number of sites in which simple linear regression was significant ($p < 0.05$). Asterisks denote the level of significance of the explanatory variable in a multi-level linear model using site as the random variable (*** for $p < 0.001$; ** for $p < 0.01$; * for $p < 0.05$).

Explanatory variables	5cm	20cm	50cm
Peak SWE	13***	16***	22***
Snow-free day	9***	9***	17***
Summer qtr. T_{air}	8(-)***	13(-)***	12(-)***
Summer qtr. Precip.	26***	18***	6***
Winter qtr. 5cm T_{soil}	10	9	7

CHAPTER 3

DUST AND CANOPY EFFECTS ON SNOWPACK MELT AND ECOSYSTEM PROCESSES IN A UTAH SUBALPINE FOREST

3.1 Abstract

Dust deposition lowers the albedo of snow and can significantly alter snowpack energy balance. Investigation of aeolian dust deposition in the mountains of the western U.S. has shown that these effects advance the timing of snowpack melt and spring runoff across much of the region. These studies have primarily focused on alpine snowpacks with little to no overstory vegetation. To evaluate the impacts of aeolian dust on forest ecohydrological processes, we conducted a manipulative experiment in a subalpine conifer forest in Utah's Wasatch Mountains. During the spring of 2010–2012, we added dust to the snow surface in forested plots every 1 to 2 weeks, roughly doubling the natural dust loading rate. We then measured the snowpack ablation rate in control and dust-addition treatments, along with below-snowpack and warm season soil temperature (T_{soil}), soil water content (θ), decomposition rate (D), soil respiration rate (R_s), and tree xylem water potential (ψ). Differences in ablation between control and dust-addition treatments were similar in magnitude to differences associated with the canopy structure of the forest. Seasonal patterns in T_{soil} and θ were similar between dust treatments and canopy structure groups. D, R_s, and ψ varied little between dust treatments, but there were significant differences between years. Our results suggest that interannual variability in snowfall had the greatest effect on the soil environment and ecosystem processes. We also conclude that the effects of aeolian dust on snowpack mass and energy balance are similar in magnitude to those associated with canopy structure.

3.2 Introduction

Dust and other impurities lower the albedo of snow and have additional indirect effects on the energy balance of snow- and ice-covered land surfaces (Warren and Wiscombe 1980, Hansen and Nazarenko 2004). During the spring, solar energy absorbed by particles near the snow surface can hasten the warming and melting of the snowpack (Conway et al. 1996, Painter et al. 2007, Gleason et al. 2013). Recent studies have suggested that deposition of aeolian dust on mountain snowpacks leads to a significantly

earlier timing of snowpack melt and seasonal water runoff in the hydrologic basins of the western U.S. (Painter et al. 2007, Skiles et al. 2012). Studies that model the effects of dust on snowpack dynamics have sometimes included forested areas, but experiments directly examining the effects of dust deposition on ecological processes have been limited to alpine areas where there is no vegetation canopy above the snowpack (Steltzer et al. 2009).

Snowpack energy balance in forested areas differs from that in open, alpine areas. A fraction of incoming shortwave (solar) radiation is intercepted by and warms the canopy, which may then increase the emission of longwave (terrestrial) energy towards the snow surface. Snow is an efficient absorber of longwave radiation, and this radiation becomes an important energy source for ablation in below-canopy environments (Link and Marks 1999a, 1999b, Koivusalo and Kokkonen 2002, Link et al. 2004, Pomeroy et al. 2009). Dust deposition lowers the shortwave albedo of snowpacks regardless of the presence of a canopy, but it does little to enhance the absorption of longwave radiation by snow (Warren and Wiscombe 1980, Painter et al. 2007). The efficacy of dust in perturbing snowpack energy balance below a canopy should therefore depend on the relative contributions of shortwave and longwave radiation, which are strongly influenced by canopy structure and radiative transfer (Link and Marks 1999a, Sicart et al. 2004, Ellis et al. 2011, Lawler and Link 2011). We know of no studies that have addressed the effects of dust deposition on snowpack melt in forested areas.

Reduced snowpack and earlier melt timing are associated with a variety of effects on ecosystems. Active microbial communities are present beneath seasonal mountain snowpacks, and their activity is tied to below-snowpack temperature and water availability. The melting of spring snowpacks triggers the turnover of these communities and an associated flush of nutrients (Brooks et al. 1998, Jaeger III et al. 1999, Lipson et al. 1999). The spring snow melt also marks the beginning of a more physiologically active period for plant communities, and changes in the timing of melt can alter the timing of phenological events, such as greening and flowering, in alpine plant communities (Steltzer et al. 2009). Warm season activity by plant and soil communities in snow-dominated ecosystems depends heavily on snowmelt water (Brown-Mitic et al. 2007, Litaor et al. 2008, Riveros-Iregui and McGlynn 2009), and differences in snowpack size and melt timing can have a significant effect on forest productivity (Molotch et al. 2009, Tague et al. 2009, Hu et al. 2010). Perturbations to snowpack ablation by dust events may therefore have a significant effect on a variety of ecosystem processes.

Dust deposition has changed since the settlement of the western United States, largely due to human-driven land use and land cover change (Neff et al. 2008, Painter et al. 2010, Ballantyne et al. 2011). Recent studies have revealed declining trends in snowcover extent, duration, and snowpack size in the region over this same time period (Hamlet et al. 2005, Mote et al. 2005, Mote 2006, Dyer and Mote 2007). These trends in the timing and magnitude of snowpack ablation are thought to be responsible for shifts toward earlier spring runoff timing in the hydrologic basins of the western U.S. (Dettinger and

Cayan 1995, McCabe and Clark 2005, Regonda et al. 2005, Stewart et al. 2005, Hamlet et al. 2007). The snowpack and streamflow changes reported in the interior western U.S. (Clow 2010, Nayak et al. 2010, Harpold et al. 2012) are consistent with regional and global trends in earth surface temperature change, but may also be attributable, in part, to the effects of aeolian dust deposition on mountain snowpacks (Painter et al. 2010). According to model projections, increasing trends in aridity and temperature in the western U.S. will continue and intensify in the coming century (Brown and Mote 2009, Seager and Vecchi 2010, Kapnick and Hall 2012). These trends bring a high likelihood of widespread vegetation change and greater aeolian dust fluxes (Westerling et al. 2006, Logan et al. 2010, Munson et al. 2011, Anderegg et al. 2011), which may act as a positive feedback for further hydroclimatic changes in the region.

Though numerous studies suggest that increased dust deposition in the western U.S. will lead to hydrologic and ecological change, few direct experiments have been performed. Given that changes in dust deposition are concomitant with changes in temperature, aridity, vegetation cover, and other factors, it is critical that the mechanisms of ecosystem responses to dust deposition be investigated. We added dust to the snowpack beneath a subalpine conifer forest in Utah and measured resulting changes in SWE accumulation, snow ablation rate, and the soil environment, including soil temperature (T_{soil}) and soil water content (θ). We also monitored the response of vegetation and soil biological processes, including xylem water potential (ψ), soil respiration, and decomposition, to this snowpack manipulation. We hypothesized that the dust-addition treatment would increase the rate of spring snowpack melt, leading to earlier snow melt, decrease in warm-season θ, and changes in the seasonal pattern of T_{soil}. We expected a response from vegetation and soil biological processes that would follow the timing and magnitude of changes θ and T_{soil}. The design of this experiment and fortuitous timing also allowed us to assess the important role of within-forest differences in canopy structure and high interannual variability in snowpack dynamics.

3.3 Methods

3.3.1 Site description

In the spring of 2010, 2011, and 2012 we conducted a snowpack manipulation at a Rocky Mountain subalpine forest to measure the impact of dust deposition on snow ablation below a conifer canopy. The study took place in a mature conifer forest on a south facing slope at 2895 m (40°, 36' N, 111°, 35' W) in the Wasatch Mountains near Salt Lake City, Utah. Dominant conifer species in this forest were *Abies lasiocarpa* (subalpine fir) and *Picea engelmanii* (Engelmann spruce), and there were small patches of the deciduous *Populus tremuloides* (quaking aspen). This site was chosen for its patchy, open canopy structure and southern aspect, which we assumed would allow significant transmission of shortwave radiation through the canopy.

Beneath this canopy, we delineated 10 × 60 meter study plots with long edges oriented parallel to the direction of the site slope. In 2010 we established a pilot snowpack manipulation consisting of one control and one dust-addition plot. At this stage we attempted to control for canopy structure by measuring stem density of the study forest and locating our study plots in areas of the forest with similar density. However, as we added replicates, we decided to control for canopy structure using hemispherical photography (described below). In 2011 we added two replicates to each treatment for a total of three 10 × 60 m plots per treatment. Control and dust-addition treatments were randomly assigned to the plots. In October of 2009, we installed a weather station in a clearing outside the study forest. We also installed four soil moisture sensor profiles (CS-616, Campbell Scientific, Inc., Logan, UT, USA; EC-5, Decagon Devices, Inc., Pullman, WA, USA) and two soil temperature sensor profiles (Decagon EC-5) in each treatment. In September 2010 we added an additional sensor profile for θ (Campbell CS-616) and T_{soil} (Campbell CS-107) profile, for a total of five θ and three T_{soil} profiles per treatment. The sensors in each profile were installed at 5, 20, and 60 cm below the top of the mineral soil horizon. Thirty-second readings of T_{soil} and θ were logged and then averaged every half hour with Campbell Scientific 23X dataloggers.

3.3.2 Snowpack dust addition

3.3.2.1 Dust provenance

For the 2010 pilot project, we collected dust from the Chinle-Moenkopi formation of the Colorado Plateau. This geologic formation is a source for aeolian dust for some areas of the southern Rockies (Neff et al. 2008, Lawrence et al. 2010). After the pilot project was complete, however, we learned that the Wasatch Mountains receive significant amounts of dust from Great Basin regions to the south and west (Steenburgh et al. 2012). Based on this new understanding of Wasatch dust sources, we changed the dust source for the remainder of the study. The Milford Flat fire near Filmore, UT in the summer of 2007 was the largest wildfire in Utah history, and the burned area soon became a recognized source of the windblown dust deposited in the Wasatch Mountains (Steenburgh et al. 2012, Hahnenberger and Nicoll 2012, Miller et al. 2012). In March of 2011 we collected dust from drifts of wind-deposited material along a roadway through the Milford Flat fire scar. The material collected from both dust sources was sifted to < 500 μm. This size threshold is larger than the typical size class for aeolian dust (Lawrence et al. 2010) but produced material that could be easily scattered across our 10-m wide plots.

3.3.2.2 Dust application

During the spring, dust was scattered by hand from the edge of the dust-addition plots on to the surface of the snowpack. We took care not to trample the snowpack inside the plots. We timed these dust additions to follow new snow events and, when possible, to precede clear, sunny weather. A new dust addition occurred every 1 to 2 weeks at times that maximized the exposure of the dust on the snowpack

surface to shortwave radiation, and thus, its effect on the snow melt rate. We anticipated that six artificial dust events per year, at a loading rate at roughly 5 grams per square meter would more than double the annual ambient dust loading observed in our region (Lawrence and Neff 2009). We applied dust six times in 2010 and 2011 and only four times in 2012 due to a smaller snowpack and early spring snowmelt in that year. To verify that dust-addition had increased the amount of particulate matter in our snowpack above ambient levels, we collected cores of the full snowpack column from all plots once the final dust application was made. In 2011 and 2012 we also measured ambient particulate matter loading in a clearing near our forest. In 2011 the clearing measurement was made by excavating a full snowpit on May 23 and sampling the entire snowpack in 10-cm increments. For the rest of the spring after this full snowpit collection, we collected surface cores (n = 3) on a storm board following each natural dust event, and the dust mass in these cores was added to the total dust loading from the snow pit. In 2012, three full snowpack cores were collected in the clearing on the same day as those collected in the canopy, and there were no further dust events after this collection. Snow cores and pit samples were thawed, filtered through weighed glass fiber filters (Whatman Grade GF/A, GE Healthcare Bio-Sciences, Pittsburgh, PA, USA), and the filters were oven dried and weighed to determine total particulate matter loading at each location. From these filters, we removed particulate matter that was clearly forest litter (needles, bark, scales, etc.) and weighed it separately.

3.3.2.3 Snow measurements

At six locations in each plot (n = 18 in each treatment), snow water equivalent (SWE) of the snowpack was measured prior to each dust addition, and on a roughly weekly schedule once ablation began. Measurement locations were marked and remained the same (±3 m) for the duration of the experiment. SWE measurements were made using a Federal aluminum tube snow sampler (Union Forge, Yakima, WA, USA). Precipitation and SWE data from the Brighton SNOTEL site (Site 366, USDA, Natural Resources Conservation Service, http://www.wcc.nrcs.usda.gov/snow/) were used for some of our statistical analyses. This station was located < 2 km from our study forest at an elevation of 2670 m.

3.3.3 Ecosystem process measurements

3.3.3.1 Below-snow soil respiration

During spring of 2011 and 2012 we measured soil respiration below the snowpack using the diffusion gradient method outlined in Sommerfeld et al. (1996). Nine 10-cm diameter stainless steel mesh gas inlets were placed on the soil surface before the snowpack developed in control and dust-addition treatments (18 inlets total). These inlets were routed to a central gas collection location between the plots using 0.64-cm diameter tubing (Type 1300, Synflex Specialty Products, Mantua, Ohio). Collection tubes were capped with stainless steel gas-tight removable fittings (Swagelok Co., Solon, Ohio, USA). At

sampling time, tubes were uncapped and attached to a small gas pump (NMP850, KNF Neuberger, Inc., Trenton, NJ, USA) via an inline flowmeter (Gilmont Instruments, Barrington, IL, USA). A volume of gas equal to the volume of the tubing was pumped away, and the pump was then isolated from the tubing. The gas in the tube was then sampled using a syringe (Becton, Dickinson and Company, Franklin Lakes, NJ, USA) through a septum (Hamilton Co., Reno, NV, USA) upstream of the pump and transferred to a pre-evacuated glass vial (Labco Exetainer, Labco Ltd., Lampeter, Ceredigion, UK). Three samples of air were collected using the syringe above the snowpack on each sampling date. Upon return to the laboratory, the CO_2 mole fraction in these samples was measured by injecting 0.5 ml of gas into a closed-loop infrared gas analyzer system (LI-7000, Li-Cor Biosciences Inc., Lincoln, NE, USA; see Moyes et al. 2010). Soil respiration rate was calculated using Fick's law with adjustments for snowpack properties by

$$F = \rho_a \eta \tau D \frac{dC}{dz} \tag{3.1}$$

where ρ_a is the molar density of air (adjusted for temperature and pressure), η and τ are the porosity and tortuosity of the air-filled snowpack, respectively, D is the molecular diffusivity of CO_2 in air (adjusted for temperature and pressure following Massman 1998), and C is the mole fraction of CO_2 at height z (see Bowling and Massman 2011).

3.3.3.2 Warm-season respiration

During the snow-free season we measured soil respiration from polyvinyl chloride collars roughly twice per month using a Li-Cor 6400 infrared gas analyzer with a 6400-09 soil chamber attachment. In 2010, the unreplicated pilot plots were measured (n = 10 locations per treatment), and in 2011 and 2012 four measurements were made in all six plots (n = 12 locations per treatment). Collars were inserted about 2.5 cm into the soil surface in an evenly-spaced line down the middle of each plot and were moved by 1 meter in a random direction at the start of each new season. Measurements of T_{soil} at 5 and 15 cm depth (thermocouple probe, Omega Engineering Inc., Stamford, CT, USA), and surface θ were taken at each soil respiration collar at the same time (Campbell Scientific CS-620 probe).

3.3.3.3 Warm-season xylem water potential

In spring 2010 we selected 18 mature subalpine fir trees in the pilot plots (n = 9 per treatment) and measured predawn and midday ψ using a pressure chamber (PMS Instrument Co., Albany OR, USA) roughly twice per month until the fall. In 2011 we added three subalpine fir saplings (DBH < 2cm) in each plot for measurement of ψ (n = 9 per treatment). In 2011 and 2012 we measured predawn and midday ψ in these saplings on the same schedule as soil respiration measurements. We continued in these years to measure a subset of the mature subalpine firs (n = 5 per treatment), but less frequently than

in 2010. We did not control for the horizontal area of the rooting zone of these trees, and the roots of some measurement trees may have extended beyond our plot boundaries.

3.3.3.4 Litter bag mass loss (decomposition rate)

In fall of 2010, we collected needle litter from canopy conifers at the site on tarps and oven dried. Five grams of litter were then sewn into nylon and fiberglass mesh litter bags (0.2mm nylon mesh bottom, 1.7mm fiberglass screen top). On October 15, 2010, at 36 locations in the study forest (18 per treatment), we placed a group of 5 litter bags on the forest floor and secured them with metal staples (n = 90 bags per treatment). From the time of placement until spring 2013, we returned to each litter bag group immediately following spring snowmelt and in late fall (~ Oct 15) each year to collect one bag per location. Collected bags were placed in a drying oven for 48 hours and decomposed litter was carefully removed from the bag and weighed. Bags that were disturbed or damaged by animals (n = 26) were excluded from analysis.

Mass loss was described using an exponential decay model with two pools, one fast and one slow cycling (Adair et al. 2008, Harmon et al. 2009). This model took the form

$$L_t = L_{0f}e^{-\lambda_f t} + L_{0s}e^{-\lambda_s t} \tag{3.2}$$

where L_t is the fractional litter remaining at time t, L_{0s} and λ_s are the initial fraction and decay constant of the slow-cycling litter pool, λ_f is the decay constant of the fast-cycling litter pool, and L_{0f} is the initial fraction of the fast-cycling pool and is defined as $1 - L_{0s}$. We fit this model to our data using the nonlinear least-squares method (Adair et al. 2010).

3.3.4 Hemispherical photos

On several dates in 2012, we took hemispherical photographs of the canopy at all SWE measurement, litter bag, and warm-season soil respiration locations, and at each soil sensor profile. For each photo, the camera tripod was adjusted to 1 m above the snow or soil surface, the camera lens was leveled, and upward looking photos were taken with a circular fisheye lens (8 mm F3.5 EX DG Circular Fisheye, Sigma Corporation, Kanagawa, Japan). In order to capture the with- and without-leaves canopy structure, we took photos at SWE measurement locations on April 24 (no leaves), at soil profiles and litter bag/respiration locations on July 17 (after leaf out) and again at soil profiles on October 17 (after leaf fall). We analyzed each digital photo using Gap Light Analyzer v2.0 software (Frazer et al. 1999). For each photo, this software calculates a value of canopy openness, the percent of a 180° sky view not occupied by canopy, and direct-beam transmissivity, the percentage of above-canopy radiation transmitted to the forest floor. The size of our ψ measurement trees and their variable rooting area prevented meaningful characterization of canopy structure above them.

3.3.5 Statistical analysis

We compared the effect size of dust versus canopy structure on snowpack ablation rate by fitting a simple statistical model to our data. In this model, parameters for incoming solar radiation (measured as PAR), air temperature, and new snowfall (as SWE measured at the Brighton SNOTEL site) were used to predict the change in SWE between one measurement date and the next. The basic form of this model was

$$dSWE_{it} = \beta_0 + \beta_1 AirT_{it} + \beta_2 Snow_{it} + \beta_3 Pin_{it} + \epsilon_{it} \tag{3.3}$$

where $dSWE_{it}$ was the change in SWE measured at location i and time t, $AirT_{it}$, Pin_{it}, and $Snow_{it}$ are the integrated air temperature, incoming solar radiation, and snowfall measured at time t, respectively, $\beta_{0...3}$ were the intercept and regression coefficients for these independent variables, and ϵ_{it} was the residual error. We fit this model to our SWE measurements using least-squares regression. Because we expected the influence of these independent variables to vary according to treatment and canopy structure, we also tested the significance of interaction terms between our independent variables and treatment (control or dust-addition), canopy radiation transmission (high or low), and canopy openness (open or closed).

We used multilevel linear model analysis of variance (ANOVA) to test for differences in SWE during the accumulation period, which we defined as the first four SWE measurement dates of the spring field season. We compared differences in SWE between treatments, canopy groups, and years with this technique. Similar multilevel model ANOVA tests were used for comparisons of soil respiration rate and xylem water potential.

3.4 Results

The Wasatch Mountains, including our study site, experienced three very different winters during the years of our snowpack manipulation experiment (Fig. 3.1). In 2011, this region had a near record breaking large snowpack, and in 2012 it had a near record breaking small snowpack. The 2010 snowpack was intermediate, and peak SWE was similar to the long-term average. These differences allowed us to compare our snowpack and ecosystem process measurements between widely contrasting years.

3.4.1 Snowmelt manipulation

Our dust-addition treatment successfully increased the load of particulate matter in the snowpack beyond the ambient snowpack dust load at the site. We measured the total particulate content of the snowpack in an adjacent clearing (no canopy present) and in control and dust-addition treatments and found that our dust additions roughly tripled the mass of particulates found in the clearing and doubled the load found in the control snowpack (Table 3.1). A large proportion of the particulate matter found in both control and dust-addition snowpacks was forest litter probably derived from the canopy (Table 3.1).

A similar proportion of the total particulate loading of the clearing snowpack in 2012 was also forest litter (Table 3.1).

Our experimental treatment resulted in small differences in measured SWE and the ablation rate between the control and dust-addition treatments (Fig. 3.2a, b, and c). During the accumulation period of the 2010 pilot study, there was significantly less SWE ($p < 0.01$) in the dust-addition treatment when compared to the control (Fig. 3.2a). During 2011 and 2012, however, the difference in SWE between treatments was indistinguishable (Fig. 3.2b and 3.2c).

There was a large range of variability in canopy structure in our forest, and this appeared to influence snow accumulation and ablation rate. Canopy openness, the percentage of a 180° sky view not occupied by the tree canopy, ranged from 16.7 to 50.7%. Canopy transmission, the percentage of above-canopy solar radiation (adjusted for seasonal solar zenith) transmitted to the forest floor, ranged from 11.5 to 68%. Mean values for each measurement location type and season are given in Table 3.2. There was greater SWE under open and high transmission canopy areas when compared to closed and low transmission canopy areas (Fig. 3.2d, 3.2e, and 3.2f, canopy transmission groups not shown). These differences were statistically significant in 2011 and 2012 ($p < 0.05$ and $p < 0.01$, respectively).

Interannual variations in SWE within our study forest were much larger than the differences between treatments or between canopy groups in any single year. All pairwise comparisons of accumulation period SWE between individual years showed significant differences in SWE ($p < 0.0001$).

3.4.2 Empirical ablation model

Visual inspection of the spring SWE depletion curves in 2010–12 revealed similar ablation rates for control and dust-addition treatments (Fig. 3.2a, b, and c), but indicated a slightly higher rate in the open compared to the closed canopy groups (Fig. 3.2d, e, and f). We tested whether this difference was significant by fitting a statistical model of snowpack ablation to our SWE measurements for 2011 and 2012 (Fig. 3.3). Without interaction effects, our model fit the data reasonably well in 2011 ($R^2 = 0.70$) and 2012 ($R^2 = 0.78$). Air temperature, snowfall, and incoming solar radiation were all significant predictors of variation in *dSWE* in both years ($p < 0.002$).

Dust treatment and canopy structure both significantly impacted the ablation rate during at least part of the experiment. We tested several interaction terms in our statistical model to test whether the differences between treatment and canopy structure groups were significant. There were significant differences in ablation between the control and dust-addition treatments in 2011 ($p < 0.02$). In 2012, however, the treatments were not statistically distinguishable. We also assigned each measurement location to an open or closed canopy and a high or low canopy transmissivity group and tested these groups as interactions in the model. Areas with high canopy transmissivity had higher ablation rates in

2011 ($p < 0.05$) and in 2012 ($p < 0.001$). Areas beneath an open canopy had higher ablation rates in 2011 ($p < 0.02$) and in 2012 ($p < 0.001$).

3.4.3 Soil temperature and water content

Average θ and T_{soil} were similar between treatments during 2011 and 2012. We constructed 95% confidence intervals around the mean θ and T_{soil} data from all sensors in control or dust-addition plots and from all sensors classified as open and closed canopy (Fig. 3.4 and 3.5). During the majority of each year, these intervals overlapped, indicating that the means of θ and T_{soil} were not statistically different between treatment or canopy groups. There were some minor differences in the dynamics of these variables between treatments or canopy groups that are detailed in the Discussion section.

When we examined the seasonal mean values of θ and T_{soil} over the 3 years of our study, we did find some consistent patterns. During winter (Jan., Feb., Mar.), θ at all depths was higher in the dust addition treatment (compared to control) in 2011 and 2012 (Fig. B.1). Soils were also wetter at open-canopy sensors during winter 2011 at all depths (Fig. B.1). In the warm-season (Jul. and Aug.), dust-addition soils measured at 20 and 60 cm depths were slightly wetter than the control treatment during 2011 and 2012. Compared to measurements beneath closed canopies, warm-season θ in the open (all depths) was slightly lower in all years measured (Fig. B.1).

Winter T_{soil} showed few differences between treatment and canopy groups, except that T_{soil} in open canopy locations was lower than in closed locations in 2012 (Fig. B.2). During the warm-season of 2010, 2011, and 2012, T_{soil} was similar between control and dust-addition treatments at all depths but 20 cm. Warm season T_{soil} at 5 and 60 cm depths was higher beneath open canopies compared to closed in all years. In 2011, 20 cm sensors in the dust-addition and open canopy groups were significantly cooler than their control or closed canopy counterparts.

Overall, interannual variability was the largest driver of variability in θ and T_{soil} (Fig. B.1 and B.2). The large snowpack year, 2011, had the highest winter θ and the highest warm-season θ. In the warm-season, soils were drier by a substantial amount in the lowest snowpack year, 2012. This pattern held at all depths and whether sensors were grouped by treatment or canopy structure. Winter T_{soil} was highest beneath the large 2011 snowpack and considerably cooler in 2010 and 2012. Warm season T_{soil} was highest in 2012 at almost every depth and treatment or canopy grouping level.

3.4.4 Ecosystem processes

Ecosystem processes showed few significant differences between control and dust-addition treatments in 2010, 2011, or 2012. Below-snow soil respiration was not significantly different between control and dust-addition treatments in 2011, but respiration was slightly greater in the dust-addition treatment in the winter of 2012 ($p = 0.05$, Fig. 3.6). During the warm season, there were no significant differences in

soil respiration rate between treatments in any year (Fig. 3.7). Xylem water potential (ψ) did not vary in response to the dust treatment (Fig. 3.8). Neither saplings nor mature firs showed significant differences in xylem ψ between control and dust-addition treatments in any year tested.

The two pool decay model fit our litter bag mass loss data well, and there were small differences in litter decomposition between the treatments (Fig. 3.9). The λ_f and λ_s for the control locations were 6.0×10^{-3} and 6.7×10^{-5}, respectively, and 7.8×10^{-3} and 8.2×10^{-5} for the dust-addition treatment, respectively. The proportion of litter mass in the slow-cycling pool was slightly higher in the dust-addition treatment (82% vs 77%) and the dust-addition bags lost slightly less mass over the first winter.

There were significant differences in ecosystem processes between years. Below-snow soil respiration was significantly higher in 2011 than in 2012 (Fig. 3.6, $p < 0.0001$). Warm season soil respiration was significantly lower in 2010 than in the two following years ($p < 0.01$), but respiration rates in 2011 and 2012 were not significantly different from each other (Fig. 3.7). It is important to note that the respiration was measured at differing and fewer locations in 2010. Sapling predawn water potential was slightly lower in 2012 ($p < 0.001$) as was sapling midday water potential ($p < 0.01$). Water potential values of mature firs did not differ significantly between years (Fig. 3.8).

3.5 Discussion

3.5.1 Snow accumulation and melt

There were few statistically significant differences in SWE accumulation or ablation rate between the control and dust-addition treatments. The primary radiative effect of dust or other impurities in snow is to lower the shortwave albedo of the snow surface and thereby increase its absorption of solar radiation. Secondary effects of dust, such as increases in snow grain size, exposure of below-snow surfaces, and changes in surface roughness also impact snowpack energy balance during the ablation season (Hansen and Nazarenko 2004, Fassnacht et al. 2009). Our dust-addition treatment likely altered the energy balance of the snowpack by one or more of these mechanisms. Several possible reasons may explain the smaller than expected differences in ablation rate. The first possibility is that the added dust did not significantly change the energy balance of the snowpack relative to the control. Another possibility is that added dust had a smaller effect on snowpack energy balance than did variations in snowpack energy balance resulting from differences in canopy structure within our forest. A third possibility is that higher accumulation and/or sublimation rates at open-canopy locations in our forest compensated for the higher ablation rate in the dust-addition treatment. These three explanations are discussed below.

Our snowpack manipulation increased the dust load relative to the control, but may have had a smaller than expected effect on albedo. When we measured the mass of particulate matter in our snowpacks near the close of each ablation season, the mass in the dust-addition treatment exceeded the control by a factor of two (Table 3.1). The control snowpack, however, had roughly double the particulate matter found

in a nearby clearing. A large percentage of the total particulate matter in the control and dust-addition treatments was composed of forest litter in 2011 (24–32% litter) and 2012 (64–70% litter), indicating that particles other than our added dust probably impacted the snow surface albedo in both treatments. Snowpack albedo is often lower in forests when compared to clearings (Melloh et al. 2002), and a number of prior studies have indicated that forest litter is highly effective at reducing the albedo and increasing the ablation rate of subcanopy snowpacks (Hardy et al. 2000, Melloh et al. 2001, Winkler et al. 2010, Pugh and Small 2012).

Significant variation in ablation rate was explained by canopy structure and its effect on radiative energy balance. In alpine or other snowpacks without overstory vegetation, net shortwave radiation is commonly the most significant component of snowpack radiative energy balance during the spring ablation season (Marks and Dozier 1992). In forested areas, incoming shortwave radiation is intercepted by the canopy (shading), and a portion of this absorbed energy is re-emitted down to the snowpack as thermal radiation (longwave irradiance). The relative importance of shading and longwave irradiance to subcanopy snowpack energy balance depends greatly on canopy structure and solar angle. In forests with open or discontinuous canopies, such as can be found in an aspen forest in winter, there is less longwave irradiance to the snowpack from the canopy, but greater transmission of shortwave radiation through the canopy. This is particularly true in late spring as sun angle increases (Pomeroy and Dion 1996, Hardy et al. 2004, Pomeroy et al. 2008, Lawler and Link 2011). Accordingly, we found higher ablation rates under open canopy locations in our forest during the spring melt (Fig. 3.3). As canopy closure increases, longwave irradiance also increases, and under some conditions, higher canopy longwave irradiance compensates for declines in shortwave transmission and becomes the major contributor of snowpack ablation energy (Link and Marks 1999a, Sicart et al. 2004). Our study forest had a heterogeneous and fairly open canopy structure, and it is probable that this led to high variability in the radiative energy balance of our snowpack. The albedo effect of dust acts primarily in the solar portion of the spectrum. If a large portion of the energy available for snowpack ablation in our forest came from canopy longwave irradiance, our dust-addition treatment would have been less effective in perturbing snowpack energy balance.

The potential for snow interception, sublimation, and redistribution also varied with canopy structure in our forest. Forest canopies intercept snowfall and facilitate water loss through redistribution and sublimation (Hedstrom and Pomeroy 1998). Consequently, it is common to find greater snow accumulation beneath forest canopy openings relative to closed canopies (Hardy et al. 1997, Koivusalo and Kokkonen 2002). Our data clearly showed that more SWE accumulated beneath an open canopy (Fig. 3.2d, 3.2e, and 3.2f), indicating less snowfall interception, sublimation, and/or redistribution in these areas. If we assume that dust-addition lowered snowpack albedo and thus increased the ablation rate in our study forest, the effect would be highest in these same open areas where greater shortwave

radiation was available to melt snow. It is possible that higher accumulation rates compensated for the higher ablation rate in dust-addition locations, making differences between treatments difficult to observe. Similar compensatory effects have occurred in other forest snowpack studies. Biederman et al. (2012) found lower snow interception during the grey phase in a mountain pine beetle impacted forest stand (presumably more open), but this was compensated for by higher sublimation rates in these stands.

Our empirical model results support the idea that canopy structure had a similar, or perhaps greater effect on snowpack ablation and accumulation than dust. Though it is important to recognize that our empirical model was not a full energy balance model, it successfully reproduced changes in SWE in our study forest. Snow accumulation was slightly higher in the control than in the dust-addition treatment during the accumulation phase of each year (Fig. 3.3). Given that, on average, control locations had a slightly more open canopy than the dust-addition treatment (Table 3.2), it is unclear whether this occurred due to the effects of dust or canopy structure. Later in the spring of 2011 and 2012, the control and dust-addition treatments showed a very similar rate of ablation, indicating that dust had a small effect on snowpack energy balance between treatments (Fig. 3.3). In both years, however, there were significant differences in snowpack ablation rate below high and low transmission canopies, indicating that differences in canopy structure led to differences in snowpack energy balance. Snowpacks below more open canopies also had significantly greater snow accumulation during early spring, probably due to low canopy interception. These two effects together resulted in similar timing in the disappearance of snow below these contrasting canopy types (Fig. 3.3). This is in line with other studies showing greater accumulation and more rapid snow ablation beneath openings in conifer forest canopies (Hardy et al. 1997, Koivusalo and Kokkonen 2002, Musselman et al. 2012a).

Our results indicate a high dependence of snow accumulation and ablation rates on canopy structure, and highlight the need for more detailed study of subcanopy dust-on-snow effects. Though this is, to our knowledge, the first such dust manipulation in a forested area, several studies have attempted to use distributed hydrological models to calculate the effect of dust deposition on snowpack dynamics and spring runoff across large areas of the western U.S. (Painter et al. 2007, 2010). Models used in these studies employ realistic, full energy balance calculations for forested areas, but the driving data for overstory vegetation, subcanopy albedo, and their effects on snowpack energy balance tend to be coarsely defined. The VIC model, for example, uses a 1 km vegetation grid, with leaf area index (LAI) specified for the vegetated fraction of each grid cell using a global LAI database derived from 1981–1994 averages values (Liang et al. 1994, Myneni et al. 1997, Gao et al. 2010). Solar radiation attenuation, longwave irradiance, snow interception and redistribution, and other canopy-dependent snowpack energy and mass balance parameters are calculated based on this gridded data. With realistic estimates of subcanopy solar and thermal radiation, accurate estimates of snowpack dynamics can be made at point or distributed

scales (Link and Marks 1999a, 1999b, Musselman et al. 2012b), but obtaining or estimating this data at or beyond the watershed scale is not an easy task. Our results suggest that even under open, heterogeneous canopy cover, which is common in western U.S. mountains, the canopy may interfere with the strong effect that dust has on snowpack ablation in other areas.

The albedo of subcanopy snowpacks plays an underappreciated role in determining their radiative energy balance. A sensitivity study by Sicart et al. (2004) found that when subcanopy snow albedo is high, the radiative energy balance of the snowpack changes little in response to variations in canopy density. At low albedos (< 0.5), however, the radiative energy balance of the snowpack becomes sensitive to increases in shortwave transmission through a canopy. Thus, aeolian dust deposition should be expected to alter the radiative energy balance of some forests. A number of studies provide interesting context, but many of these have taken place in disturbed forests. In the western U.S., where the mountain pine beetle is currently impacting forests at a large scale, Pugh and Small (2012) found that high rates of litter deposition in beetle impacted conifer forests lowered snowpack albedo. They estimated that this increased the snowpack ablation rate to a greater extent than other radiative or atmospheric effects resulting from tree death in the forest. Gleason et al. (2013) found a 200% increase in net shortwave radiation at the snowpack surface in a recently burned conifer forest. This change was due to the combined effects of higher solar radiation transmission by the canopy and lower snowpack albedo due to the deposition of burned woody debris. So, though it is established that changes in albedo impact the energy balance of a subcanopy snowpack, the conditions under which this results in higher ablation rates are not documented in a broad number of forest types, with notably few studies in undisturbed forests. Without more detailed, spatially explicit data on canopy structure and subcanopy snowpack albedo, it may remain difficult to predict the effect of aeolian dust deposition on the subcanopy snowpacks at a broad spatial scale.

3.5.2 Impacts on the soil biophysical environment

Our snowpack manipulation had little effect on the soil environment. There were no significant differences between mean θ and T_{soil} in the control and dust-addition treatments (Fig. 3.4 and 3.5), which is consistent with the small effects our treatment had on snowpack dynamics during the spring. Differences between mean θ and T_{soil} in open and closed canopy groups were also not significant. Despite this, a few interesting patterns emerged when comparing the dynamics of θ and T_{soil} between groups. Winter θ was higher in the dust addition treatment (compared to control) and higher in open canopy locations (compared to closed, Fig. B.1). Snowpacks that absorb greater solar radiation, whether due to lower albedo or higher incident radiation (under a more open canopy) can experience winter melt events in which liquid water reaches the soil, but this is more likely in areas where snowpacks are at or near an isothermal state during winter (Bales et al. 2011). We view it as somewhat unlikely that winter melt events of this type would occur between January and March in our high-elevation forest. Our

snowmelt results indicate greater radiative exposure and earlier snowmelt in areas below an open canopy, and this may also have led to greater evapotranspiration and earlier declines in surface θ during the spring (Fig. 3.4) (Molotch et al. 2009, Bales et al. 2011). These open canopy areas also had slightly lower warm-season θ (Fig. B.1). Surface T_{soil} began to increase from a near-zero level below the snowpack at or near the moment snowcover disappeared, consistent with other observations in snow-covered ecosystems (Lundquist and Lott 2008). This occurred a few days earlier in the dust-addition treatment (compared to the control), and in open locations (compared to closed), during 2011 and 2012 (Fig. 3.5), perhaps indicating an earlier completion of ablation, on average, in these groups. In the warm-season, T_{soil} was higher beneath an open canopy than a closed canopy, again suggesting greater radiation exposure in these areas.

Interannual variability in θ and T_{soil} was larger than any difference due to our dust treatment or canopy structure. The large snowpack year, 2011, had the highest winter and warm-season θ of any year (Fig. B.1). Warm season θ was lowest, by a substantial amount, during 2012, the year with the smallest snowpack. These patterns held at all depths and when sensors were grouped by treatment or canopy structure (Fig. B.1). Average winter T_{soil} was also highest in 2011, suggesting that the large snowpack more effectively insulated the soil from temperature fluctuations at the snow surface (Zhang 2005). Warm-season T_{soil} was highest in 2012 following the lowest snow year (Fig. B.2). This suggests that either low water availability limited evapotranspiration or that air temperature during July and August 2012 was warmer than other years.

3.5.3 Impacts on ecosystem processes

Differences in ecosystem processes between control and dust-addition plots were not significant in the majority of cases (Fig. 3.7 and 3.8). We believe this to be because there were only small differences in T_{soil} and θ between these treatments. Litter decomposition rate was slightly slower in the dust-addition treatment (Fig. 3.9), but there were no consistent differences in T_{soil} or θ between the treatments that explained this.

There were significant differences in ecosystem processes between years. Interannual variability in snowpack and the soil environment appeared to be linked, and we interpret this to mean that differences in θ and T_{soil} led to different soil respiration rates and xylem ψ between years. Of the three winters observed in our experiment, soils were warmest and wettest below the 2011 snowpack, and the highest below-snow soil respiration occurred in this year. A number of studies have highlighted that significant amounts of CO_2 are respired from soil below seasonal snowpacks and that these fluxes may vary significantly in response to changes in the below-snowpack soil environment (Monson et al. 2006a, 2006b, Liptzin et al. 2009, Aanderud et al. 2013). Snow-molds, for example, are a group of fungi that colonize forest litter below Rocky Mountain (and probably other) snowpacks in the spring and are highly sensitive to small

fluctuations in temperature (Schmidt et al. 2009). Soil microbial physiology such as this may explain the higher below-snowpack respiration rate we observed in 2011.

Of the warm-seasons observed in our experiment, soils were warmest and driest after the 2012 snowpack. This did not impact on soil respiration rates, but did influence water availability for trees. High T_{soil} and low θ in the warm-season of 2012 resulted in predawn and midday sapling ψ that was significantly lower in 2012. This result agrees with other studies in our region indicating that years with lower SWE and earlier snow melt result in diminished soil water availability for vegetation (Molotch et al. 2009, Hu et al. 2010)

3.6 Conclusions

We artificially increased the load of aeolian dust in a subcanopy mountain snowpack. This dust-addition treatment did not substantially alter snow accumulation, ablation rate, and the timing of snowmelt in our study forest. The influence of the canopy, through the combined effects of snow interception and shading, overwhelmed the effects of dust on snowpack albedo and radiative energy balance. Both SWE amount and the ablation rate were significantly greater beneath open as compared to closed canopy areas in our study forest, supporting this explanation.

Dust addition produced no significant effects on the soil environment or on ecosystem processes. There were, however, significant differences in ecosystem processes between years, and this interannual variability was larger than any within-year effect of dust or canopy. Interannual differences in soil temperature and soil water content were in the direction expected given the year's snowpack size and melt timing. The resulting variation in the soil environment appeared to drive the differences in ecosystem processes we observed.

The limited efficacy of our dust manipulation in this forest suggests that the impacts of aeolian dust on snowpack energetics are complex and likely to be site specific. In this system, within-forest and interannual variation in snowpack mass and energy balance were larger than the effect of dust. Both field and modeling studies of aeolian dust's impacts on snowpack ablation would benefit from better representation of canopy and its influence over snowpack energy balance. Future research on this topic should target interactions between canopy structure and snowpack albedo to better understand the conditions under which dust deposition may influence ecohydrological processes.

3.7 Acknowledgments

The authors wish to thank Mark Blonquist, Andrew Moyes, Allison Chan, Raili Taylor, LaShaye Ervin, Tara Trammel, Meghan Avolio, Ryan Bares, Ryan Dillingham, Dave Eiriksson, Laurel LeGate, and Michael Bernard for donating valuable time to fieldwork. Discussions with Tom Painter helped greatly with experimental design and interpretation of results. Thanks to Jim Steenburgh and Tim Bard-

sley for providing helpful comments on early versions of this manuscript. Randy Doyle (Brighton Mountain Resort), Park City Mountain Resort, and Royal Street Holdings permitted and facilitated access to the Hidden Canyon study site. Ed Grote, Paul Gettings, and Kevin Hultine assisted with technical matters. Mark Miller (NPS), Lisa Bryant, Dave Whitaker, and Randy Beckstrand (BLM) were helpful in sourcing the dust used in this experiment. The University of Utah Global Change and Sustainability Center, U.S. Department of Energy (grant DE-SC0005236), and the University of Utah SEED grant program each supported a portion of this research.

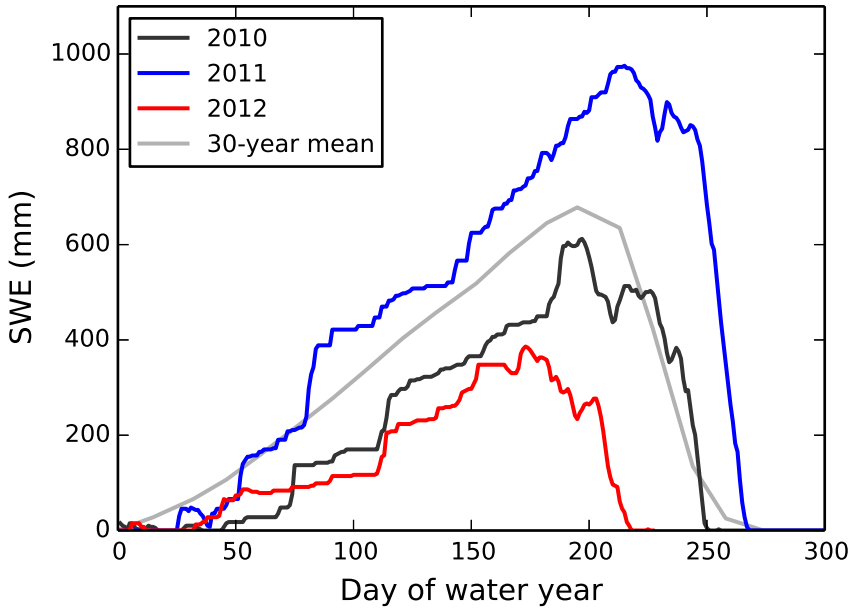

Figure 3.1. Snow water equivalent at the Brighton SNOTEL site, located about 2 km from Hidden Canyon, for the study years 2010 to 2012. The multiyear mean for the site was calculated at 2-week intervals for the years 1971–2000 by the NRCS Snow Survey and is plotted for reference in gray.

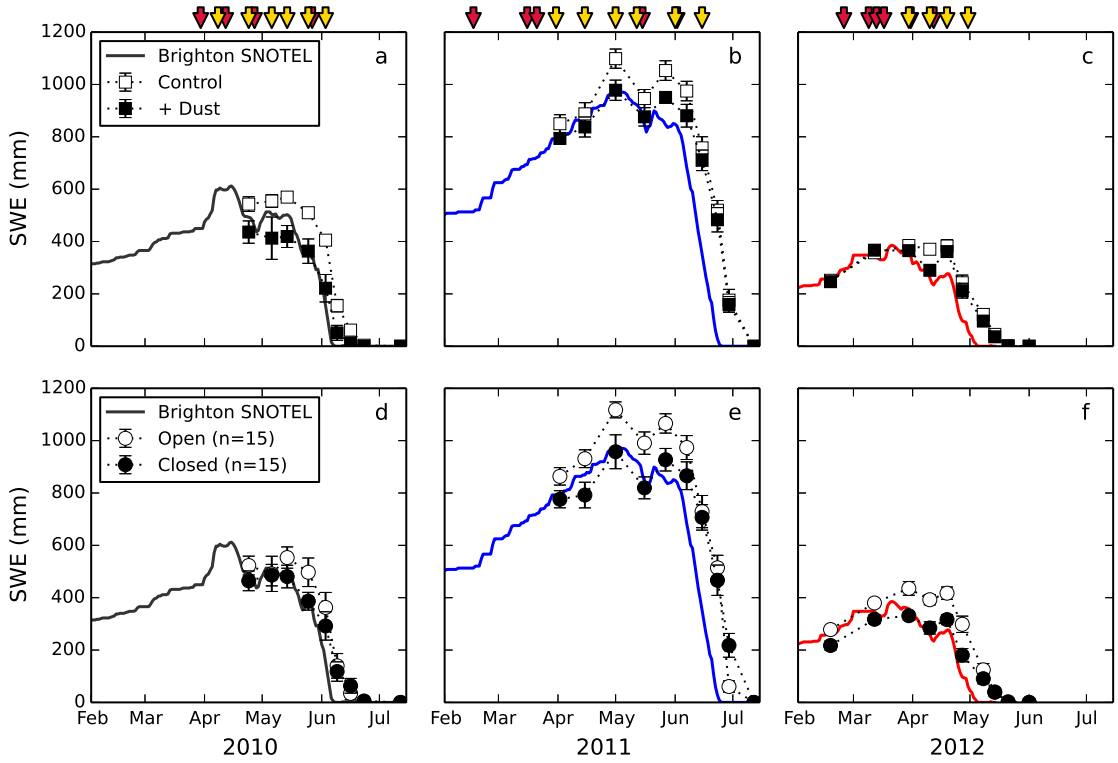

Figure 3.2. Snow water equivalent during 2010, 2011, and 2012. Measurements made during this study were grouped and averaged in two ways in this figure. Panels (a), (b), and (c) compare the means of measurements made in control versus dust addition treatment plots (n = 18 per treatment). Panels (d), (e), and (f) compare the means of measurements made in open verus closed canopy locations in the forest (n = 15 per group, 6 median locations were excluded). Red arrows indicate the timing of natural dust events and yellow arrows indicate experimental dust additions. SWE observations from the Brighton SNOTEL site is shown for reference (as in Fig. 3.1).

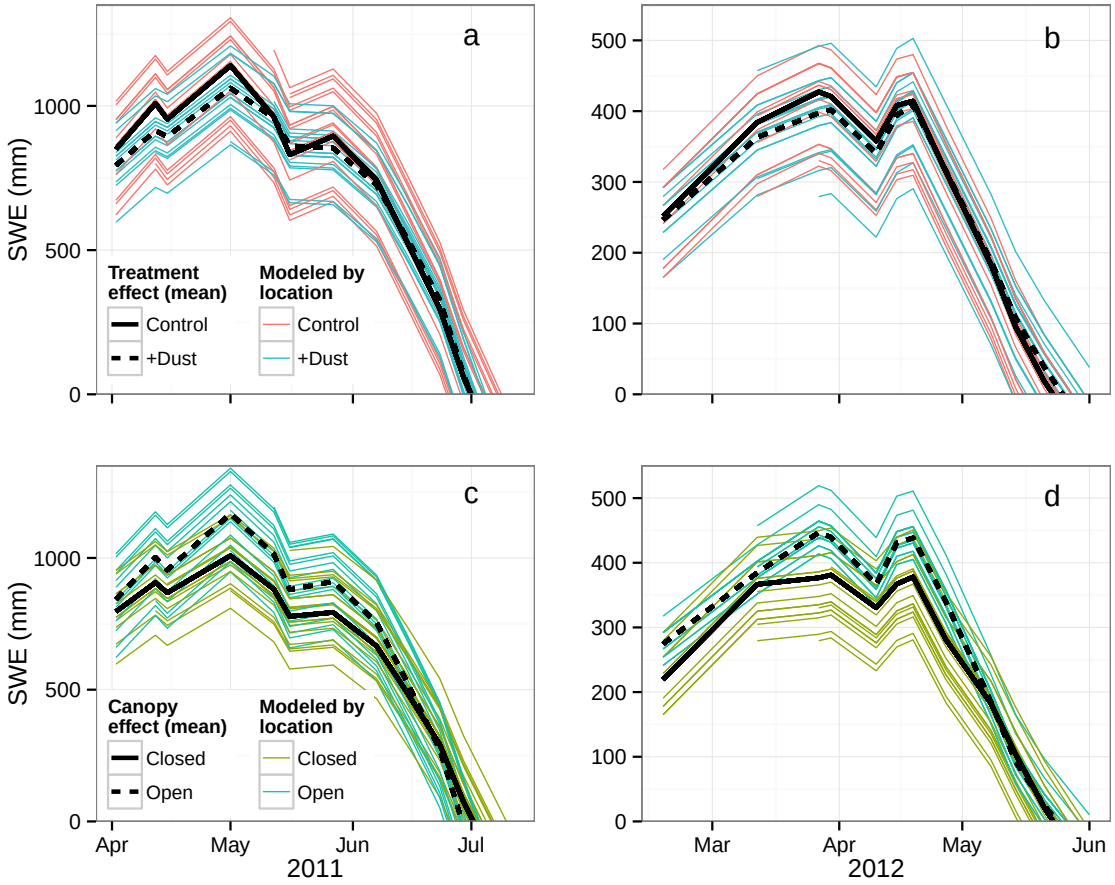

Figure 3.3. Modeled SWE during the spring of 2011 in panels (a) and (c), and the spring of 2012 in panels (b) and (d). Modeled SWE values were based on measured SWE during at the start of the experiment and linear model estimates of *dSWE* fit using measured SWE and climate data from the site. The model start day is different in 2011 and 2012, and two variations of the model were tested in each year. The model used in panels (a) and (b) includes a treatment interaction effect, and in the panels (c) and (d) includes a canopy transmission interaction effect. Thick black lines represent mean SWE of all locations in each treatment or canopy group, beginning at each group's mean SWE on the starting day. Finer colored lines are modeled for individual locations, beginning at each location's measured SWE on the starting day.

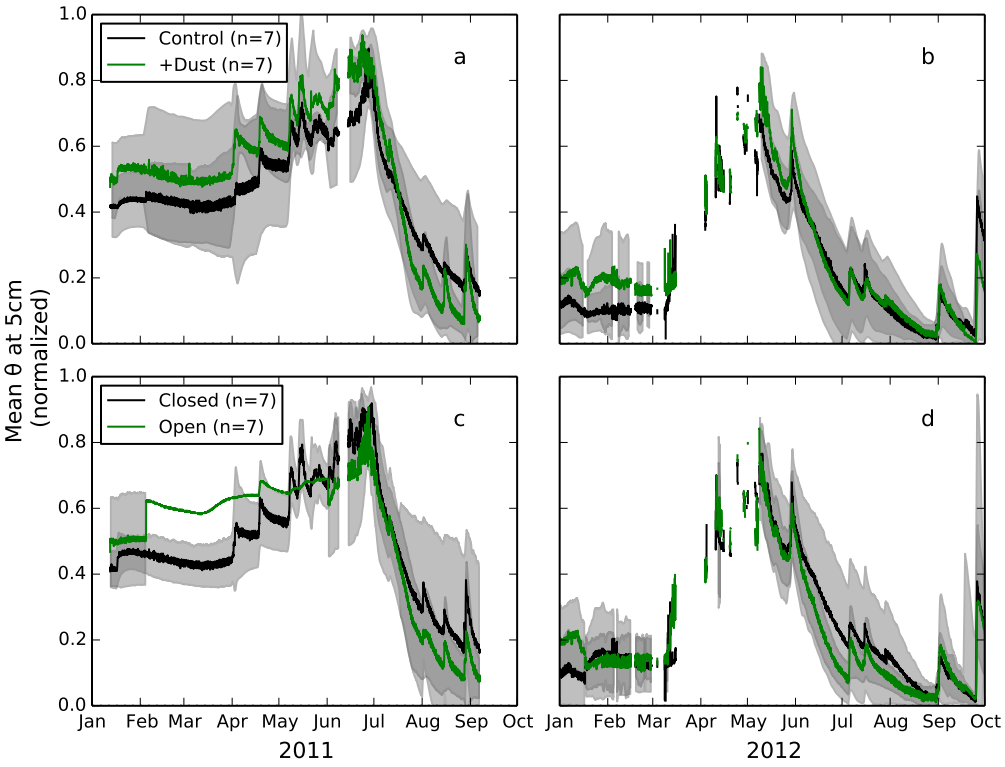

Figure 3.4. Comparison of mean volumetric soil water content (θ, normalized) at 5 cm depth in the study plots. Lines represent the mean value of all sensors grouped by treatment in panels (a) and (b) or by canopy openness in panels (c) and (d). Shading represents the 95% confidence interval for data from all sensors used to calculate each mean.

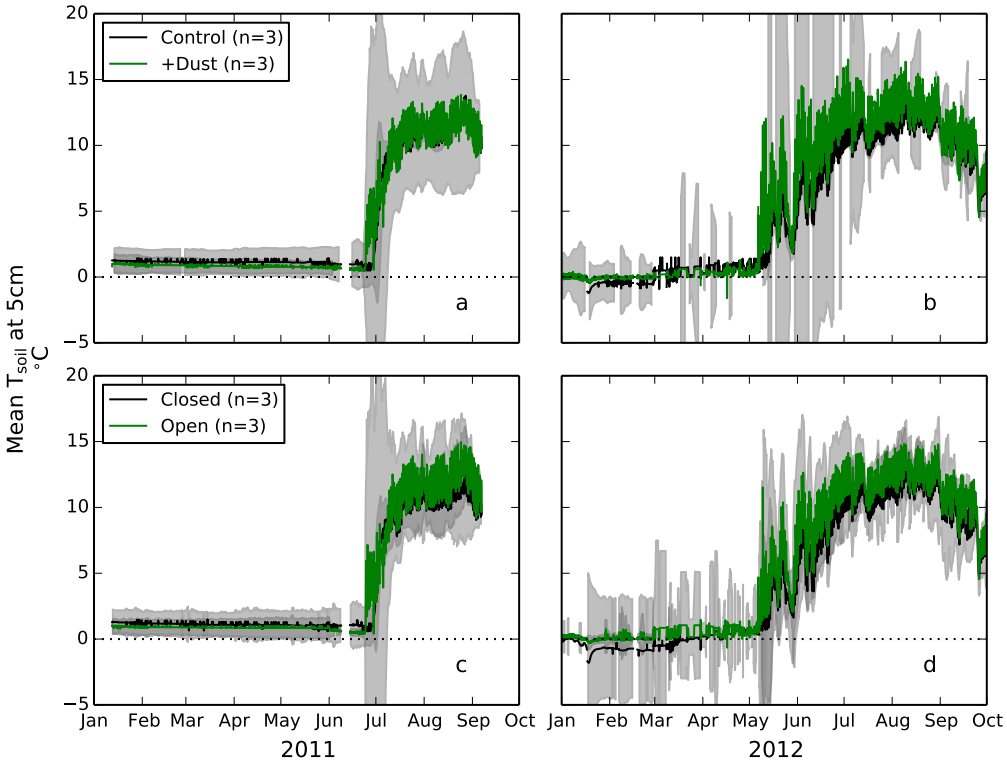

Figure 3.5. Comparison of mean soil temperature at 5 cm depth in the study plots. Lines represent the mean value of all sensors grouped by treatment in panels (a) and (b) or by canopy openness in panels (c) and (d). Shading represents the 95% confidence interval for data from all sensors used to calculate each mean. A dotted line at 0 °C is plotted for reference.

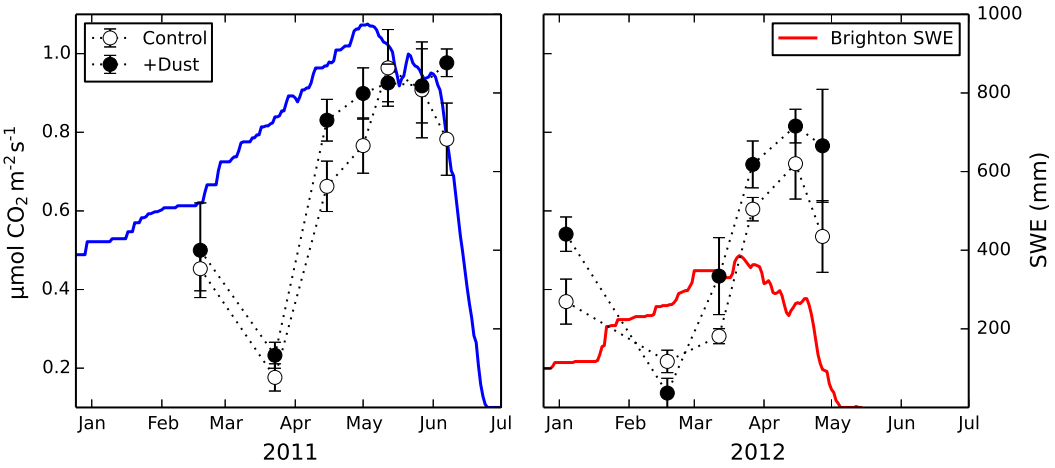

Figure 3.6. Mean values and standard errors of below-snowpack soil respiration rates measured in control and dust addition treatment plots (n = 9 for each treatment, left axis) during sampling dates in 2011 and 2012. These measurements were made using the diffusion gradient method. The Brighton SNOTEL SWE observations during the corresponding time period is shown with colored lines for reference (right axis).

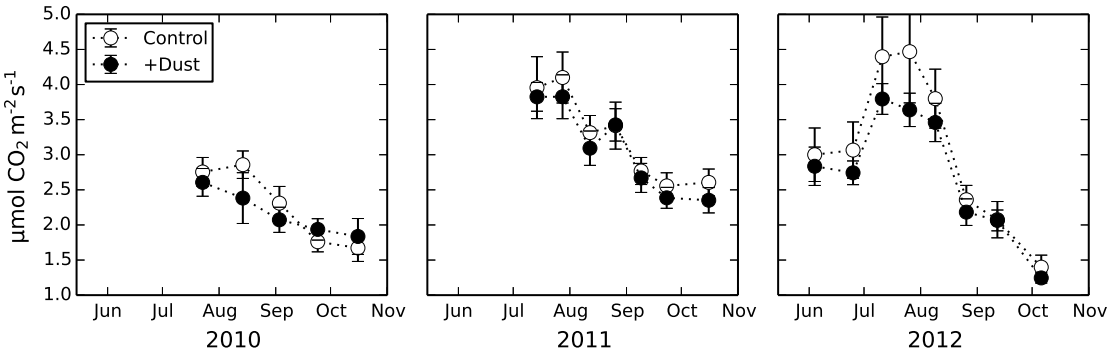

Figure 3.7. Mean values and standard errors of warm season soil respiration rates measured in control and dust addition treatments (n = 18 for each treatment) during 2010, 2011, and 2012 sampling dates. Note the difference in scale with Fig. 3.6.

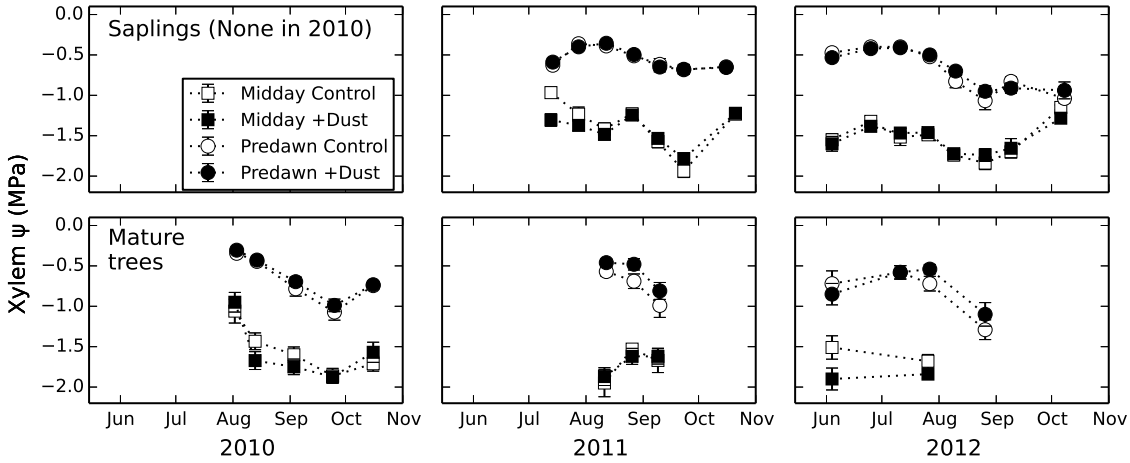

Figure 3.8. Mean values of xylem water potential (ψ) in juvenile and mature subalpine fir measured in control and dust addition treatments (n = 9 for each treatment) during 2010, 2011, and 2012 sampling dates. No saplings were measured in 2010. Means and standard error bars, which are smaller than the symbols in many cases, are shown.

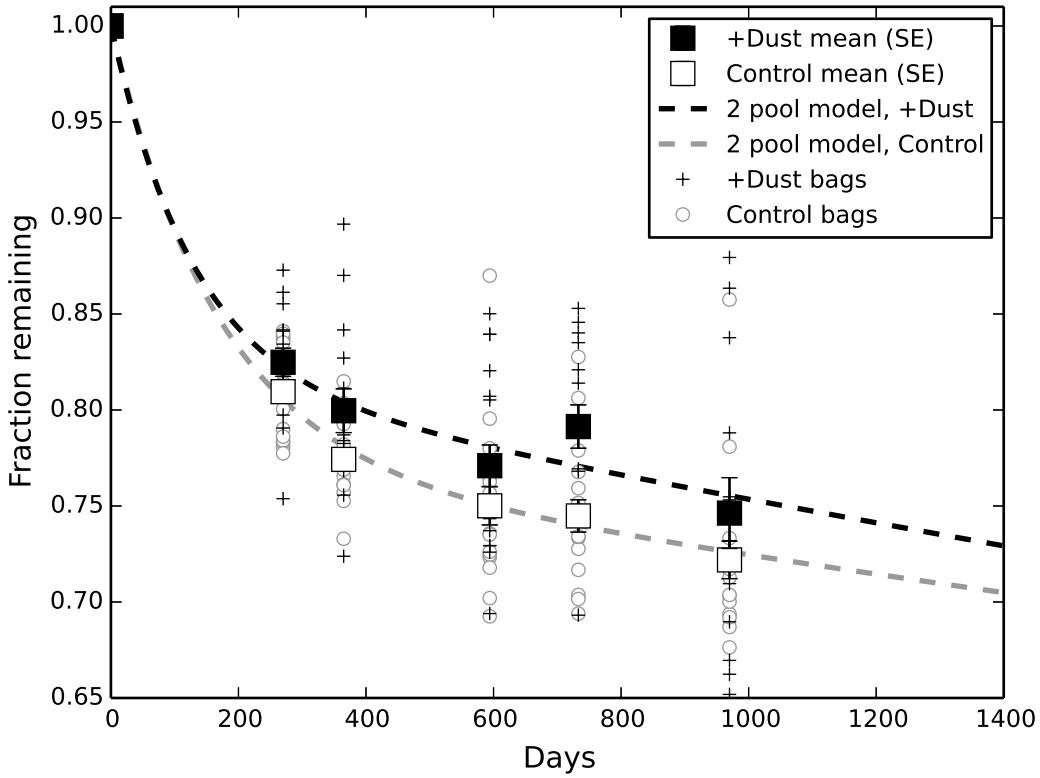

Figure 3.9. Litter bag mass loss between fall 2010 and spring 2013. Individual litter bag samples are shown (small circles or crosses), along with the mean and standard error of control and dust addition treatments for each collection date (n = 18 per treatment per date). The dashed lines were calculated using a 2 pool exponential decay function fit using non-linear least-squares. Decay constants for each pool (λ_f and λ_s) in each treatment are given in the text.

Table 3.1. Snowpack particulate loading for 2011 and 2012 in a nearby clearing (no canopy) and in control and dust-addition treatments (with canopy). Mean total loading in g/m^2 and standard errors are given, along with the mean forest litter (in g/m^2) extracted from the total. Three full-snowpack core samples were taken for each location/year, except in 2011 (explained in the text)

	Clearing		Control		+ Dust	
	Total (SE)	Litter (SE)	Total (SE)	Litter (SE)	Total (SE)	Litter (SE)
2011	18.3 (NA)	NA	32.7 (8.5)	10.5 (5.1)	64.2 (20.2)	15.8 (8.0)
2012	19.1 (6.8)	13.3 (7.5)	38.5 (2.0)	24.9 (4.3)	73.4 (11.6)	49.8 (13.1)

Table 3.2. Means of the canopy structure measurements derived from hemispherical photographs, including the percentage of sky view not occupied by canopy (% Open) and the percentage of incoming solar radiation transmitted by the canopy (% Transmitted) in control and dust-addition treatments. Locations were photographed during time periods with overstory deciduous leaves present, without deciduous leaves present, or both. Standard deviations of the means are in parentheses.

		Control		+Dust	
	Meas. Location	% Open	% Transmitted	% Open	% Transmitted
With leaves	Litterbags	19.4 (5.9)	30.8 (11.7)	21.8 (4.4)	34.8 (11.2)
	Soil respiration	19.6 (6.4)	31.8 (12.5)	20.9 (4.4)	32.5 (11.0)
	Soil profiles	19.6 (4.9)	33.1 (10.1)	22.5 (3.9)	34.9 (8.4)
Without leaves	SWE locations	30.2 (8.8)	45.0 (14.2)	27.7 (5.9)	40.6 (12.6)
	Soil profiles	22.9 (4.5)	34.1 (13.0)	24.4 (7.7)	35.7 (17.3)

CHAPTER 4

FOREST SOIL CARBON STOCKS AND ISOTOPIC COMPOSITION ALONG MOUNTAIN CLIMATE GRADIENTS OF THE INTERIOR WESTERN UNITED STATES

4.1 Abstract

Forest soils and detritus contain globally significant carbon pools, and processes controlling the size of these pools are strongly influenced by variation in temperature and water availability. In the mountains of the interior western U.S., these drivers overlap across the landscape from warm, arid lowlands to cold, mesic highlands. Seasonal snowpacks also vary across the landscape and have large impacts on winter soil temperature and warm-season water availability. We studied the effect of temperature and water availability on the size and isotopic composition of soil and detrital organic matter stocks in conifer forests along climatic gradients in the Wasatch and Uinta mountains of Utah. Carbon stocks generally increased with mean annual precipitation, probably as a result of increasing forest litter inputs. In contrast to similar studies, we found significantly higher accumulation of total and mineral C stocks in warmer, lower elevation forests. Water availability declined in low elevation forests as snowpacks melted earlier and warm season precipitation diminished. We also found evidence of limits on forest productivity at high elevation, including longer periods of subzero air temperature, low soil moisture, and greater stand age. The balance of evidence suggests that decomposition was limited at low and high elevation (by water and temperature, respectively) and that elevational declines in litter inputs were greater than declines in organic matter decomposition. Elevational patterns in the carbon isotope composition of needles and roots suggested low elevation forests were more water limited, but that later-melting snowpacks did little to improve plant water availability. The nitrogen isotope composition of needles, roots and detrital organic matter declined with elevation, indicating greater losses of nitrogen at low elevation. Overall, a small fraction of the variability in stock size and distribution was explained by temperature and water availability. Seasonal snowpacks had an important, though limited, role in moderating these climatic drivers.

4.2 Introduction

Forest ecosystems contain a substantial fraction of the global terrestrial carbon inventory, with the majority of this carbon in soil and detrital organic matter pools (Dixon et al. 1994, Moore and Braswell 1994, Jobbágy and Jackson 2000). The size and structure of these pools reflect the climate under which ecosystem and soil development has taken place over variable timescales (Jenny 1941, Amundson and Jenny 1997). In the interior western U.S., forest ecosystems occur largely in montane areas where complex topography leads to high spatial variability in climate, vegetation, soils, and ecosystem processes (Houghton and Hackler 2000, Schimel et al. 2002). Additionally, seasonal snow cover strongly influences the soil environment in this region (Maurer and Bowling, in review), with important effects on vegetation productivity and soil biogeochemical processes (Monson et al. 2006b, Liptzin et al. 2009, Hu et al. 2010, Tague and Peng 2013). The size and structure of soil carbon stocks and their relation to climate have been investigated at local, regional, and global scales (Post et al. 1982, Guo et al. 2006), but few studies have examined such relations within seasonally snow-covered forests.

The size of soil and detrital carbon pools is determined by the balance between carbon inputs and outputs (Jenny 1941, Schlesinger 1977, Amundson 2001). Carbon inputs come primarily from plant production of leaf litter, root litter, and root exudates. Carbon outputs occur primarily through the decomposition of this detrital organic matter and the associated soil respiration flux by the soil microbial community (though carbon exports such as leaching and fire are sometimes important). Plant production, decomposition, and respiration are each highly sensitive to temperature, precipitation, soil water content, and other climatic variables (Gholz 1982, Orchard and Cook 1983, Lloyd and Taylor 1994, Schimel et al. 1994, Kirschbaum 1995, Gholz et al. 2000, Amundson 2001). Consequently, when disturbances are absent, these ecosystem carbon pools reach a steady state (inputs = outputs) that reflects long-term acclimation to climate and other site-specific characteristics, such as parent material, topography, and biota.

Climosequence studies provide a means to isolate the effects of temperature, precipitation, and other climatic drivers by examining the structure and function of ecosystems along climatic gradients. With careful selection, factors such as parent material, species composition, and time since disturbance can be held similar across a set of sites that vary in climate (Jenny 1941, Amundson and Jenny 1997). This approach has been used to understand how climate influences many ecosystem processes, including plant production, decomposition, and the accumulation of soil and detrital organic matter. Numerous studies have shown increases in soil carbon stocks with elevation (Vitousek et al. 1988, Amundson et al. 1989, Townsend et al. 1995, Trumbore et al. 1996, Garten Jr et al. 1999, Kueppers et al. 2004, Kueppers and Harte 2005, Garten and Hanson 2006, Tewksbury and Van Miegroet 2007, Leifeld et al. 2009). To explain this trend, these studies have presented evidence that cooler temperature at high elevation

sites slows decomposition and increases carbon turnover times, with accompanying increases in organic matter accumulation. Other studies have identified precipitation as a driver of carbon stock size, with increases as available water, plant production, and forest litter inputs increase in tandem (Post et al. 1982, Amundson 2001, Bird et al. 2004, Campbell et al. 2004, Sun et al. 2004). Few of these studies have focused on colder, high elevation, seasonally snow-covered ecosystems, despite evidence that temperature limits production and carbon storage in these systems (Gholz 1982, Trumbore et al. 1996, Wang et al. 2000).

Examining the stable isotope ratios of carbon and nitrogen in vegetation and soils along climate gradients provides additional information about ecosystem processes. As precipitation increases, greater water availability commonly leads to discrimination against the heavier isotope of carbon, ^{13}C, by vegetation (Stewart et al. 1995, Bowling et al. 2002). Increases in mean annual temperature may have variable effects on ^{13}C discrimination by plants depending on their water status, elevation, and species (Körner et al. 1991, Hultine and Marshall 2000, Warren et al. 2001). Ecosystem nitrogen losses occur at higher rates under warm, dry conditions. These losses are mediated largely by microbial processes that fractionate against the heavier isotope of N, leading to ^{15}N enrichment of the remaining nitrogen pool (Austin and Vitousek 1998, Handley et al. 1999, Amundson et al. 2003). The stable isotope composition of plant tissues and the soil and detrital organic matter derived from them thus reflect long-term biological and ecosystem process responses to climate drivers. A reasonable, but simplified, expectation for the mountains of the western U.S. would be that organic matter pools become progressively depleted in ^{13}C and ^{15}N, due to improved site water balance and lower overall rates of nitrogen cycling, as elevation increases.

Seasonal snow cover strongly influences soil temperature and water content, with significant impacts on ecosystem processes occurring below snowpacks and during the warm season. In the interior western U.S., a significant fraction of annual precipitation falls as snow, and snowpacks persist for much, if not most, of the year. Snow cover alters the thermal environment of soils, insulating soils from fluctuations in energy balance at the snow surface and keeping winter soil temperature warm relative to the atmosphere (Bartlett et al. 2004, Zhang 2005). Warmer soil temperature enhances below-snow biological activity, with the result that ecosystem processes such as decomposition and soil respiration occur at substantial rates in winter (Hobbie and Chapin 1996, Lipson et al. 1999, Schmidt et al. 2009). Snowpack ablation and infiltration of melt water into soils may last well into the warm season and deliver water to ecosystems as evaporative demand rises (Pataki et al. 2000, Molotch et al. 2009). This water can support ecosystem processes during the normally dry warm season, enhancing soil biogeochemical activity and primary production (Brown-Mitic et al. 2007, Litaor et al. 2008, Riveros-Iregui and McGlynn 2009, Hu et al. 2010). Seasonal snowpacks thus facilitate year-round soil carbon cycling and subsidize water-dependent

ecosystem processes during the warm season.

The western U.S. is experiencing a period of significant change in regional temperature and hydrologic processes with concomitant impacts on some ecosystems (Milly et al. 2005, Seager et al. 2007, Seager and Vecchi 2010). These climatic changes are causing alterations in the dynamics of seasonal snow cover, and numerous studies have found trends toward reduced snow cover extent and snowpack size (Hamlet et al. 2005, Mote et al. 2005, Mote 2006, Dyer and Mote 2007, Clow 2010, Nayak et al. 2010, Harpold et al. 2012), earlier timing of spring runoff (Dettinger and Cayan 1995, McCabe and Clark 2005, Stewart et al. 2005, Hamlet et al. 2007) and increases in the ratio of rain to snow (Hamlet et al. 2005, Regonda et al. 2005, Knowles et al. 2006, Gillies et al. 2012). Such changes are linked to a variety of consequences for western U.S. forests, including more frequent fire and drought (Brown et al. 2004, Westerling et al. 2006, Cayan et al. 2010), and extensive forest mortality due to tree hydraulic failure and insect outbreaks (Logan et al. 2010, Anderegg et al. 2011). The current relationship between soil and detrital carbon stocks and the climate of western U.S. mountains has not been extensively studied, but alterations in carbon stock size and distribution are a likely result of these changing climate and disturbance regimes.

To elucidate relationships between climate, forest carbon cycle processes, and carbon storage, we examined the size and isotopic composition of soil and detrital carbon stocks at 21 conifer forests in the Wasatch and Uinta mountains of Utah. These forests were located across broad gradients in mean annual temperature, precipitation, snowmelt timing, and snowpack duration. Prior research in the western U.S. (Trumbore et al. 1996, Kueppers and Harte 2005) suggests that decomposition declines, site water balance improves, and soil and detrital carbon stocks increase with elevation. Our study sites spanned most of the elevational distribution of conifer forests in these mountain ranges and received a majority of annual precipitation as snowfall. At the highest elevation sites, we expected forest productivity to be limited by temperature or growing season length. Through their enhancement of winter soil temperature and warm-season soil moisture, we also expected that seasonal snowpacks would increase year-round decomposition of soil and detrital organic matter and alleviate warm season drought effects on vegetation. We therefore hypothesized that

1. Carbon stocks would decline as elevation increased, due to reductions in forest litter production in excess of reductions in decomposition.
2. Plant and organic matter ^{13}C content would decline (greater ^{13}C discrimination) at sites with later-melting snowpacks due to lower incidence of warm season soil drought.
3. Plant and organic matter ^{15}N content would remain unchanged as elevation, snowpack melt timing, and snowpack duration increased due to greater below-snowpack decomposition.

4.3 Methods

4.3.1 Description of sites

The USDA/NRCS SNOTEL network (http://www.wcc.nrcs.usda.gov/snow/) is composed of automated stations located in middle and upper elevation basins throughout the western U.S. This network's purpose is to provide data for water supply forecasting in regions where significant fractions of annual precipitation fall as snow. The standard set of SNOTEL measurements includes snow water equivalent (SWE), accumulated precipitation, snow depth, and air temperature. Instrument specifications for these measurements are documented in the NRCS Snow Survey and Water Supply Forecasting National Engineering Handbook (Natural Resources Conservation Service 2010). At all sampled SNOTEL sites measurements of the temperature and water content of the soil profile at 5, 20, and 60 cm depths were made using Stevens Hydraprobe II sensors (Stevens Water Monitoring Systems, Inc., Portland, OR, USA).

We selected 21 SNOTEL stations in the Wasatch and Uinta mountain ranges of Utah as study sites. Climate and biometric data for each site are given in Table 4.1. These sites spanned the elevation and mean annual precipitation ranges present at SNOTEL sites in these mountains and throughout the region (Fig. 4.1). We visited these sites in the summers of 2008, 2009, 2011, and 2012 and collected a suite of biometric measurements, plant samples, soil samples, and site data from three 10-meter diameter sampling plots per site.

At each site, we first recorded the slope and aspect of the site at the location of SWE measurements. If the station was within a suitable conifer forest (the most common scenario), we designated a start point at the nearest tree in a randomly generated direction from the station's precipitation gauge. If the station was not located in a conifer forest, we chose the nearest accessible conifer stand according to three selection criteria. First, we required a similar slope and aspect to the adjacent SNOTEL site. Second, the stand had to be large enough to accommodate our sampling plot design, which required at least 100 meters of continuous forest. Third, forests with evidence of recent fire, harvest, or other disturbance were avoided. At 6 of the 21 sites, these criteria could not be met within the immediate area of the SNOTEL site, and we sampled in the nearest neighboring drainage with a suitable stand. These alternate sample sites were never more than 5 km from the SNOTEL station. Once the stand was selected, the start point was designated 50 meters into the interior of the forest in a direct line from the SNOTEL station.

4.3.2 Field sampling procedures

From the start point, we designated three sampling plot center points using randomly generated angles and distances (between 10 and 50 m) from the start point. At the center point of each plot, we anchored the end of a tape measure to the ground using a tent stake and used a 5 m length of this tape to mark the boundary of the plot. The diameter at breast height (dbh), species, and health (alive/dead) of all stems

within 5 m of the plot center point were recorded. Stems less than 2 cm in diameter were recorded as saplings. We measured the length and the center diameter of each piece of coarse woody debris (CWD) greater than 3 cm diameter in the plot. We also collected one tree bole increment core and a sample of the most recent 5 years of needles (bulked) from the south side and lower branches of each of the 3 largest conifers in each plot (species varied).

In each plot, we collected soil samples from six (five in 2008) soil quadrats. Quadrat locations were chosen using random angles and distances from the center point of the plot. At each location, we placed a 15 × 15 cm wooden frame on the surface of the litter layer to delineate the quadrat. From within the quadrat, all woody debris and the loose litter (Oi horizon) sitting on the top of the partially decomposed organic layer were collected. Pieces of wood greater than 3 cm in diameter that were in or above the quadrat were discarded because they were already sampled as CWD. The organic layer (Oe and Oa horizons) in the quadrat was then excavated and bagged. Once the organic layer was removed, we sampled the mineral soil below (A/B horizon) to 10 cm depth using a 2 cm diameter hand driven soil corer (3 cores per quadrat). Soil samples of each type (litter, organic, and mineral) were separately bulked. In each plot intact samples of the mineral soil were collected into a 5.1 × 15 cm wooden frame on the surface of the litter layer to delineate the quadrat. From within the quadrat, all woody debris and the loose litter (Oi horizon) sitting on the top of the partially decomposed organic layer was collected. Pieces of wood greater than 3 cm in diameter that were in or above the quadrat were discarded because they were already sampled as CWD. The organic layer (Oe and Oa horizons) in the quadrat was then excavated and bagged. Once the organic layer was removed, we sampled the mineral soil below (A/B horizon) to 10 cm depth using a 2 cm diameter hand driven soil corer (3 cores per quadrat). Soil samples of each type (litter, organic, and mineral) were separately bulked. In each plot intact samples of the mineral soil were collected into a 5.1 × 10.2 cm diameter sleeve using a soil corer. A series of three intact cores was collected in 10 cm depth increments starting at the top of the mineral soil (0–10 cm, 10–20 cm, and 20–30 cm) for bulk density measurement and carbon (C) and nitrogen (N) analysis. At ~20% of plots, the soil was too rocky to collect cores at all depths, but at least one core from each depth was collected for every site.

4.3.3 Laboratory processing of plant and soil samples

Plant and soil samples were returned to the lab within 24 hours and dried for 1 week at ~65 °C. Once dry, all rocks (if any) were removed from the litter and organic soil samples, and the bulk weight of the litter and organic layer samples was then recorded. From each litter and organic soil sample, fine woody debris (FWD) greater than 0.5 cm diameter (branches, some conifer strobili, roots) was removed and the sample was reweighed. The mass of FWD was calculated from the difference between these two masses. Mineral soil samples were sifted through a 2 mm screen, and the mass of all rocks greater than

2 mm in diameter was recorded. At this stage, intact fine roots were sampled from the organic soil and mineral soil (> 2 mm portion) samples and set aside for measurement of percent C, percent N, and C and N stable isotope ratios. The bulk litter (minus FWD), organic soil (minus FWD), and mineral soil (< 2 mm portion) samples were then homogenized and ground, and portions of each sample were archived and subsampled for elemental and isotope analysis. The mineral soil samples were treated with 0.5 N hydrochloric acid (HCl) to remove carbonates prior to this analysis. After drying, intact soil cores were removed from their sleeves and the bulk sample was weighed and then sifted to 2 mm. The mass of the sifted soil from each core was recorded, and the mass of the > 2 mm rocks in each core was calculated as the difference between the bulk weight and the sifted sample. A subsample of the sifted soil from each core was homogenized, treated with 0.5 N HCl, and then sent for elemental and isotope analysis.

4.3.4 Elemental and isotope analysis

Subsamples of all plants and soils (needles, litter, organic, and mineral soil) were ground in a stainless steel ball mill (Retsch MM200, Retsch GmbH, Haan, Germany) before being weighed for elemental and isotopic composition measurement. The percent C, percent N (%C and %N), and stable isotope composition of these samples were determined by continuous flow elemental analysis and isotope ratio mass spectrometry (EA-IRMS). Samples were combusted in a Fisons 1110 CHN elemental analyzer (CE Elantech, Inc., Lakewood, NJ, USA) and the isotope ratios of combustion gases were determined using a Finnegan DELTAplus Advantage mass spectrometer (Thermo Scientific Inc., West Palm Beach , FL, USA). Isotope ratio results are reported in δ^{13}C and δ^{15}N notation, which indicate parts per thousand (or per mil, ‰) deviation relative to Vienna Pee Dee Belemnite (V-PDB) for C, and atmospheric N_2 for N.

4.3.5 Biometric calculations

From our soil sampling and biometric measurements, we calculated the ground-area basis of a number of organic matter stocks. The volume of each measured piece of CWD was estimated using Huber's formula (see Waddell 2002). We calculated the mass of each piece of CWD by multiplying its volume times a specific gravity of wood for the dominant species in the plot (Jenkins et al. 2003). Decomposition reduces the density of wood over time, but we did not qualitatively rank the decay class of CWD pieces in our plots. To account for this, we adjusted the wood specific gravity for decay in each plot by selecting most abundant decay class (class 3) in our region based on national survey data (Woodall et al. 2013) and a decay reduction factor for the each plot's dominant species (Harmon et al. 2008) at that decay class. The biomass of CWD (M_w) in each plot was thus calculated as

$$M_{wi} = \sum_{k=1}^{n_i} V_k \times \rho_i \tag{4.1}$$

where V_k is the volume of any piece of CWD and ρ_i is the decay adjusted (class 3) specific gravity in g/cm^3 of wood for the dominant tree species in plot i. We calculated the carbon content of the CWD (C_w) in each plot as

$$C_{wi} = M_{wi} \times \tau_w \tag{4.2}$$

where τ_w was the carbon concentration of wood and was given a value of 0.521 (Birdsey 1992, Schlesinger 1997). Each plot's biomass and carbon content was calculated on an area basis by dividing by plot area.

The biomasses of litter and organic layer pools were calculated on an area basis by dividing by the summed area of all quadrats sampled in each plot. The carbon contents of these two pools (C_l and C_o) were then calculated as

$$C_{li} = M_{li} \times \tau_{li} \quad \text{and} \quad C_{oi} = M_{oi} \times \tau_{oi} \tag{4.3}$$

where M_{li} and M_{oi} were the biomass of the litter and organic pools in plot i, respectively, and τ_{li} and τ_{oi} were the carbon concentration of these pools measured by EA-IRMS.

After intact cores were dried, sifted, and weighed, the bulk density of the mineral soil at each depth was calculated by dividing the sifted (rock-free, < 2mm) soil mass by the volume of the sample collected. We used these bulk densities to calculate the mass of rock-free mineral soil on an area basis by 10 cm depth increments (M_{md}), and then used %C to calculate the carbon content of each layer. For each plot, the carbon content of mineral soil to 30 cm depth (C_m) was then calculated as

$$C_{mi} = \sum_{d=1}^{3} M_{mdi} \times \tau_{mdi} \tag{4.4}$$

where M_{mdi} was the mass of the of mineral soil at depth d (0–10, 10–20, or 20–30cm) in plot i, and τ_{mid} was its carbon concentration measured by EA-IRMS.

With each of these pools quantified, we then calculated the total carbon storage (C_t) in each plot. This was calculated as

$$C_{ti} = C_{wi} + C_{li} + C_{oi} + C_{mi} \tag{4.5}$$

We also used basal area and stand age as covariates in our analysis. The basal area (B) of each plot was calculated as

$$B_i = \frac{\sum_{k=1}^{n_i} \pi r_k^2}{A_i} \tag{4.6}$$

where r_k is the radius in meters of each tree in plot i, and A_i is the area of the 10 m diameter plot. We assumed that the mean age of the three largest trees from all plots at a site (n = 9) represented the mean stand age of the site.

4.3.6 Ancillary climate data

We used weather and soil data from 2000 to 2011 from the SNOTEL station adjacent to each sampled forest to calculate climate summary variables and monthly mean soil temperature and water content. Daily air temperature, cumulative precipitation, SWE, and soil temperature and moisture (3 depths) data from 11 water years (1 October to 30 September) were collected for each site. Incomplete years (< 1 full year) were excluded, and all data were plotted and visually screened to remove obvious errors. When air temperature, soil temperature, soil water content, or SWE data were more than three standard deviations from the 10 day moving-window mean of a time series, they were classified as outliers and removed. Following these quality control steps, air temperature data were aggregated into multiyear mean air temperature values (MAT). Cumulative precipitation values for June, July, and August were aggregated into multiyear mean summer precipitation (P_{jas}). Time series of SWE were used to calculate several snowpack metrics. Snowmelt date (D_{sm}) was calculated as the first date with < 2.5 mm SWE after the day that peak SWE occurred. Snowpack duration (T_{sc}) was the total number of days with > 5 mm of SWE. Soil temperature and water content for the 11 year dataset were aggregated into 12 monthly means, and four quarterly means (Oct–Dec, Jan–Mar, Apr–Jun, Jul–Aug). When calculating any of the values above, time periods missing more than 5% of data were excluded. The NRCS provides 30 year mean (1971–2000) values of precipitation and peak SWE for most SNOTEL stations in Utah. We used these as our values of mean annual precipitation (MAP) and mean peak SWE (SWE_p) for all sites except one newer site (LM) for which these data were not available. For this we used means of the 11 year dataset.

4.3.7 Statistical analysis

We examined relationships among elevation, basal area, stand age, soil nitrogen, litter quality, and climate summary variables at all sites using Pearson correlation coefficients. Trends in carbon stocks, $\delta^{13}C$, and $\delta^{15}N$ along gradients in climate or site variables were evaluated by fitting a simple linear model by least-squares regression. The three plots sampled at each plot were treated as independent replicates in regression. We used probablility (p) values lower than 0.05 to judge the significance of correlation coefficients in both of these analyses.

Our dataset allowed us to use two subsets of sites to independently evaluate the effect of elevation/MAT and MAP gradients on carbon stocks and isotope ratios. Sites in the temperature subgradient (n = 8) had a limited range in MAP (828-1061 mm/yr, Coefficient of variation (C_v) = 0.08), but variability in elevation between 1994 and 3230 m (C_v = 0.17) and in MAT between 0.5 and 7.2 °C (C_v = 0.64). Sites in the precipitation subgradient (n = 9) had a limited range in elevation (2316–2523 m, C_v = 0.03) and MAT (3.9–5.6 °C, C_v = 0.14), but variability in MAP between 602 and 1628 mm per year (C_v = 0.36). Trends in carbon stocks and isotope ratios along the subgradients were evaluated the same way as the full set of sites.

4.4 Results

4.4.1 Climate gradients and forest characteristics

The SNOTEL sites we sampled spanned a large portion of the range in elevation and mean annual precipitation measured across the entire SNOTEL network of the interior western U.S. (Fig. 4.1). Among our forests, there were ranges of 1450 meters in elevation and 1130 mm in mean annual precipitation (MAP). Ranges in snowpack characteristics were also large, spanning 879 mm in mean peak SWE, 48 days in snowmelt date, and 81 total snow-covered days.

High elevation sites were colder and had longer lasting snow cover. There was a highly significant negative correlation ($p < 0.001$) between elevation and mean annual temperature (Table 4.2). Mean monthly air temperature remained below 0 °C for a greater proportion of the year at high elevation sites (Fig. 4.2). The duration of snow cover, as measured by T_{sc}, increased with elevation as MAT declined (Table 4.2, Fig. 4.3). Sites with longer lasting snow cover experienced longer periods of time in which soil temperature remained near 0 °C (Fig. 4.2).

Total precipitation did not change systematically with elevation, but there were still changes in seasonal water availability with elevation. Among all sites, MAP and SWE_p varied independently of elevation (Table 4.2, Fig. 4.3). Snowpacks were larger and melted later (greater SWE_p and D_{sm}) at sites with higher MAP (Table 4.2, Fig. 4.3), but this did not significantly increase seasonal soil water content at these sites (data not shown). There were significant increases in D_{sm}, probably due to temperature declines, and P_{jas} with elevation (Table 4.2, Fig. 4.3), but it was unclear whether this influenced warm-season soil water content. Mean soil water content during the summer quarter (Jul, Aug, and Sep) did increase with elevation, but the change was not significant (data not shown). During the fall and winter quarters, soil water content was lower at high elevation (Fig. 4.2). During the spring quarter, soil water content peaked later at high elevation sites, but was otherwise similar to other elevations (Fig. 4.2). There was no significant increase in P_{jas} with MAP (Table 4.2, Fig. 4.3).

Basal area, stand age, and organic matter nitrogen (N) content, all had variable relationships to elevation and precipitation. Forest basal area varied between 21 and 126 m^2/ha, and stand age ranged from 43 to 175 years, but only two forests were younger than 80 years. Stand age increased slightly at higher elevation and cooler sites (with greater D_{sm}, and T_{sc}), but basal area had no correlation to elevation (Table 4.2, Fig. 4.4). Basal area did increase with MAP and snowpack influence (SWE_p, D_{sm}, and T_{sc}), but stand age did not (Table 4.2, Fig. 4.4). Leaf N, soil N, and litter quality (measured as litter C:N ratio) all decreased significantly with elevation and P_{jas} (Table 4.2, Fig. 4.4, litter C:N shown). There was no trend in leaf N, soil N, or litter quality with MAP, but leaf and soil N declined in older stands (Table 4.2).

4.4.2 Soil and detrital carbon stocks

We found significant variability in soil and detrital carbon pools among our sites. Total soil and detrital carbon stocks (total C) ranged between 58 and 153 Mg/ha among all sites (Fig. 4.5). Mineral soil carbon (0–30 cm, mineral C) and organic layer carbon (organic C) made up the largest fraction of this total, with mineral C varying from 29–81% and organic C from 10—50%. The litter and coarse woody debris carbon pools (litter C and CWD C, respectively) were smaller and more variable among sites, with litter varying from 1.9–17%, and coarse woody debris from 0.4–13%.

Total C decreased significantly at higher elevation sites, which were cooler, had lower soil N, and greater P_{jas} (Table 4.3, Fig. 4.6). Among the components of total C, only mineral C showed a similar pattern of decline with elevation. Total and mineral C increased significantly with MAP (Fig. 4.6), but were not correlated with basal area (which did correlate with MAP, Table 4.3). There was also less mineral C in older forests, which were more prevalent at higher elevation (Table 4.3). Neither CWD C, litter C, nor organic C showed any correlation with elevation, precipitation or snowpack characteristics (Table 4.3). There was more organic C at sites with greater basal area, and total, litter, and organic C declined as litter quality, measured as C:N ratio, decreased.

There were also changes in soil and detrital carbon storage along the temperature and precipitation subgradients. When elevation was constant (Fig. 4.6, Table C.1), litter C decreased as MAP, SWE_p, D_{sm}, and T_{sc} increased, and mineral C increased at sites with greater SWE_p. When MAP was constant, total and mineral C carbon stocks followed similar patterns to those found on the full gradient (Fig. 4.6, Table C.2), declining at higher elevation sites with longer lasting snowpacks and greater P_{jas}.

4.4.3 Stable isotope composition

There was a clear pattern of stable isotope enrichment with depth in the soils of our study forests (Fig. 4.7). Mineral soil had enriched $\delta^{13}C$ and $\delta^{15}N$ values relative to the organic and litter layer. Relative to forest litter, the organic layer was enriched in ^{15}N at all sites and enriched in ^{13}C at most, but not all, sites.

There were few significant correlations between $\delta^{13}C$ and climatic variables, but $\delta^{13}C$ was correlated to forest age and nitrogen content. The $\delta^{13}C$ of litter increased with elevation, but all other organic matter pools showed no significant relationship to elevation, temperature, precipitation, or snowpack variables (Table 4.4, Fig. 4.8). Organic layer and mineral soil organic matter were significantly enriched in ^{13}C in older stands. There was a significant pattern of ^{13}C depletion in litter and organic layer organic matter as soil N increased and enrichment in litter C as C:N ratios increased (Table 4.4).

The $\delta^{15}N$ value of organic matter was significantly correlated with temperature and precipitation. The $\delta^{15}N$ of all organic matter pools but mineral soil had significant negative correlations with elevation and P_{jas} (and a positive correlation with MAT, Table 4.4, Fig. 4.9). There were also negative correlations

with snowpack duration (greater D_{sm} and T_{sc}). There were no correlations between $\delta^{15}N$ and MAP, or SWE_p, however, suggesting that depletion was primarily driven by temperature (Table 4.4, Fig. 4.9). At sites with higher nitrogen content (leaf and soil N), most organic matter pools were enriched in $\delta^{15}N$, and as litter C:N increased (lower litter quality), the $\delta^{15}N$ of pools declined (Table 4.4).

By using the subgradients, we were able to resolve separate temperature and precipitation effects on the $\delta^{13}C$ and $\delta^{15}N$ values of soil organic matter pools. When elevation and MAT were constant, the $\delta^{13}C$ value of organic and mineral soil declined significantly with higher MAP and SWE_p (Fig. 4.8, Table C.3), possibly indicating greater discrimination by plants. Longer lasting snowpacks (D_{sm} and T_{sc}) were also correlated with lower $\delta^{13}C$. Mineral soil organic matter showed significant depletion $\delta^{15}N$ when temperature was constant and MAP, SWE_p, or snowpack influence increased (Fig. 4.9, Table C.3). When precipitation was constant, the $\delta^{13}C$ of the organic layer was significantly enriched at higher elevations where temperature was low, P_{jas} was high, and snowpacks were longer lasting (Fig. 4.8, Table C.4). The $\delta^{15}N$ values of the litter and organic layer pools were depleted under these same conditions (Fig. 4.9, Table C.4).

4.5 Discussion

Our estimates of the size of soil and detrital carbon pools are similar to other estimates for central Rocky Mountain conifer forests. Three studies have estimated coarse wood, forest floor (litter and organic layer), and soil organic matter carbon stocks in the central Rocky Mountains (Arthur and Fahey 1992, Kueppers and Harte 2005, Bradford et al. 2008) and are therefore suitable for comparison to this study (see Table 4.5). Our average estimates of total soil and detrital C are lower than the Bradford et al. (2008) and Arthur and Fahey (1992) studies and higher than the Kueppers and Harte study (2005). Our measurements of component stocks (coarse wood, litter, organic layer, mineral soil) were also comparable to these studies (Table 4.5). The forests in these prior studies were higher than the average elevation of forests in our study. Of the forests above 2850 meters in our study, the mean total C value was 77 MgC/ha. This is closest to, but still slightly higher than the Kueppers and Harte study. We assumed 50% C content in the organic matter stocks of the Arthur and Fahey study to make these comparisons.

We found significantly larger total soil and detrital carbon stocks (total C) at warmer, lower elevation forests, and significant increases in total C at sites with greater MAP (Table 4.3, Fig. 4.6). Of the component stocks making up the total C pool, mineral C increased significantly with MAT (declining with elevation) and MAP. Other stocks showed no significant changes along these climatic gradients (Fig. 4.6, Table 4.3), suggesting that elevational trends in total C were due to changes in the C content of mineral soil. A number of other studies, including several in the western U.S., have observed that cool temperature at high elevation leads to longer carbon turnover times, and consequently, greater organic matter accumulation at high elevation (Vitousek et al. 1988, Amundson et al. 1989, Townsend et al. 1995,

Trumbore et al. 1996, Garten Jr et al. 1999, Kueppers et al. 2004, Kueppers and Harte 2005, Garten and Hanson 2006, Tewksbury and Van Miegroet 2007, Leifeld et al. 2009). Of the three central Rocky Mountain studies above, only Kueppers and Harte (2005) examined variation in forest carbon stocks along an elevation gradient. Along their 500 meter elevation transect, CWD and mineral C stocks increased significantly as elevation increased and air temperature declined. Our results stand in contrast to this well-established pattern and support our hypothesis that mechanisms other than temperature limitation of decomposition influence the elevational distribution of soil and detrital carbon stocks. The relationship between carbon stocks and MAP that we observed was consistent with studies of other precipitation gradients (Post et al. 1982, Law et al. 2004, Sun et al. 2004).

4.5.1 Relation between carbon stocks and climate

Elevational patterns in carbon stock size support our hypothesis that plant production declined more rapidly with elevation than did decomposition. Some of this pattern is most likely attributable to climate. Gradients in air temperature, precipitation, and snowpack influence were large among our forests, and we found associated differences in soil temperature and moisture (Fig. 4.2). Presumably, variations in climate and the soil environment drove site differences in plant production and microbial activity, which, in turn, influenced the carbon inputs to and outputs from soil and detrital organic matter pools. Without detailed data on ecosystem processes, we cannot determine rates of production or decomposition, so we examine the evidence for, and climatic drivers of, elevational change in both processes in the following paragraphs.

In low elevation forests, decomposition of soil and detrital organic matter was probably limited by water availability. Low elevation sites had higher MAT and soil temperature (Table 4.2, Fig. 4.2), and in the absence of other limiting factors (e.g., water or nutrients), this would lead to enhanced heterotrophic microbial activity and more rapid decomposition of organic matter. Microbial breakdown of organic matter and associated fluxes of CO_2 in respiration are significantly slowed under dry conditions (Orchard and Cook 1983, Skopp et al. 1990, Raich and Schlesinger 1992, Aerts 1997, Davidson et al. 1998, Borken and Matzner 2009, Manzoni et al. 2011). This has been shown to limit decomposition and soil respiration at lower sites in carbon cycle studies along semi-arid elevation gradients (Amundson et al. 1989, Running 1994, Conant et al. 1998, Murphy et al. 1998, Wang et al. 2000). There was no correlation between elevation and MAP among our sites, but snowmelt occurred significantly earlier at low elevations, and summer precipitation (P_{jas}) was significantly greater at high elevation (Table 4.2, Fig. 4.3). This suggests that, in comparison to high elevations, low elevation forests had greater evaporative demand and longer periods of warm-season drought. In comparison to high elevation sites, we expected that lower elevation soils would be drier during the warm season but found no significant evidence of this. The only carbon stock that increased at drier sites was the litter pool, which, when elevation was

constant, increased significantly as MAP and the size and duration of snowpacks declined (Table C.1). This suggests a reduction in litter decomposition at low elevation sites.

At high elevation, plant production and inputs to soil and detrital carbon pools may have been limited by temperature and/or water. In high-elevation (and high-latitude) conifer forests, photosynthesis is substantially downregulated, and growth is limited during cold winter periods (Körner 1998, Savitch et al. 2002, Öquist and Huner 2003, Zarter et al. 2006a, Koh et al. 2009, Bauerle et al. 2012), leading to reductions in potential productivity (Gholz 1982, Case and Peterson 2005, Littell et al. 2008). However, when environmental conditions become favorable again, forest carbon uptake resumes rather rapidly (Ensminger et al. 2004, Monson et al. 2005, Zarter et al. 2006b). High elevation forests in our study experienced cold winter air temperature for a longer proportion of the year (Fig. 4.2), indicating that periods of diminished growth and photosynthetic capacity limited the productive potential of these forests. Mean below-snowpack soil temperature was lower at high elevation sites (Fig. 4.2), but still remained above zero, making it highly likely that there was active decomposition and soil respiration below the snowpack at all sites. Given the high temperature sensitivity of winter soil biological activity, however, decomposition rates may have been considerably lower at high elevation (Monson et al. 2006b, Schmidt et al. 2009). Below-snowpack soil moisture was lowest at high elevation sites (Fig. 4.2), reflecting dry fall conditions at the onset of snowpack accumulation (Maurer and Bowling, in review). Research at other high elevation forests in the region has shown that forest productivity can be limited by water availability even at high elevation and that percolation of snowmelt water into soil is a key requirement for the transition to carbon uptake in high elevation forests (Villalba et al. 1994, Monson et al. 2005, Zarter et al. 2006b). Thus, even when air temperature was favorable for late-fall or early-spring photosynthesis, it is likely that soil water was limiting at some high elevation sites.

Basal area, stand age, and leaf and soil nitrogen content varied with climate and are evidence of changing ecosystem carbon inputs and outputs. Leaf area is generally tightly correlated with basal area at the individual and forest level (Gholz 1982, Waring et al. 1982, Pearson et al. 1984), though following canopy closure, forest leaf area often plateaus as basal area continues to increase (Oliver 1980, Vogt et al. 1987, McDowell et al. 2002). We sampled mature conifer forests and found no change in basal area with elevation. We did find, however, a significant increase in stand age with elevation (Table 4.2, Fig. 4.4), indicating possible age-related declines in leaf area with elevation (Gower et al. 1996, Ryan et al. 1997, Law et al. 2004) Along with leaf area, needle retention time is a key determinant of litterfall rates in conifer forests and tends to increase at less fertile sites, leading to lower litterfall rates (Vogt et al. 1987, Trofymow et al. 1991, Gower et al. 1992). The leaf and soil N content of our forests declined significantly with elevation (Table 4.2, Fig. 4.4), evidence that there were longer needle retention times and consequent declines in litterfall at high elevation. Older and nutrient-poor forests, however, have also

been observed to allocate greater fractions of their productivity to fine root biomass (Vogt et al. 1987, Ryan et al. 1997, Klopatek 2002). Increases in the C:N ratio of litter and soil organic matter were an additional consequence of declines in leaf and soil nitrogen with elevation (Table 4.2, Fig. 4.4). Higher C:N ratios indicate poorer litter quality and may have led to lower decomposition rates at high elevation (Aerts 1997, Seneviratne 2000).

Temperature, water, and other ecosystem process drivers covary across the landscape, making attribution of changes in ecosystem carbon stocks and related processes difficult in this study. Our data provide indirect evidence that decomposition and respiration were water limited at low elevation, and limited by declines in MAT, soil temperature, and litter quality at the opposite end of the elevation gradient. We also find it likely that leaf area and litterfall were limited by water availability at lower, drier sites (Grier and Running 1977, Gower et al. 1992, Campbell et al. 2004), and at high elevation sites by cold temperature, increased stand age, and low N availability. It is also likely that trees allocated significant amounts of carbon to fine roots to enhance water uptake at drier, low elevation sites (Law et al. 2003) and nutrient uptake at less fertile high elevation sites. Thus, the expected effects of temperature, moisture, or other drivers of ecosystem process rates were often opposing across the elevation gradient. We made no direct measurements of the rates of these ecosystem process rates and therefore can only speculate on their relative importance in determining carbon stock sizes.

Our results indicate that temperature and water availability jointly control the size and distribution of soil and detrital carbon stocks in the western U.S. Though a preponderance of studies conducted along forest elevation or temperature transects have found increasing soil and detrital carbon accumulation with elevation (and negative relationships to MAT), studies highlighting other patterns are also common. Positive relationships between MAT and soil carbon stocks have been observed in upland forests in northern Europe (Liski and Westman 1997, Vucetich et al. 2000, Callesen et al. 2003) and some regions of the continental U.S. (Homann et al. 1995, Guo et al. 2006). Guo et al (2006), in a study of soil organic carbon stocks across the continental U.S., found declines in carbon stocks with elevation and a nonlinear relationship between MAT and carbon storage. In the temperature range matching our sites (0 to 6 °C), soil organic carbon stock sizes were positively related to temperature. The correlation we observed between carbon stock size and MAP agrees with a number of studies along forest precipitation gradients. In Oregon, for example, above- and belowground conifer forest productivity and total soil carbon stocks generally increased from east to west as precipitation increased (Campbell et al. 2004, Law et al. 2004, Sun et al. 2004). Forest floor carbon stocks in this study, however, were largest at the dry, eastern site due to low decomposition rates (Running 1994).

These results do come with limitations, however. Climatic drivers explained a relatively small fraction of the variability in the size of soil and detrital carbon stocks among our forests, suggesting that controllers other than climate were important. The forests of the western United States vary considerably

in disturbance history, and though we tried to control for this, we do not know the actual disturbance history of our forests. Given that some of our forests were relatively young, there remains the possibility that either steady-state carbon stock size had not been reached, or that legacy carbon with long turnover times was included in our estimates of soil and detrital carbon stocks (Sun et al. 2004, DeLuca and Aplet 2008). Species differences can cause differences in carbon allocation within the soil profile, litter quality, or a number of other important effects (Jobbágy and Jackson 2000, Djukic et al. 2010). We sampled only conifer forests but still found variation in both dominant conifer and understory (including broad-leaved species) species assemblages among our sites. There are also important effects of hillslope (Yoo et al. 2006) and aspect (Villalba et al. 1994, Kunkel et al. 2011) on soil and detrital carbon storage. We limited our sampling to slopes less than 25°, but did not standardize aspect in our study. Finally, soil texture is well known to influence soil carbon accumulation and stablility (Schimel et al. 1994, Six et al. 2002), and we did not account for this. There is evidence that soil carbon storage in western U.S mountains may be particularly dependent on soil texture (Homann et al. 2007). Our results should thus be viewed with caution due to limitations in our data, and it is likely that site-level effects account for a significant amount of variability in carbon stock size among our forests.

4.5.2 Organic matter isotope composition and climate

Gradients in both water availability and elevation produce variation in the stable carbon isotope composition of plant tissue and the detrital organic matter derived from it. Enrichment in the $\delta^{13}C$ value of leaves and other plant tissue with elevation has commonly been observed, including in conifer forests in the western U.S.(Vitousek et al. 1990, Körner et al. 1991, Marshall and Zhang 1994, Hultine and Marshall 2000, Warren et al. 2001). Elevational decreases in ^{13}C discrimination that cause this pattern are thought to result from a changing balance between mesophyll demand for and conductance of CO_2, which occurs independently of plant water availability (Marshall and Zhang 1994, Hultine and Marshall 2000). Along gradients in water availability, plants discriminate against the heavy isotope, ^{13}C, more when water is not limiting, leading to lower tissue $\delta^{13}C$ values under wetter or cooler conditions (Read and Farquhar 1991, Stewart et al. 1995, Ehleringer and Cerling 1995, Sun et al. 1996, Bowling et al. 2002, Ehleringer et al. 2002). When water does not limit plant carbon uptake along an elevation transect, the first pattern, enrichment with elevation, should predominate. When water is limiting, however, spatial patterns in ^{13}C discrimination may depend on plant physiological responses to drought (Stewart et al. 1995, Warren et al. 2001, Wei and Jia 2009).

Conifer needle, root, and detrital $\delta^{13}C$ indicated that some of our study forests were periodically limited by drought (Table 4.4). In the absence of an elevational change in plant available water, we expected to find $\delta^{13}C$ enrichment with elevation in needle or root tissues. Needle and root $\delta^{13}C$ values did not change significantly with elevation (Table 4.4, Fig. 4.8), indicating that forests became increasingly water

limited at lower elevation, reducing ^{13}C discrimination and raising $\delta^{13}C$ values. Elevational patterns in air temperature, snowmelt timing, summer rain, and warm-season soil moisture support this hypothesis. When we restricted sites to elevations between 2300 and 2550 m (the precipitation subgradient), the $\delta^{13}C$ value of the organic layer and mineral soil declined as MAP increased, and snowpacks melted later (Fig. 4.8, Table C.3). This suggests that at these elevations, forests with low MAP and smaller, short-duration snowpacks were more drought limited. When we restricted sites to MAP values of ~900 mm (the temperature subgradient), the $\delta^{13}C$ value of organic layer pools became significantly enriched with elevation (Fig. 4.8, Table C.4). We interpret this to mean that, at a constant precipitation level, there was no elevational change in overall plant available water, despite changes in snowmelt timing, summer rain, or soil moisture. This elevational enrichment was thus most likely due to various other effects of changing altitude (Körner et al. 1991, Marshall and Zhang 1994, Hultine and Marshall 2000, Warren et al. 2001). Both mechanisms of isotopic variation, elevational enrichment and enrichment at dry sites, were evident, but drought effects on vegetation obscured any broader elevational pattern in $\delta^{13}C$.

These data provide mixed support for our hypothesis that plant water availability improved and ^{13}C discrimination increased at sites with later-melting snowpacks. On the one hand, elevational patterns in $\delta^{13}C$ and relationships to MAT suggested that low elevation forests were more water limited. On the other hand, evidence of improved water availability at higher elevation disappeared when MAP was constant. This may suggest that at the time of conifer tissue growth, which occurs later at high elevation (Beedlow et al. 2013), water availability and the $\delta^{13}C$ values of new tissues (and derived organic matter) were similar regardless of elevation. Some western U.S. studies also suggest that the water subsidy provided by snowmelt is a fairly limited resource for high elevation conifer forests (Monson et al. 2002, Hu et al. 2010). Therefore, high and low elevations may have experienced similar incidence of drought during periods of active growth. We did not find statistically significant evidence that high elevation soils were wetter during the warm season, and many high elevation sites had very dry soils in other parts of the year (Fig. 4.2). Climate driven patterns in $\delta^{13}C$ values, however, may be masked by interspecific differences in ^{13}C discrimination and/or leaf traits along our transect of sites (Schulze et al. 1998, Hultine and Marshall 2000). In addition, the $\delta^{13}C$ values of low elevation conifer leaves may have been elevated due to higher nitrogen content and associated increases in leaf water use efficiency (Lajtha and Getz 1993, Sparks and Ehleringer 1997).

Ecosystems readily lose ^{15}N depleted forms of nitrogen under warmer and drier conditions, and at many spatial scales this leads to increasing plant and soil $\delta^{15}N$ as MAT increases and MAP declines (Austin and Vitousek 1998, Handley et al. 1999, Schuur and Matson 2001, Amundson et al. 2003, Craine et al. 2009). At the local scale, however, denitrification in saturated, anaerobic conditions may alter this general pattern (Farrell et al. 1996). Our forests displayed consistent $\delta^{15}N$ enrichment as depth

in the soil profile increased from litter to mineral soil, indicating a pattern of nitrogen loss over time at our sites (Fig. 4.7). The δ^{15}N values of needles, roots, litter, and the organic layer were also negatively correlated with elevation (Fig. 4.9, Table 4.4). We do not know the isotopic range of N inputs to our forests, but if we assume that they are similar at all sites, these data suggest that the rate of ecosystem N losses were higher at low elevation, leading to ^{15}N enrichment of these pools. The δ^{15}N of organic matter pools was not correlated to precipitation (Fig. 4.9, Table 4.4) except when MAT (and elevation) was held constant (Table C.3), indicating that N losses in mineral soil organic matter were low at wet sites with later melting snowpacks.

This does not support our hypothesis that similar rates of decomposition occur along gradients of increasing snowmelt timing and snowcover duration. Instead, these data suggest increasing microbial activity at warmer, drier forests. There are some alternative explanations for this pattern, however. Nutrient poor ecosystems produce and lose less inorganic nitrogen, and therefore, less fractionation is expected relative to N rich systems (Austin and Vitousek 1998, Schuur and Matson 2001, Amundson et al. 2003). Because nitrogen abundance declined with elevation (Table 4.2), changes in δ^{15}N at our sites may reflect increasingly efficient and conservative nitrogen cycling at high elevation. Some variation in δ^{15}N values can be expected as dominant tree species and functional types of associated mycorrhizae change (Craine et al. 2009, Hobbie and Ouimette 2009). Only conifer forests were sampled in this study, and therefore we expect ectomycorrhizal symbionts, which tend to deplete ^{15}N in foliage relative to soils, to dominate. We suspect, however, that long-lasting snowpacks at high elevation (Fig. 4.3, Table 4.2) facilitated activity by fungal symbionts and that this led to ^{15}N depletion of foliage and the forest floor and enrichment in mineral soil pools where fungal necromass accumulated (Högberg et al. 1996). This speculation is supported by our data (Fig. 4.7, Fig. 4.9), and other studies in snow-dominated ecosystems have observed high rates of below-snowpack fungal activity (Lipson et al. 2002, Schadt et al. 2003, Schmidt et al. 2009).

4.5.3 Conclusions

The balance of evidence in this study suggests that there is significant climatic control over the size of soil carbon stocks in the mountain forests of the western U.S. We found significant declines in soil carbon stocks with elevation and increases with precipitation. Both forest production and decomposition were potentially limited by climate (temperature and moisture) at high elevation, so this pattern appeared to result from elevational declines in forest litter inputs that were more rapid than corresponding reductions in decomposition. Changes in the stable carbon isotope composition of plant tissue and soil and detrital organic matter along climatic gradients indicated that forests were impacted by drought and that water supplied by seasonal snowpacks did fairly little to ameliorate this. Patterns in nitrogen isotope composition suggested that the rate of decomposition declined with elevation, but that fungi became a

more prominent part of the decomposer community at higher sites with more persistent snowpacks. We thus found only indirect evidence that seasonal snowpacks enhance warm-season water availability or year-round decomposition. Nevertheless, the unexpected distribution of soil and detrital carbon stocks that we observed warrants further investigation of the ecosystem processes that determine them, with particular attention to the role of seasonal snowpacks.

4.6 Acknowledgments

The authors wish to thank Richard Malyn, Davis Unruh, Tasha Heilwiel, Michael Bernard, and Lori Long for assistance in the field or the laboratory. The staff of the SIRFER lab, including Brad Erkkila, Abby Howell-Dinger, and Lesley Chesson, provided generous assistance in isotope analysis and data reduction. The University of Utah Global Change and Sustainability Center, U.S. Department of Energy (grant DE-SC0005236), and the University of Utah SEED grant program each supported a portion of this research.

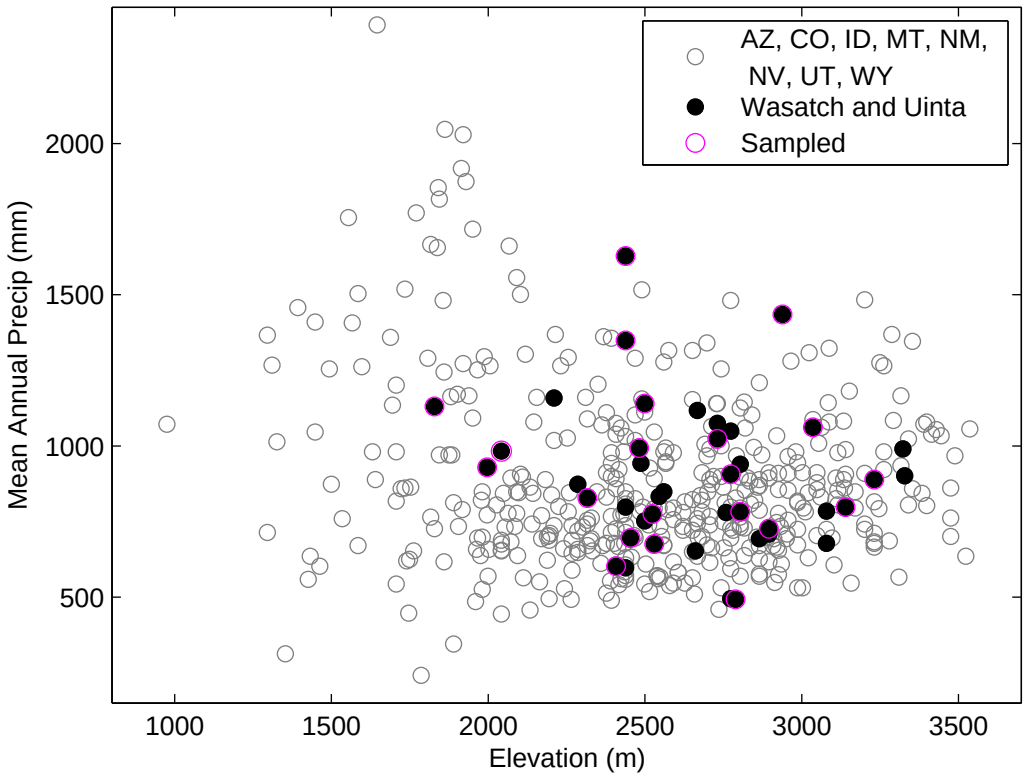

Figure 4.1. Values of mean annual precipitation (MAP) and elevation at all SNOTEL sites in the interior western U.S. states (n = 470), those in the Wasatch and Uinta mountains of Utah (n = 38), and sites sampled during this study (n = 21). MAP data are 30-year (1971–2000) means provided by the USDA/NRCS.

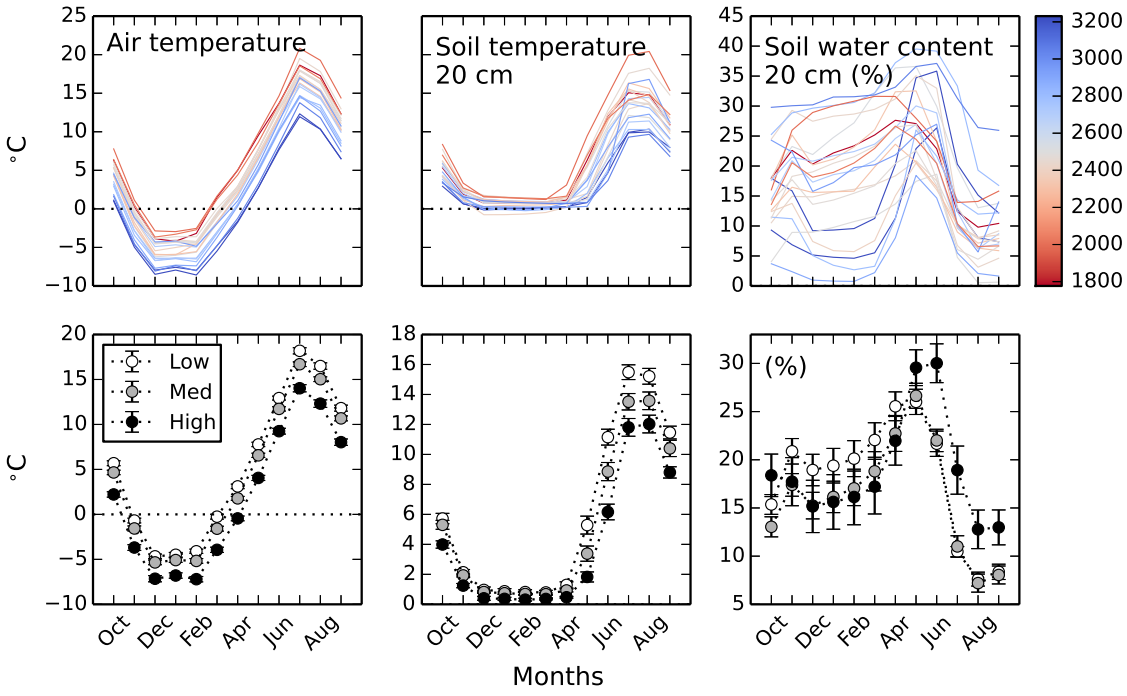

Figure 4.2. Mean monthly air temperature, 20 cm soil temperature, and 20 cm soil water content at sampled SNOTEL sites. Colored lines in the top three panels are monthly means at each of the 21 sites, colored by elevation. In the lower three panels these data are grouped into low (1775–2439 m, white circles), middle (2439–2731 m, grey circles), and high (2788–3231 m, black circles) elevation classes (n = 7 in each group). Bars represent one standard error of the means for all sites in each group. Note that in the lower panels the y axes were adjusted to better display the range in the data. Dotted lines at $y = 0$ are plotted for reference.

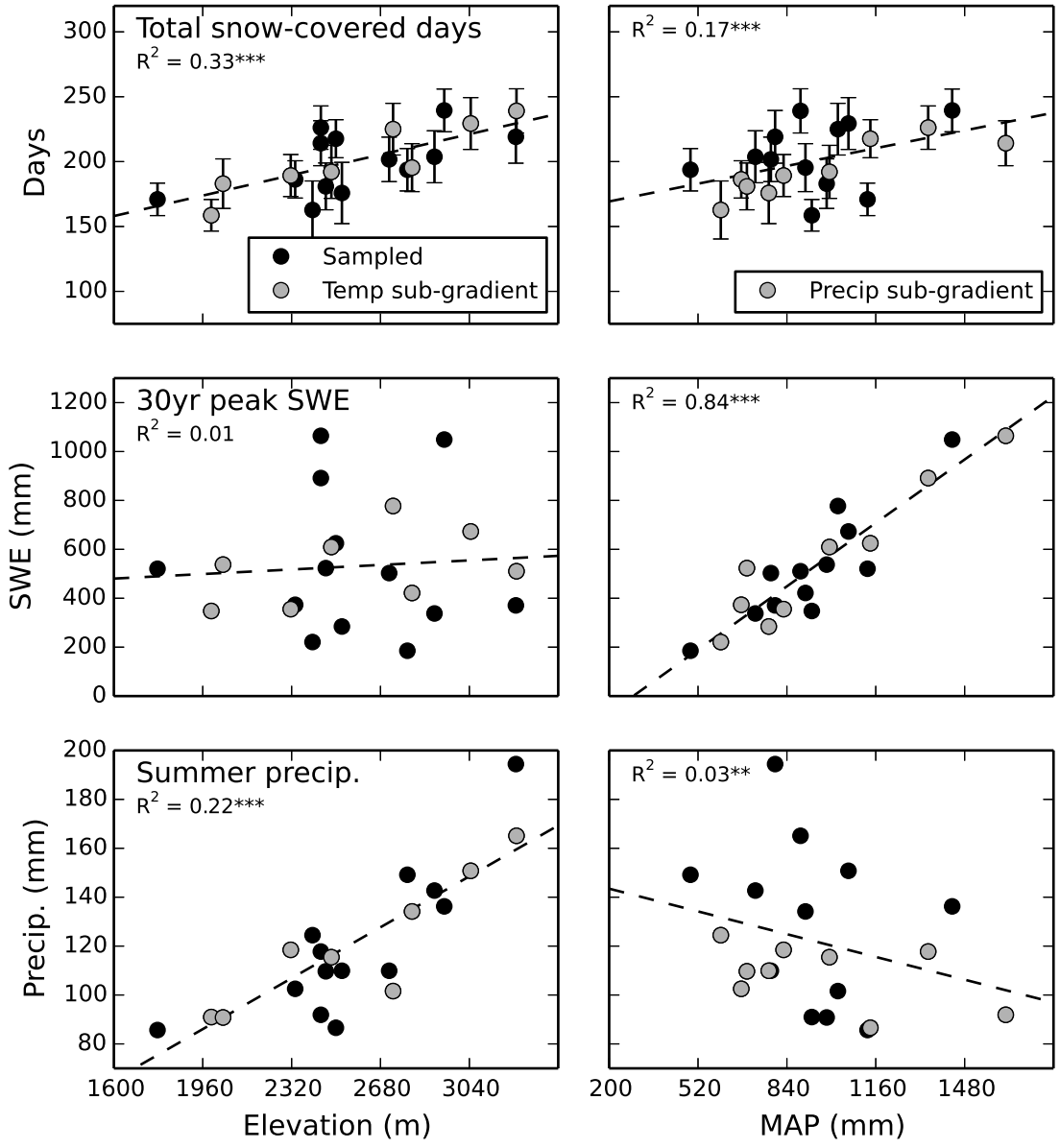

Figure 4.3. Trends in snowpack size, snow cover duration (SWE_p and T_{sc}) and summer precipitation (P_{jas}) along gradients in elevation and MAP. Temperature subgradient (left panels, grey) sites vary minimally in mean annual precipitation, and precipitation subgradients (right panels, grey) sites vary minimally in elevation and MAT. Least squares linear fits (dashed lines, $y = a + bx$) and R^2 values are calculated using data for all sites. Asterisks indicate the significance of the linear model (*** for p < 0.001; ** for p < 0.01; * for p < 0.05). Pearson correlation coefficients and their significance are given in Table 4.2.

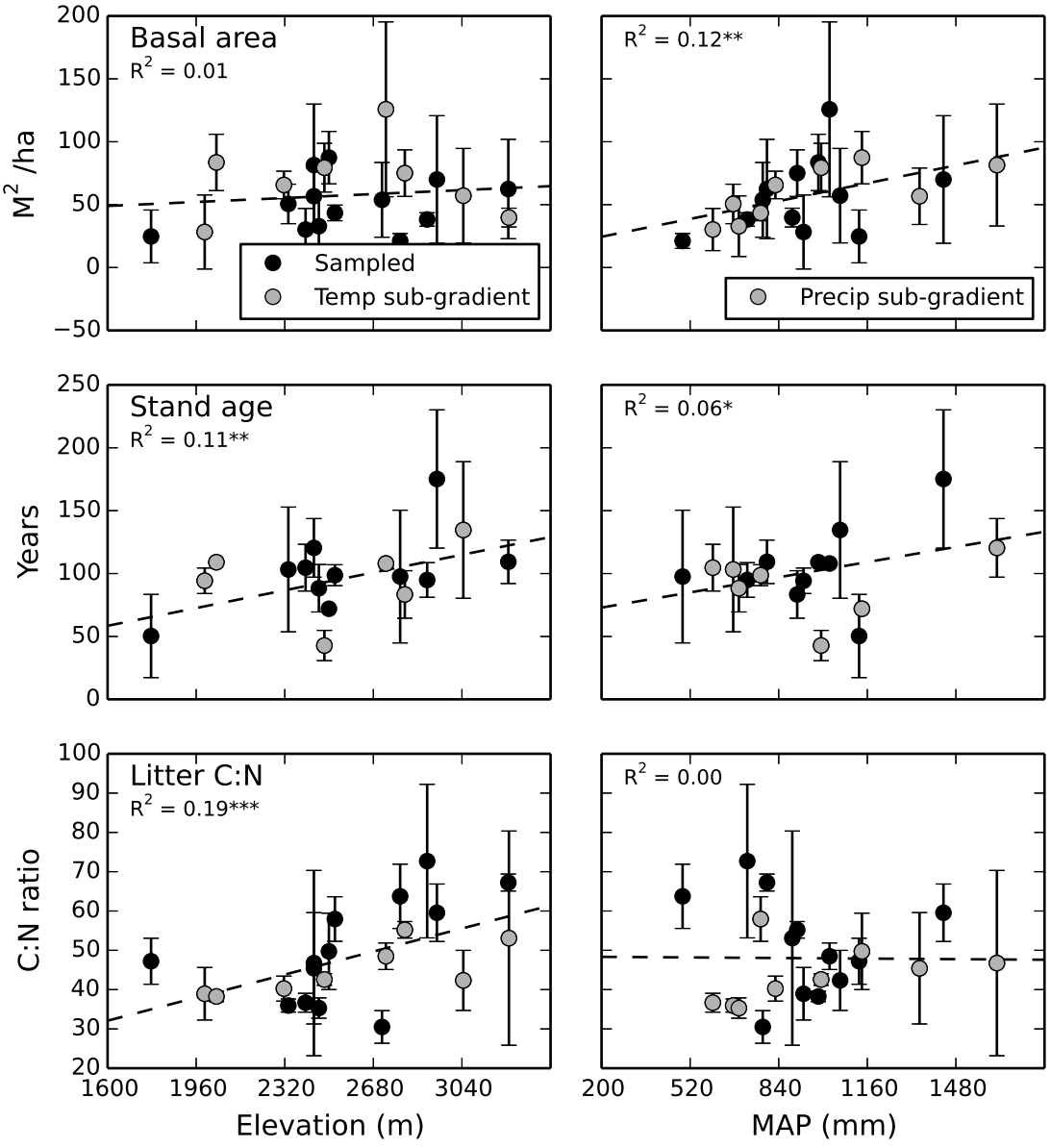

Figure 4.4. Trends in basal area, stand age, and soil N along gradients in elevation and MAP. Temperature subgradient (left panels, grey) sites vary minimally in mean annual precipitation, and precipitation subgradient (right panels, grey) sites vary minimally in elevation and MAT. Least squares linear fits (dashed lines, $y = a + bx$) and R^2 values are calculated using data for all sites. Asterisks indicate the significance of the linear model (*** for $p < 0.001$; ** for $p < 0.01$; * for $p < 0.05$). Pearson correlation coefficients and their significance are given in Table 4.2.

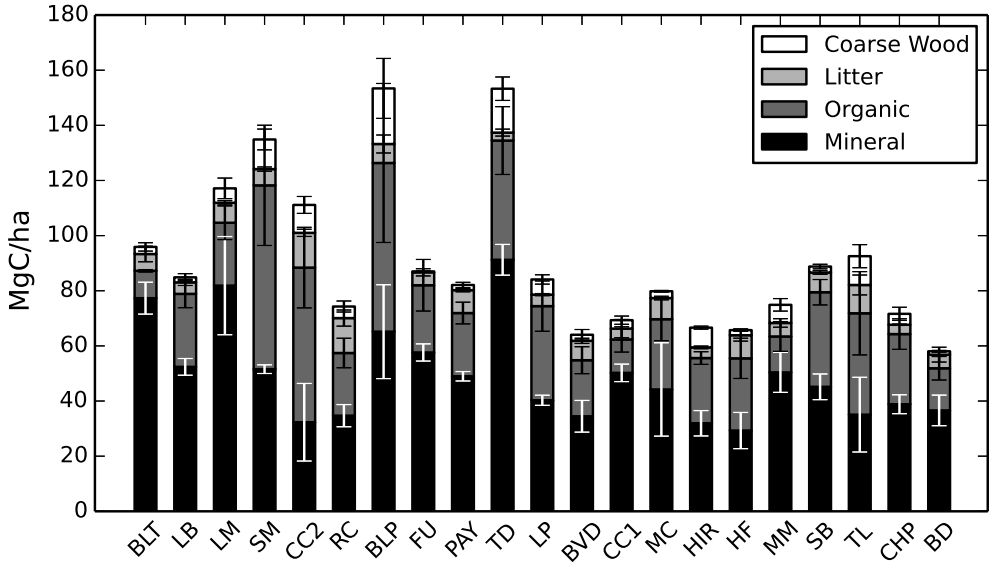

Figure 4.5. Stacked bar chart of carbon stock size in detrital and soil organic matter pools at the 21 sampled sites. Overall bar height indicates the total of all measured C pools. Sites are ordered by elevation from left (1777 m) to right (3231 m). Bars indicate one standard error from the mean of three plots per site.

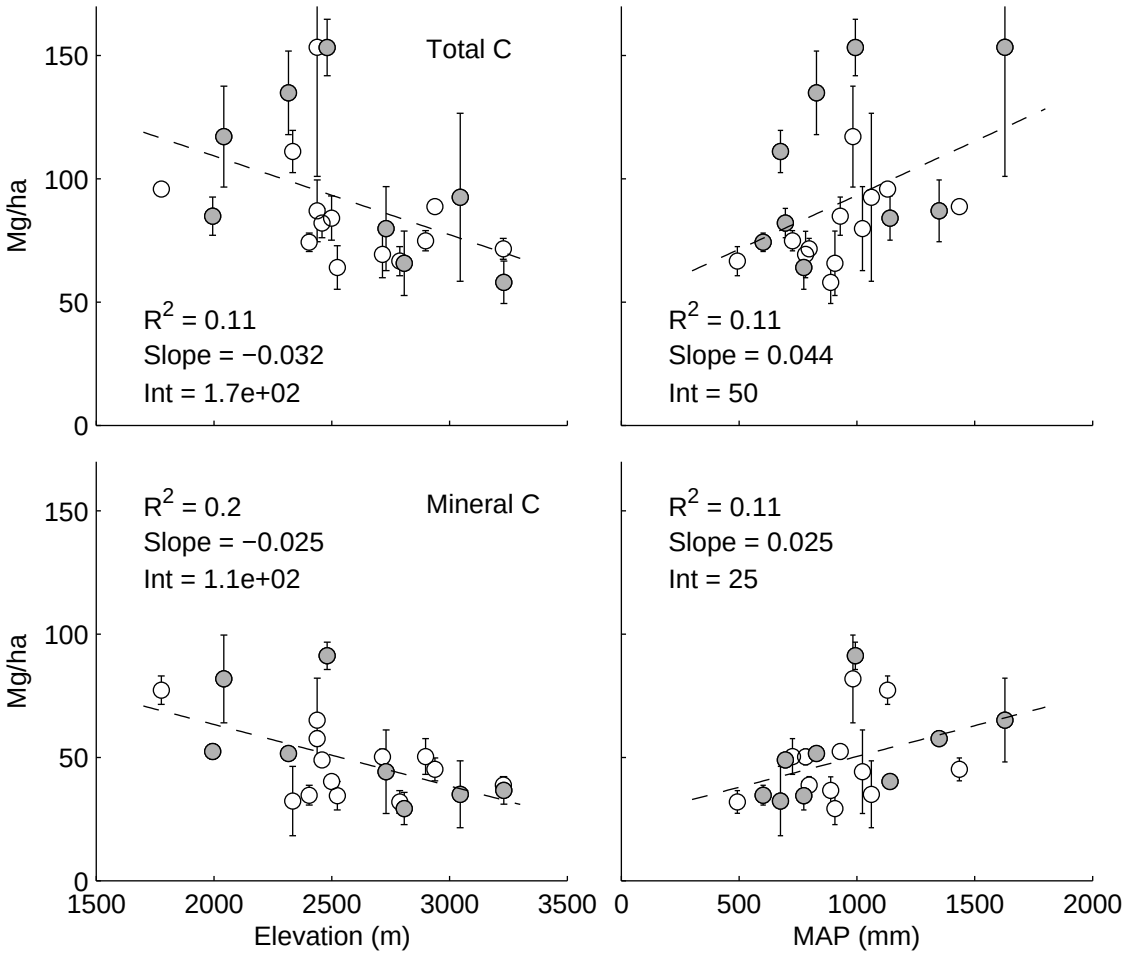

Figure 4.6. Trends in total soil carbon stocks and mineral soil carbon stocks versus elevation and MAP. Temperature subgradient (left panels, grey) sites vary minimally in MAP, and precipitation subgradient (right panels, grey) sites vary minimally in elevation and MAT. R^2, slope, and intercept values are calculated for the least squares linear fit (dashed lines, $y = a + bx$) using all data points. All fits were significant at $p < 0.05$. These and other correlation coefficients and their significance values are given in Tables 4.3, C.1, and C.2.

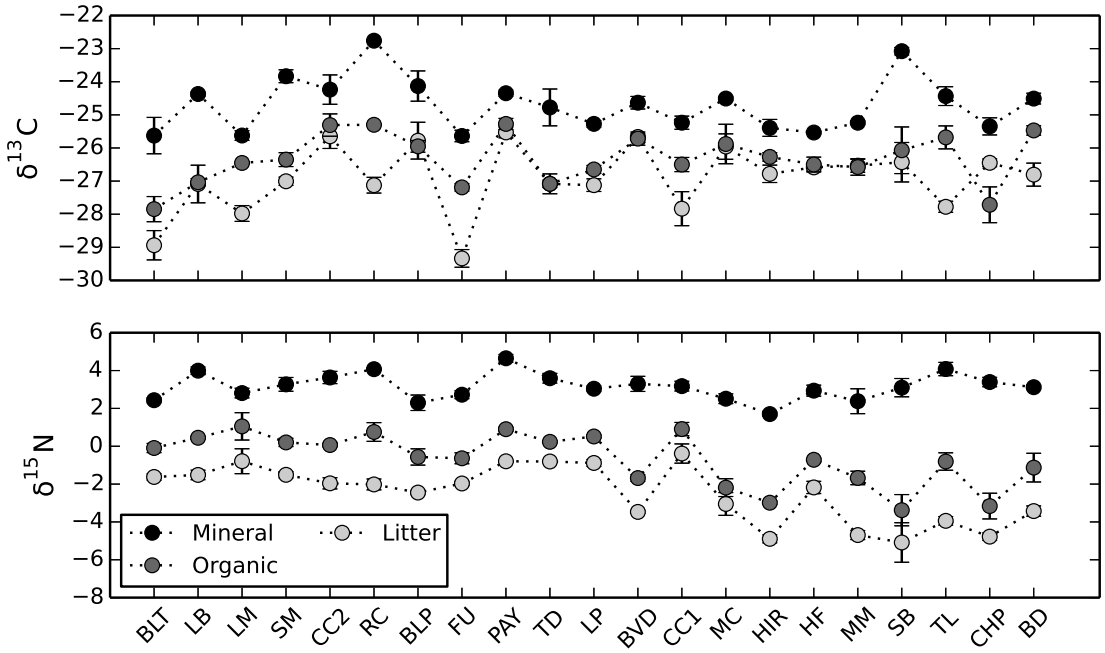

Figure 4.7. Mean δ^{13}C and δ^{15}N in three detrital and soil organic matter pools at the 21 sampled sites. Sites are ordered by elevation from left (1777 m) to right (3231 m). Bars indicate one standard error from the mean of three plots per site and are smaller than the symbols in some cases.

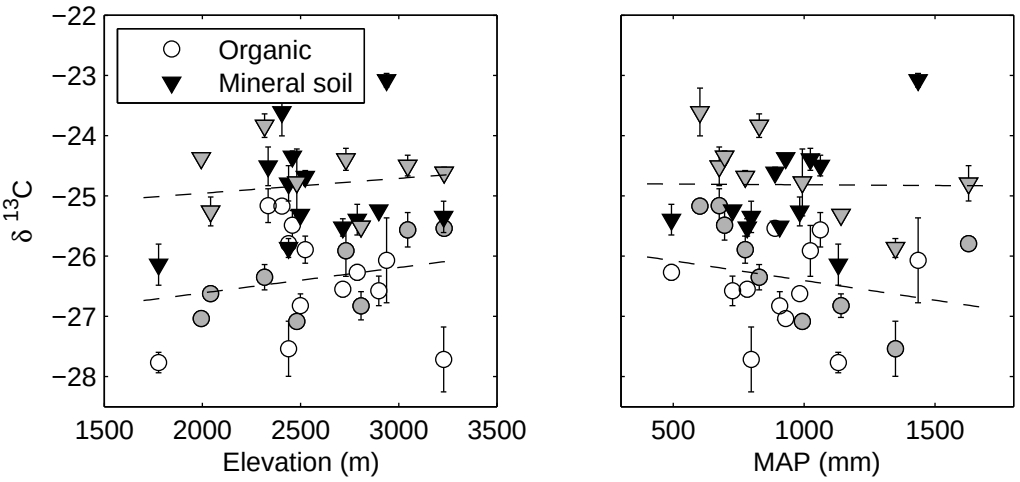

Figure 4.8. Trends in δ^{13}C versus elevation and MAP at the study sites. Organic and mineral soil organic matter values are shown. Temperature subgradient (left panels, grey) sites vary minimally in MAP, and precipitation subgradient (right panels, grey) sites vary minimally in elevation and MAT. The least-squares linear fit (dashed lines, $y = a + bx$) were calculated using all data points and were not significantly different from zero ($p > 0.05$). These and other correlation coefficients and their significance values are given in Tables 4.4, C.3, and C.4.

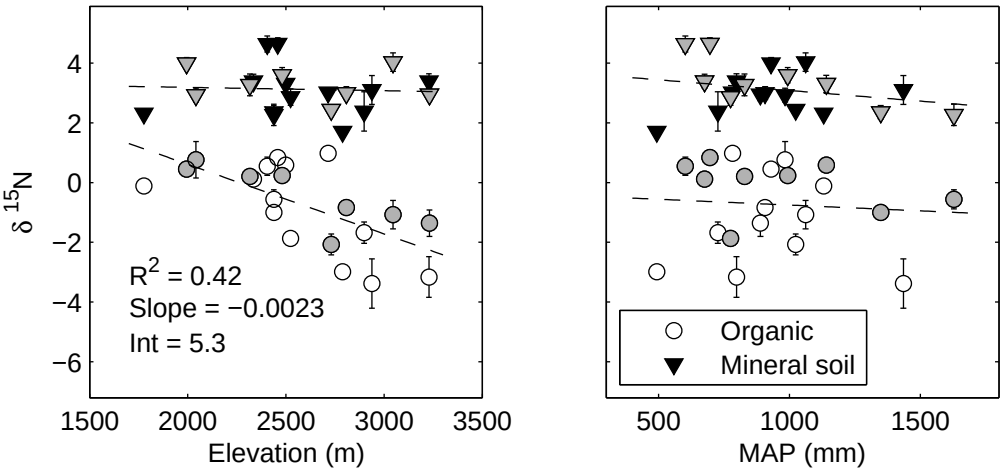

Figure 4.9. Trends in δ^{15}N versus elevation and MAP at the study sites. Organic and mineral soil organic matter values are shown. Temperature subgradient (left panels, grey) sites vary minimally in MAP, and precipitation subgradient (right panels, grey) sites vary minimally in elevation and MAT. R^2, slope, and intercept values were calculated for the least squares linear fit (dashed lines, $y = a + bx$) using all data points and are given only for relationships that were significant at $p < 0.05$. These and other correlation coefficients and their significance values are given in Tables 4.4, C.3, and C.4.

Table 4.1. Location, climate, and biometric data of all sampled forests. MAP and SWE_p data are 30-year (1971–2000) averages calculated by the NRCS. Other climate data are means calculated from 11 years of data collected from the SNOTEL site adjacent to each forest and are defined in the text. Methods for stand age and basal area calculations are given in the text. Standard deviation in parentheses.

Site abbr.	Mtn. range	Elevation (m)	Mean air temp. (MAT, °C)	Mean ann. precip. (MAP, mm)	Summer precip. (P_{jas}, mm)	Mean Peak SWE (SWE_p, mm)	Snowmelt date (D_{sm}, d)	Snowpack duration (T_{sc}, d)	Stand age (yrs)	Basal area (m^2/ha)
BD	Uinta	3231	0.5 (0.8)	889	165 (38)	511	Jun 15 (14)	239 (17)	NA	40
BLP	Wasatch	2438	5.6 (0.5)	1628	92 (54)	1064	Jun 08 (13)	214 (17)	120	81
BLT	Wasatch	1777	6.2 (0.5)	1130	86 (45)	521	May 09 (11)	171 (13)	50	25
BVD	Uinta	2524	3.9 (0.3)	775	110 (33)	284	May 05 (20)	176 (24)	99	43
CC1	Wasatch	2715	4.0 (0.5)	782	110 (31)	503	May 26 (13)	202 (17)	NA	54
CC2	Wasatch	2334	4.1 (0.5)	676	103 (27)	373	May 12 (11)	186 (14)	103	51
CHP	Uinta	3228	0.3 (0.6)	798	194 (42)	371	May 02 (14)	219 (20)	109	62
FU	Wasatch	2438	4.8 (0.5)	1349	118 (48)	892	May 28 (11)	226 (17)	NA	57
HF	Uinta	2808	2.6 (0.5)	907	134 (47)	422	Jun 11 (15)	195 (18)	83	75
HIR	Uinta	2789	2.5 (0.6)	493	149 (26)	185	Jun 19 (17)	194 (16)	98	21
LB	Wasatch	1995	7.2 (0.5)	930	91 (31)	348	Jun 07 (12)	159 (12)	94	28
LM	Wasatch	2042	6.1 (0.4)	983	91 (33)	538	May 23 (16)	183 (19)	109	84
LP	Wasatch	2499	4.7 (0.5)	1140	87 (30)	625	May 19 (13)	218 (15)	72	87
MC	Wasatch	2731	3.0 (0.5)	1024	102 (46)	777	May 03 (15)	225 (20)	108	126
MM	Uinta	2899	1.9 (0.6)	726	143 (47)	338	May 13 (17)	204 (20)	95	38
PAY	Wasatch	2459	5.4 (0.5)	696	110 (40)	523	May 19 (11)	181 (18)	88	33
RC	Uinta	2405	4.7 (0.6)	602	124 (29)	221	Jun 09 (13)	163 (22)	105	30
SB	Wasatch	2938	4.2 (0.5)	1435	136 (46)	1049	May 14 (13)	239 (16)	175	70
SM	Uinta	2316	3.9 (0.4)	828	118 (40)	356	May 21 (14)	189 (16)	NA	66
TD	Wasatch	2481	5.1 (0.5)	993	115 (38)	610	May 23 (14)	192 (20)	43	79
TL	Uinta	3046	1.1 (0.5)	1062	151 (28)	673	Jun 08 (16)	229 (20)	135	57

Table 4.2. Pearson correlation coefficients (*r*) between elevation, climate summary variables, and biometric data from all study sites. Boldface indicates a significant correlation at $p < 0.05$.

	Elevation	MAT	MAP	P_{jas}	SWE_p	D_{sm}	T_{sc}	Stand age	Basal area
Elevation	**1.00**								
MAT	**-0.90**	**1.00**							
MAP	-0.10	0.29	**1.00**						
P_{jas}	**0.84**	**-0.87**	-0.29	**1.00**					
SWE_p	0.07	0.18	**0.92**	-0.21	**1.00**				
D_{sm}	**0.59**	-0.40	**0.63**	0.28	**0.76**	**1.00**			
T_{sc}	**0.73**	**-0.59**	**0.49**	**0.46**	**0.64**	**0.97**	**1.00**		
Stand age	0.47	-0.29	0.29	0.33	0.42	**0.49**	**0.53**	**1.00**	
Basal area	0.13	-0.03	**0.48**	-0.20	**0.56**	**0.53**	**0.47**	0.15	**1.00**
Leaf N	**-0.74**	**0.61**	0.10	**-0.64**	-0.11	-0.48	-0.57	-0.57	0.06
Soil N	**-0.76**	**0.77**	0.32	**-0.62**	0.17	-0.30	**-0.45**	-0.48	0.08
Litter C:N	**0.55**	**-0.57**	-0.01	**0.58**	-0.08	0.28	0.37	0.16	-0.04

Table 4.3. Correlation coefficients (*r*) from linear regression of carbon stocks on the variables shown in Table 4.2. Values in italics are signicant at p < 0.05. Asterisks indicate the significance of this correlation (*** for p < 0.001; ** for p < 0.01; * for p < 0.05).

	Coarse wood	Litter	Organic layer	Mineral soil	Total
Elevation	-0.06	-0.08	-0.09	*-0.45****	*-0.33***
MAT	0.06	0.03	0.10	*0.48****	*0.35***
MAP	0.17	-0.09	0.20	*0.33***	*0.33***
P_{jas}	-0.09	-0.10	-0.12	*-0.37***	*-0.31**
SWE_p	0.15	-0.03	0.19	*0.27**	*0.29**
D_{sm}	0.03	-0.16	0.06	-0.05	-0.01
T_{sc}	0.02	-0.14	0.05	-0.16	-0.07
Stand age	-0.04	0.26	0.15	*-0.32**	-0.10
Basal area	0.18	-0.02	*0.25**	0.15	*0.27**
Leaf N	0.07	0.07	0.31	0.09	0.25
Soil N	0.18	-0.16	0.13	*0.75****	*0.53****
Litter C:N	-0.16	*-0.25**	*-0.27**	-0.18	*-0.32**

Table 4.4. Correlation coefficients (*r*) from linear regression of $\delta^{13}C$ and $\delta^{15}N$ values of organic matter pools on the variables shown in Table 4.2. Values in italics are significant at p < 0.05. Asterisks indicate the statistical significance of the correlation (*** for p < 0.001; ** for p < 0.01; * for p < 0.05).

	$\delta^{13}C$					$\delta^{15}N$				
	Needles	Roots	Litter	Organic layer	Mineral soil	Needles	Roots	Litter	Organic layer	Mineral soil
Elevation	0.13	0.10	*0.28**	0.19	0.04	*-0.74****	*-0.48**	*-0.63****	*-0.59****	-0.04
MAT	0.05	-0.03	-0.18	-0.13	0.09	*0.67****	*0.53***	*0.64****	*0.56****	0.10
MAP	0.01	-0.13	-0.21	-0.20	0.03	0.19	0.27	0.03	-0.06	-0.20
P_{jas}	0.03	-0.01	0.10	-0.00	0.00	*-0.71****	*-0.41**	*-0.67****	*-0.58****	0.02
SWE_p	0.10	0.23	-0.10	-0.02	0.11	-0.01	0.09	0.00	-0.11	-0.14
D_{sm}	0.12	0.23	-0.07	0.01	-0.05	*-0.44**	-0.22	*-0.31**	*-0.38***	*-0.26**
T_{sc}	0.02	0.28	-0.00	0.04	-0.04	*-0.56****	-0.33	*-0.44****	*-0.48****	-0.23
Stand age	0.07	0.37	0.26	*0.38***	*0.49****	*-0.47**	*-0.62***	*-0.56****	*-0.45****	0.03
Basal area	-0.20	-0.12	0.13	-0.02	-0.04	0.09	-0.15	0.12	-0.07	-0.16
Leaf N	-0.35	-0.53	-0.11	-0.16	-0.04	*0.78****	0.54	*0.69****	*0.49***	0.08
Soil N	-0.34	-0.15	*-0.34***	*-0.39***	-0.03	*0.72****	*0.60****	*0.62****	*0.53****	0.07
Litter C:N	0.20	-0.37	*0.28**	-0.12	-0.21	*-0.42**	-0.20	*-0.63****	*-0.63****	*-0.44****

Table 4.5. Comparisons of site characteristics and carbon stock estimates between the present study and three other studies in the central Rocky Mountains. The forest floor carbon stock is the sum of litter and organic layer stocks, which were seperately measured in our study. We assumed an organic matter carbon content of 0.5 to estimate carbon stocks from the organic matter biomass data reported in the Arthur and Fahey study.

	Present study	Arthur & Fahey 1992	Kueppers & Harte 2005	Bradford et al. 2008
Species	Pine, spruce, fir	Spruce-fir	Pine, spruce, fir	Pine, spruce, fir
Elevation	1777–3231 m	3100–4000 m	3040–3552 m	2850–3100 m
MAP	493–1628 mm	~1000 mm	442 mm	737–1000 mm
Carbon stocks (Mg/ha)				
Coarse wood	5.7	26	5.7	13
Forest floor	36	34	15	72
Mineral soil (depth)	49 (30 cm)	63 (variable)	27 (30 cm)	61 (15 cm)
Total soil & detrital	91	123	48	146

APPENDIX A

PRINCIPAL COMPONENT ANALYSIS OF CLIMATE AND SOIL DATA FROM THE SNOTEL NETWORK

A.1 Introduction

In our study of data from 252 SNOTEL sites around the western U.S., we found high intersite variability in below-snow soil temperature (T_{soil}), winter quarter soil water content (θ), and summer quarter soil θ. To test whether this variability in the soil environment was related to snowpack and other climatic variables across these study sites, we used multiple regression analysis with PCA scores as the explanatory variables. This analysis complements our examination of interannual variability in soil temperature and moisture and adds support to hypotheses tested using simple linear regression in the main body of the article. The following sections describe the methodology and results of this analysis.

A.2 Methods

We performed principal components analysis (PCA) using two multivariate datasets. These were constructed as matrices with each row containing observations from one individual site in 1 year and columns containing the explanatory variables observed at those sites and in those years. The first dataset contained variables relevant to the below-snow soil environment (snowpack metrics, Oct.–May mean monthly T_{air} and SWE, presnowpack temperature and θ, and below-snow means). The second dataset contained variables relevant to the warm season soil environment (snowpack metrics, May–Sept. mean monthly T_{air} and precipitation, JJA T_{air} and precipitation means, and JFM T_{soil} and θ). Below-snow T_{soil}, winter quarter (JFM) θ, and summer quarter (JJA) θ were the variables examined for dependence on these datasets. Principal components analyses were run for both datasets, which generated a number of new orthogonal axes (principal components). Each new axis was weighted with a loading value for every explanatory variable in the original dataset, signifying the importance of the explanatory variable on the axis. All observations in the dataset received scores indicating their placement along each new axis.

From each set of principal components, we rejected all axes that explained less than 100/N percent of the variance in the dataset, where N was the number of explanatory variables in the dataset. We used

the remaining axes to test our hypotheses using multiple regression. The explanatory variables with the three highest loadings were assumed to be the most important for each axis, and we used them to assist in interpreting the multiple regression results. This condensed all correlated environmental quantities down to a few orthogonal, composite variables that could be used in multiple regression analysis. We chose mean below-snow T_{soil}, winter quarter mean θ, and summer quarter mean θ as the dependent variables for multiple regression analysis because these were the most suitable values for testing our hypotheses. The generalized regression model used was

$$y = PC1 + PC2 + PC3 + PC4 \tag{A.1}$$

where y was the dependent variable (snow-cover period T_{soil} , winter quarter θ, or summer quarter θ), and PC1–4 are the scores for principal component axes 1–4. We ran each PCA and performed the multiple regression analysis with all years of data and then separately for 2007, 2009, and 2011 data.

A.3 Below-snow results

We retained the first four principal component axes from the below-snow PCA. These four principal components explained 78% of the variance in the dataset for all years, and 86, 86, and 88% for the 2007, 2009, and 2011 subsets, respectively (Table A.1). The explanatory variable loadings on these axes were fairly consistent in all years (Table A.2), and we used these loadings to characterize the axes. We termed below-snow PC1 the spring snowmelt axis because total snow-covered days, snow-free date, and spring SWE and T_{air} (April and May) were the most important explanatory variables (had the highest loadings) on this axis. We termed PC2 the winter temperature axis because mean T_{air} during the snow-cover period was most important. January through March SWE were also important in the 2007, 2009, and 2011 PC2 axes. We termed PC3 the snowpack start temperature axis because presnowpack T_{soil}, T_{air}, and snowpack start day were most important. Below-snow PC4 was termed the fall snow/soil axis because fall SWE (Oct. and Nov.), presnowpack θ, and presnowpack T_{soil} were most important. Observation scores along these axes were used as explanatory variables in multiple regression analysis of snow-cover period T_{soil} and winter quarter θ (see Tables A.3 and A.4).

In multiple regression tests, mean below-snow T_{soil} was significantly dependent on the winter temperature (PC2) and snowpack start temperature (PC3) axes in all years tested (Table A.3). Below-snow T_{soil} was higher at sites with warmer winter T_{air} (PC2), suggesting that soils were not fully insulated from the thermal environment above the snowpack. Below-snow T_{soil} was cooler at sites that had lower presnowpack T_{soil} and T_{air}, and these sites tended to have a later snowpack start date (PC3). Below-snow T_{soil} was also warmer at sites with greater early-winter SWE (PC1 & 4), though this relationship was not significant in one of the individual years tested. In some years, soils were warmer at sites with higher presnowpack soil moisture (PC4), perhaps indicating an effect related to the high heat capacity of water or

latent heat release during soil freezing. Relationships with the spring snowmelt axis (PC1) were generally weak and inconsistent between the years tested.

Mean winter quarter θ was significantly dependent on winter temperature (PC2) and fall snowpack/soil (PC4) axes in all years tested (Table A.4). Winter quarter θ was higher at sites where winter T_{air} was warm (PC2). This may suggest that winter and early spring melt events recharged soil moisture, but a relationship between elevation and soil water content is also a possibility. Winter quarter θ had a positive relationship to the fall snowpack/soil axis (PC4), indicating that winter soil moisture was higher at sites with either greater October and November SWE or higher presnowpack θ, depending on the years of data used in the model. In some of the years tested, winter quarter θ was lower at sites where presnowpack T_{soil} and T_{air} were high (PC3). These results suggest that a combination of precipitation and temperature conditions during the fall and early-winter are important determinants of winter quarter θ.

A.4 Warm season results

We retained the first three principal component axes from the warm-season PCA. These four principal components explained 67% of the variance in the dataset for all years, and 75, 73, and 76% for the 2007, 2009, and 2011 subsets, respectively (Table A.5). We termed warm season PC1 the summer T_{air} axis because summer quarter T_{air} was the most important explanatory variable (Table A.6). We termed PC2 the spring snowmelt/summer precip axis because summer quarter precipitation was the most important explanatory variable for all years, and peak SWE, snow-free date and spring precipitation were most important in the axes for 2007, 2009, and 2011. We termed PC3 the winter T_{soil} axis because winter quarter T_{soil} was most important for all axes except the 2011 axis, in which May precipitation loaded the highest. Overall, the importance of explanatory variables for the warm-season PCA axes changed between years more than for the below-snow PCA axes. Observation scores along these axes were used as explanatory variables in multiple regression analysis of summer quarter θ (see Table A.7).

Mean summer quarter θ was significantly dependent on the summer T_{air} axis (PC1) in all years tested, but precipitation and snowpack were also important explanatory variables in some years (Table A.7). Summer quarter θ was lower at sites with higher summer T_{air} (PC1), suggesting greater rates of warm-season evapotranspiration. Summer quarter θ could be higher at sites with greater warm season precipitation, higher peak SWE, and later snow-free date (PC2 & 3), but these relationships did not hold for all years that we tested. Interestingly, winter T_{soil} also appeared to influence summer quarter θ in some of our multiple regression tests. Though the statistical relationships between summer quarter θ and our explanatory variables were inconsistent between years, they do indicate that warm season T_{air}, warm season precipitation, and snowpack characteristics were responsible for intersite differences in summer soil moisture during some years.

Table A.1. Standard deviation and variance explained (percent and cumulative) by the first four principal component axes for the below-snow PCA analyses. The results of four separate PCA analyses are shown, PCA using observations from all years together, and using 2007, 2009, and 2011 subsets of the observations.

	PC 1				PC 2				PC 3				PC 4			
	All	2007	2009	2011	All	2007	2009	2011	All	2007	2009	2011	All	2007	2009	2011
Std. Deviation	3.18	3.47	3.46	3.52	2.38	2.43	2.51	2.52	1.51	1.49	1.46	1.53	1.18	1.17	0.99	0.93
% Var. Explained	0.40	0.48	0.48	0.50	0.23	0.24	0.25	0.25	0.09	0.09	0.09	0.09	0.06	0.05	0.04	0.03
Cum. Var. Explained	0.40	0.48	0.48	0.50	0.63	0.72	0.73	0.75	0.72	0.81	0.82	0.84	0.78	0.86	0.86	0.88

Table A.2. Explanatory variables used in the below-snow PCA analyses and their loading values on each of the first four principal component axes. Again, the results of four separate PCA analyses are shown (all years, 2007, 2009, and 2011). The highest loadings for each column were assumed to be the most important variables for the respective axis.

	PC 1				PC 2				PC 3				PC 4			
Explanatory variables	All	2007	2009	2011	All	2007	2009	2011	All	2007	2009	2011	All	2007	2009	2011
Elevation	-0.14	0.17	-0.16	-0.13	-0.21	0.19	0.15	0.19	-0.05	0.28	0.18	-0.12	0.08	-0.25	0.11	-0.45
Snow-covered days[a]	-0.28	0.26	-0.26	-0.26	0.00	-0.07	-0.06	-0.05	-0.14	0.10	0.13	-0.10	0.05	-0.11	0.04	-0.07
Snow-free day	-0.27	0.18	-0.25	-0.25	0.04	-0.13	-0.10	-0.09	-0.08	0.12	0.04	-0.05	-0.10	-0.19	0.04	-0.05
Snowpack start day	0.19	-0.21	0.18	0.19	0.03	-0.01	0.07	0.00	0.46	-0.38	-0.48	0.46	-0.08	-0.21	0.09	0.14
Peak SWE	-0.25	0.20	-0.20	-0.21	0.23	-0.28	-0.26	-0.25	0.10	-0.10	-0.11	0.12	-0.17	0.01	-0.03	0.04
Below-snow T_{air}[b]	0.07	-0.09	0.12	0.11	0.37	-0.35	-0.34	-0.34	-0.10	0.15	0.04	-0.06	0.06	-0.17	0.12	-0.15
Oct. Mean T_{air}	0.15	-0.24	0.23	0.19	0.27	-0.21	-0.23	-0.25	0.11	-0.04	-0.01	0.00	-0.09	0.02	0.01	0.24
Nov. Mean T_{air}	0.18	-0.23	0.23	0.22	0.18	-0.17	-0.22	-0.24	-0.11	0.17	-0.03	-0.01	-0.28	0.00	0.05	0.01
Dec. Mean T_{air}	0.13	-0.20	0.23	0.21	0.28	-0.24	-0.19	-0.21	0.06	0.14	0.05	-0.06	0.12	-0.22	0.11	-0.26
Jan. Mean T_{air}	0.13	-0.18	0.21	0.17	0.26	-0.23	-0.21	-0.26	-0.14	0.16	0.05	-0.03	-0.03	-0.24	0.10	-0.13
Feb. Mean T_{air}	0.20	-0.25	0.22	0.22	0.26	-0.20	-0.23	-0.24	-0.05	0.00	-0.03	-0.01	0.05	0.05	0.00	0.00
Mar. Mean T_{air}	0.21	-0.24	0.24	0.24	0.21	-0.22	-0.18	-0.19	-0.02	-0.01	0.02	-0.02	0.26	0.05	0.01	-0.06
Apr. Mean T_{air}	0.23	-0.24	0.23	0.24	0.20	-0.16	-0.19	-0.12	0.05	-0.07	-0.09	0.00	0.20	0.24	-0.03	-0.12
May Mean T_{air}	0.22	-0.23	0.25	0.24	0.19	-0.18	-0.16	-0.15	0.09	-0.07	0.00	0.06	0.15	0.20	0.07	0.09
Oct. Mean SWE	-0.19	0.23	-0.17	-0.23	-0.01	-0.02	-0.01	-0.03	-0.03	0.14	0.01	-0.09	0.48	-0.01	0.49	-0.01
Nov. Mean SWE	-0.22	0.25	-0.24	-0.25	0.07	-0.14	-0.12	-0.07	0.11	-0.08	-0.07	0.04	0.51	0.11	0.21	-0.04
Dec. Mean SWE	-0.24	0.22	-0.22	-0.22	0.17	-0.23	-0.18	-0.22	0.18	-0.14	-0.12	0.10	0.21	0.18	0.00	0.02
Jan. Mean SWE	-0.23	0.19	-0.18	-0.18	0.24	-0.27	-0.27	-0.27	0.16	-0.15	-0.15	0.14	0.01	0.14	-0.10	-0.04
Feb. Mean SWE	-0.23	0.19	-0.17	-0.19	0.24	-0.28	-0.29	-0.26	0.14	-0.14	-0.11	0.14	-0.12	0.13	-0.08	-0.01
Mar. Mean SWE	-0.24	0.20	-0.19	-0.19	0.23	-0.27	-0.28	-0.27	0.13	-0.12	-0.12	0.13	-0.16	0.05	-0.05	0.02
Apr. Mean SWE	-0.26	0.22	-0.22	-0.22	0.19	-0.21	-0.23	-0.23	0.07	-0.08	-0.08	0.09	-0.21	-0.15	-0.04	0.08
May Mean SWE	-0.26	0.20	-0.22	-0.24	0.13	-0.15	-0.18	-0.18	0.09	-0.03	-0.19	0.08	-0.08	-0.23	0.14	0.06
Presnowpack θ[c]	0.01	0.07	-0.04	0.03	-0.06	0.10	0.00	0.00	0.22	-0.19	-0.22	0.35	0.27	0.44	-0.75	-0.74
Presnowpack T_{soil}[c]	-0.06	0.02	-0.03	0.02	0.12	0.00	-0.17	-0.13	-0.53	0.49	0.54	-0.53	0.06	0.48	-0.19	-0.12
Presnowpack T_{air}	-0.09	0.07	-0.04	-0.06	0.20	-0.19	-0.22	-0.20	-0.48	0.50	0.49	-0.50	0.08	0.13	-0.11	-0.03

[a] Yearly total

[b] Mean for below-snow period

[c] At 20 cm depth

Table A.3. Results of the multiple regression analyses using below-snow T_{soil} as the dependent variable and the below-snow principal component axes as explanatory variables. Results for four separate analyses are shown (all years, 2007, 2009, and 2011). Regression coefficients for each principal component axis are shown with their standard error (S.E.), p value, and significance as explanatory variables in the model (*** for p < 0.001; ** for p < 0.01; * for p < 0.05).

	All years			2007			2009			2011		
Explanatory vars.	Coeff.	S.E.	p	Coeff.	S.E.	p	Coeff.	S.E.	p	Coeff.	S.E.	p
(Intercept)	0.735	0.023	0.000 ***	0.661	0.050	0.000 ***	0.548	0.058	0.000 ***	0.877	0.036	0.000 ***
PC 1	-0.023	0.007	0.001 **	0.017	0.014	0.234	-0.015	0.017	0.376	0.032	0.010	0.002 **
PC 2	0.140	0.009	0.000 ***	-0.089	0.021	0.000 ***	-0.153	0.023	0.000 ***	-0.113	0.014	0.000 ***
PC 3	-0.038	0.015	0.010 *	0.077	0.033	0.023 *	0.128	0.040	0.002 **	-0.074	0.024	0.002 **
PC 4	0.124	0.019	0.000 ***	0.236	0.044	0.000 ***	-0.148	0.059	0.013 *	-0.015	0.039	0.692
Model adj. R^2	0.216			0.280			0.282			0.316		

Table A.4. Results of the multiple regression analyses using winter quarter θ as the dependent variable and the below-snow principal component axes as explanatory variables. Results for four separate analyses are shown (all years, 2007, 2009, and 2011).Regression coefficients for each principal component axis are shown with their standard error (S.E.), p value, and significance as explanatory variables in the model (*** for p < 0.001; ** for p < 0.01; * for p < 0.05).

	All years			2007			2009			2011		
Explanatory vars.	Coeff.	S.E.	p	Coeff.	S.E.	p	Coeff.	S.E.	p	Coeff.	S.E.	p
(Intercept)	0.465	0.007	0.000 ***	0.489	0.015	0.000 ***	0.444	0.015	0.000 ***	0.570	0.015	0.000 ***
PC 1	0.004	0.002	0.044 *	-0.004	0.004	0.316	0.010	0.004	0.018 *	0.019	0.004	0.000 ***
PC 2	0.043	0.003	0.000 ***	-0.021	0.006	0.001 **	-0.047	0.006	0.000 ***	-0.043	0.006	0.000 ***
PC 3	0.018	0.004	0.000 ***	-0.051	0.010	0.000 ***	-0.017	0.010	0.088 .	0.015	0.010	0.128
PC 4	0.040	0.006	0.000 ***	0.093	0.014	0.000 ***	-0.088	0.015	0.000 ***	-0.043	0.016	0.008 **
Model adj. R^2	0.231			0.383			0.422			0.322		

Table A.5. Standard deviation and variance explained (percent and cumulative) by the first three principal component axes for the warm season PCA analyses. The results of four separate PCA analyses are shown, PCA using observations from all years together, and using 2007, 2009, and 2011 subsets of the observations.

	PC 1				PC 2				PC 3			
	All	2007	2009	2011	All	2007	2009	2011	All	2007	2009	2011
Std. Deviation	2.75	3.12	3.08	2.91	1.92	1.73	1.79	2.08	1.48	1.50	1.36	1.56
% Var. Explained	0.38	0.49	0.47	0.42	0.18	0.15	0.16	0.22	0.11	0.11	0.09	0.12
Cum. Var. Explained	0.38	0.49	0.47	0.42	0.56	0.64	0.63	0.64	0.67	0.75	0.73	0.76

Table A.6. Explanatory variables used in the warm season PCA analyses and their loading values on each of the first three principal component axes. Again, the results of four separate PCA analyses are shown (all years, 2007, 2009, and 2011). The highest loadings for each column were assumed to be the most important variables for the respective axis.

	PC 1				PC 2				PC 3			
	All	2007	2009	2011	All	2007	2009	2011	All	2007	2009	2011
Elevation	-0.28	0.29	-0.25	-0.26	0.16	0.08	-0.15	-0.21	0.03	0.02	-0.10	0.06
Total snow-covered days	-0.25	0.23	-0.24	-0.24	-0.27	-0.33	0.31	0.25	0.18	0.08	-0.05	0.18
Snow-free day	-0.22	0.14	-0.21	-0.23	-0.31	-0.39	0.38	0.28	0.20	0.20	-0.01	0.21
Peak SWE	-0.10	0.09	-0.09	-0.11	-0.31	-0.43	0.46	0.31	0.34	0.21	-0.11	0.32
Below-snow period T_{air}	0.22	-0.15	0.21	0.23	-0.15	-0.23	0.23	0.09	0.30	0.23	-0.25	0.35
Summer quarter mean T_{air}	0.34	-0.31	0.32	0.32	-0.11	-0.01	0.08	0.10	0.05	0.09	0.01	0.08
Apr. Mean T_{air}	0.30	-0.30	0.31	0.28	0.19	0.12	0.02	-0.23	0.13	0.13	-0.10	0.09
May Mean T_{air}	0.28	-0.31	0.30	0.31	0.17	0.06	-0.11	-0.13	0.08	0.11	-0.12	0.03
Jun. Mean T_{air}	0.27	-0.28	0.31	0.25	0.22	0.16	0.00	-0.27	0.13	0.16	-0.14	0.14
Jul. Mean T_{air}	0.33	-0.31	0.32	0.31	-0.03	-0.07	0.03	0.02	0.07	0.01	-0.03	0.09
Aug. Mean T_{air}	0.32	-0.31	0.32	0.32	-0.11	-0.02	0.05	0.10	0.08	0.08	-0.05	0.10
Sep. Mean T_{air}	0.28	-0.29	0.30	0.31	-0.16	0.09	0.15	0.15	-0.01	0.19	0.09	0.05
Summer quarter precip.	-0.16	0.21	-0.19	-0.16	0.36	0.29	-0.12	-0.33	0.35	0.34	-0.46	0.32
May precip.	-0.09	0.15	-0.08	-0.08	-0.34	-0.11	0.34	0.27	0.20	0.30	-0.09	0.36
Jun. Precip.	-0.01	-0.08	-0.07	-0.01	-0.24	-0.40	0.37	0.35	-0.02	0.17	0.21	-0.04
Jul. Precip	-0.13	0.16	-0.10	-0.15	0.31	0.29	-0.15	-0.29	0.18	0.24	-0.40	0.20
Aug. Precip	-0.15	0.20	-0.08	-0.15	0.22	0.26	0.18	-0.20	0.25	0.21	-0.02	0.29
Sep. Precip	-0.07	0.15	-0.16	-0.08	0.26	0.14	-0.19	-0.29	0.34	0.37	-0.36	0.33
Winter quarter 5 cm T_{soil}	0.06	-0.04	0.05	0.08	-0.03	0.06	0.16	0.07	0.41	0.47	-0.47	0.33
Winter quarter 20 cm θ	0.13	-0.10	0.13	0.17	-0.12	-0.09	0.22	0.08	0.35	0.26	-0.29	0.25

Table A.7. Results of the multiple regression analyses using warm season θ as the dependent variable and the warm season principal component axes as explanatory variables. Results for four separate analyses are shown (all years, 2007, 2009, and 2011). Regression coefficients for each principal component axis are shown with their standard error (S.E.), p value, and significance as explanatory variables in the model (*** for $p < 0.001$; ** for $p < 0.01$; * for $p < 0.05$).

	All years			2007			2009			2011		
Explanatory vars.	Coeff.	S.E.	p	Coeff.	S.E.	p	Coeff.	S.E.	p	Coeff.	S.E.	p
(Intercept)	0.275	0.005	0.000 ***	0.230	0.012	0.000 ***	0.271	0.012	0.000 ***	0.340	0.013	0.000 ***
PC 1	-0.022	0.002	0.000 ***	0.024	0.004	0.000 ***	-0.013	0.004	0.001 ***	-0.025	0.004	0.000 ***
PC 2	0.008	0.003	0.002 **	0.021	0.007	0.003 **	-0.002	0.006	0.809	-0.008	0.006	0.185
PC 3	0.020	0.003	0.000 ***	0.004	0.008	0.628	-0.011	0.009	0.214	0.023	0.008	0.006 **
Model adj. R^2	0.156			0.259			0.070			0.183		

APPENDIX B

ADDITIONAL HIDDEN CANYON SOIL TEMPERATURE AND WATER CONTENT FIGURES

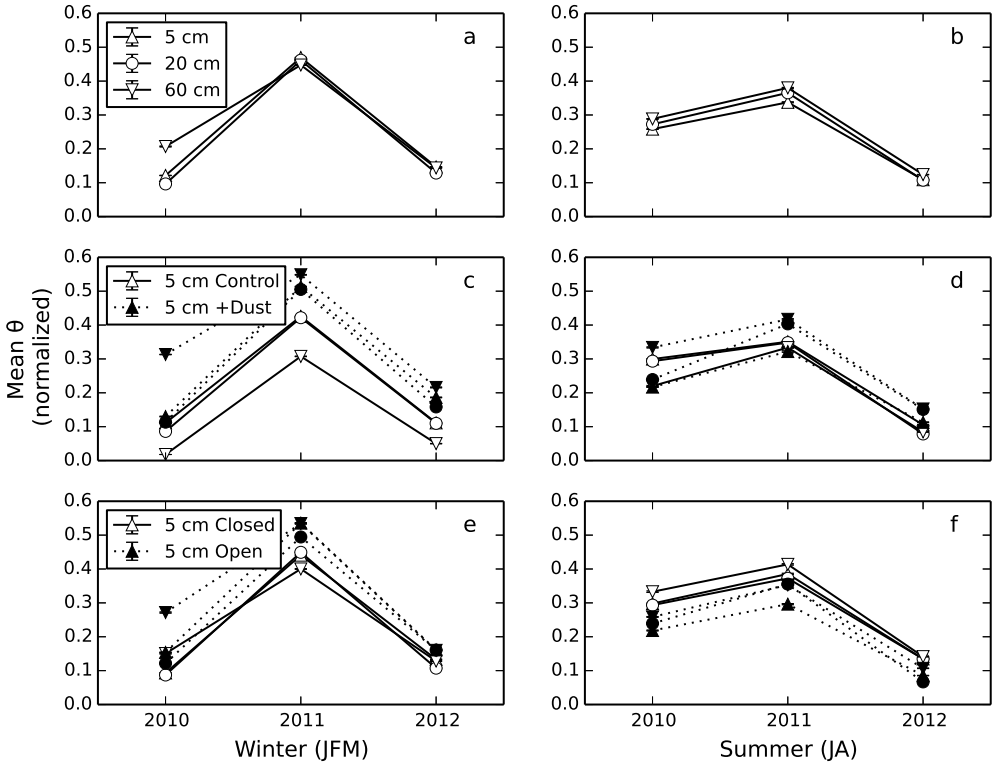

Figure B.1. Comparison of mean volumetric soil water content (θ, normalized) during winter (Jan., Feb., Mar.) and summer (Jul., Aug.) periods in the 3 years of the study. The mean of data from all sensors at each depth are shown with standard error bars, which are smaller than the symbol in many cases. September data were excluded from all summer means due to missing data in 2011.

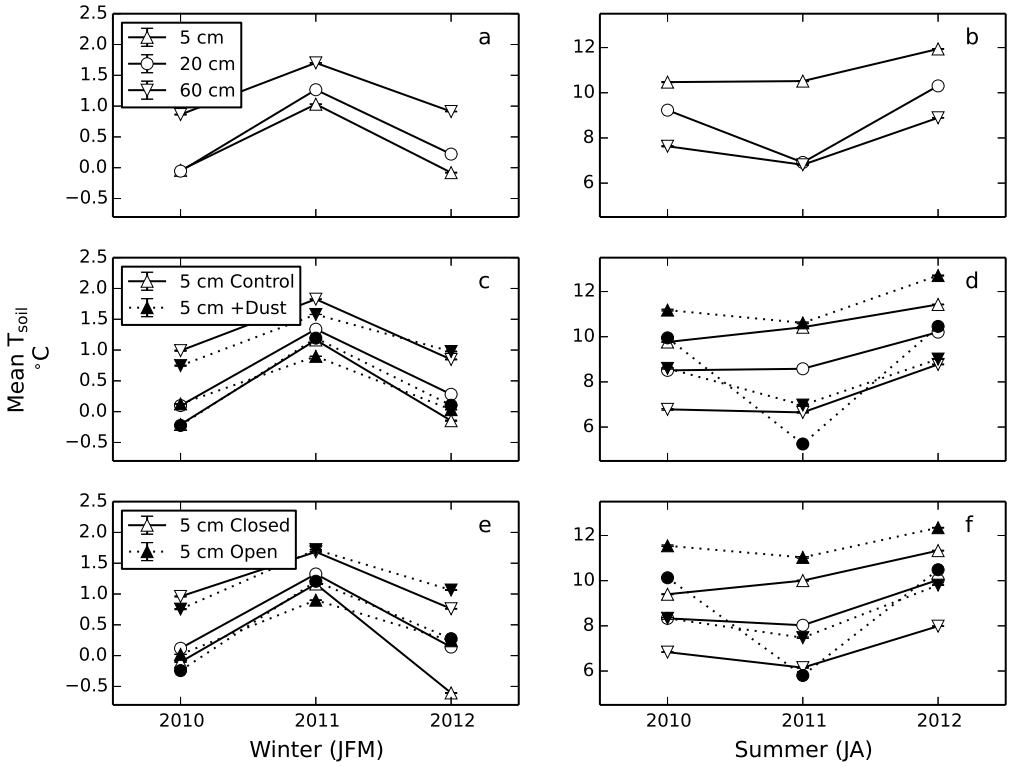

Figure B.2. Comparison of mean soil temperature during winter (Jan., Feb., Mar.) and summer (Jul., Aug.) periods in the 3 years of the study. The mean of the data from all sensors at each depth are shown with standard error bars, which are smaller than the symbol in many cases. September data were excluded from all summer means due to missing data in 2011.

APPENDIX C

CORRELATION TABLES FOR SNOTEL PRECIPITATION AND TEMPERATURE SUBGRADIENTS

Table C.1. Correlation coefficients (*r*) from linear regression of *precipitation subgradient* (constant elevation/MAT) carbon stocks on the variables shown in Table 4.2. Values in italics are signicant at p < 0.05. Asterisks indicate the statistical significance of the correlation (*** for p < 0.001; ** for p < 0.01; * for p < 0.05).

	Coarse wood	Litter	Organic layer	Mineral soil	Total
MAP	0.31	*-0.46**	0.17	*0.42**	0.33
P_{jas}	-0.23	0.14	-0.17	0.08	-0.11
SWE_p	0.28	*-0.41**	0.13	*0.47**	0.34
D_{sm}	0.16	*-0.49***	0.11	0.34	0.22
T_{sc}	0.12	*-0.51***	0.14	0.30	0.21
Stand age	-0.02	*0.55**	0.10	*-0.48**	-0.15
Basal area	*0.46**	*-0.56***	0.35	*0.46**	*0.49***
Leaf N	0.15	-0.24	0.45	-0.21	0.23
Soil N	*0.46**	*-0.48**	0.26	*0.76****	*0.58***
Litter C:N	-0.30	*-0.47**	-0.36	-0.04	-0.35

Table C.2. Correlation coefficients (*r*) from linear regression of *temperature subgradient* (constant MAP) carbon stocks on the variables shown in Table 4.2. Values in italics are signicant at p < 0.05. Asterisks indicate the statistical significance of the correlation (*** for p < 0.001; ** for p < 0.01; * for p < 0.05).

	Coarse wood	Litter	Organic layer	Mineral soil	Total
Elevation	-0.09	0.24	-0.17	*-0.51**	*-0.41**
MAT	0.08	-0.31	0.08	*0.56***	0.39
P_{jas}	0.01	0.16	-0.06	*-0.47**	-0.31
SWE_p	0.14	0.22	-0.17	0.06	-0.01
D_{sm}	-0.11	0.25	-0.26	-0.34	-0.35
T_{sc}	-0.05	0.26	-0.16	-0.39	-0.32
Stand age	-0.31	*0.55**	-0.20	-0.44	-0.40
Basal area	0.07	0.19	0.02	0.16	0.14
Leaf N	-0.09	-0.43	0.26	0.43	0.28
Soil N	0.33	-0.35	0.25	*0.77****	*0.65****
Litter C:N	-0.16	-0.06	-0.20	-0.29	-0.32

Table C.3. Correlation coefficients (*r*) from linear regression of $\delta^{13}C$ and $\delta^{15}N$ values of *precipitation subgradient* (constant elevation/MAT) organic matter pools on the variables shown in Table 4.2. Values in italics are signicant at p < 0.05. Asterisks indicate the statistical significance of the correlation (*** for p < 0.001; ** for p < 0.01; * for p < 0.05).

	$\delta^{13}C$			$\delta^{15}N$		
	Litter	Organic layer	Mineral soil	Litter	Organic layer	Mineral soil
MAP	-0.31	*-0.55***	*-0.43**	-0.07	-0.30	*-0.73****
P_{jas}	-0.35	-0.00	0.32	-0.05	0.07	0.37
SWE_p	-0.26	*-0.48**	*-0.46**	0.10	-0.16	*-0.57***
D_{sm}	*-0.45**	*-0.63****	*-0.60****	0.21	-0.09	*-0.62****
T_{sc}	*-0.47**	*-0.67****	*-0.66****	0.16	-0.17	*-0.65****
Stand age	*0.49**	*0.72****	*0.46**	*-0.65***	-0.27	-0.20
Basal area	-0.17	*-0.65****	*-0.41**	0.27	-0.07	*-0.59***
Leaf N	-0.03	*-0.77**	-0.29	0.46	0.03	0.06
Soil N	-0.10	*-0.52***	-0.02	*0.51***	0.20	-0.08
Litter C:N	0.09	-0.23	*-0.39**	*-0.42**	*-0.54***	*-0.43**

Table C.4. Correlation coefficients (*r*) from linear regression of $\delta^{13}C$ and $\delta^{15}N$ values of *temperature subgradient* (constant MAP) organic matter pools on the variables shown in Table 4.2. Values in italics are signicant at p < 0.05. Asterisks indicate the statistical significance of the correlation (*** for p < 0.001; ** for p < 0.01; * for p < 0.05).

	$\delta^{13}C$			$\delta^{15}N$		
	Litter	Organic layer	Mineral soil	Litter	Organic layer	Mineral soil
Elevation	0.24	*0.63***	0.08	*-0.77****	*-0.64****	-0.05
MAT	-0.20	*-0.70****	-0.14	*0.78****	*0.62***	0.10
P_{jas}	0.02	*0.54***	0.13	*-0.64****	-0.37	0.14
SWE_p	0.12	0.36	-0.07	-0.39	*-0.49**	-0.19
D_{sm}	0.20	*0.71****	0.01	*-0.72****	*-0.65****	-0.24
T_{sc}	0.20	*0.74****	0.13	*-0.76****	*-0.66****	-0.18
Stand age	-0.22	*0.62***	0.13	*-0.61***	-0.24	0.02
Basal area	0.32	0.07	-0.23	0.05	-0.33	*-0.57***
Leaf N	0.36	-0.54	0.12	*0.90****	0.55	-0.32
Soil N	-0.34	*-0.69****	-0.02	*0.86****	*0.75****	0.22
Litter C:N	*0.56***	0.34	0.02	-0.36	*-0.56***	-0.16

REFERENCES

Aanderud, Z. T., S. E. Jones, D. R. Schoolmaster Jr., N. Fierer, and J. T. Lennon. 2013. Sensitivity of soil respiration and microbial communities to altered snowfall. Soil Biology and Biochemistry 57:217–227.

Abu-Hamdeh, N. H., and R. C. Reeder. 2000. Soil thermal conductivity. Soil Science Society of America Journal 64:1285.

Adair, E. C., S. E. Hobbie, and R. K. Hobbie. 2010. Single-pool exponential decomposition models: potential pitfalls in their use in ecological studies. Ecology 91:1225–1236.

Adair, E. C., W. J. Parton, S. J. Del Grosso, W. L. Silver, M. E. Harmon, S. A. Hall, I. C. Burke, and S. C. Hart. 2008. Simple three-pool model accurately describes patterns of long-term litter decomposition in diverse climates. Global Change Biology 14:2636–2660.

Adams, D. K., and A. C. Comrie. 1997. The North American monsoon. Bulletin of the American Meteorological Society 78:2197–2213.

Aerts, R. 1997. Climate, leaf litter chemistry and leaf litter decomposition in terrestrial ecosystems: a triangular relationship. Oikos 79:439–449.

Amundson, R. 2001. The carbon budget in soils. Annual Review of Earth and Planetary Sciences 29:535–562.

Amundson, R. G., O. A. Chadwick, and J. M. Sowers. 1989. A comparison of soil climate and biological activity along an elevation gradient in the eastern mojave desert. Oecologia 80:395–400.

Amundson, R., and H. Jenny. 1997. On a state factor model of ecosystems. BioScience 47:536–543.

Amundson, R., A. T. Austin, E. a. G. Schuur, K. Yoo, V. Matzek, C. Kendall, A. Uebersax, D. Brenner, and W. T. Baisden. 2003. Global patterns of the isotopic composition of soil and plant nitrogen. Global Biogeochemical Cycles 17.

Anderegg, W. R. L., J. A. Berry, D. D. Smith, J. S. Sperry, L. D. L. Anderegg, and C. B. Field. 2011. The roles of hydraulic and carbon stress in a widespread climate-induced forest die-off. Proceedings of the National Academy of Sciences:201107891.

Arthur, M. A., and T. J. Fahey. 1992. Biomass and nutrients in an engelmann spruce–subalpine fir forest in north central Colorado: pools, annual production, and internal cycling. Canadian Journal of Forest Research 22:315–325.

Austin, A. T., and P. M. Vitousek. 1998. Nutrient dynamics on a precipitation gradient in Hawai'i. Oecologia 113:519–529.

Bales, R. C., J. W. Hopmans, O'GeenA. T., M. Meadows, P. C. Hartsough, P. Kirchner, C. T. Hunsaker, and D. Beaudette. 2011. Soil moisture response to snowmelt and rainfall in a Sierra Nevada mixed-conifer forest. Vadose Zone Journal 10:786.

Bales, R. C., N. P. Molotch, T. H. Painter, M. D. Dettinger, R. Rice, and J. Dozier. 2006. Mountain hy-

drology of the western United States. Water Resources Research 42:doi:10.1029/2005WR004387.

Ballantyne, A. P., J. Brahney, D. Fernandez, C. L. Lawrence, J. Saros, and J. C. Neff. 2011. Biogeochemical response of alpine lakes to a recent increase in dust deposition in the southwestern, US. Biogeosciences 8:2689–2706.

Baptist, F., N. G. Yoccoz, and P. Choler. 2009. Direct and indirect control by snow cover over decomposition in alpine tundra along a snowmelt gradient. Plant and Soil 328:397–410.

Barichivich, J., K. R. Briffa, T. J. Osborn, T. M. Melvin, and J. Caesar. 2012. Thermal growing season and timing of biospheric carbon uptake across the northern hemisphere. Global Biogeochemical Cycles 26:GB4015.

Barnett, T. P., J. C. Adam, and D. P. Lettenmaier. 2005. Potential impacts of a warming climate on water availability in snow-dominated regions. Nature 438:303–309.

Barnett, T. P., D. W. Pierce, H. G. Hidalgo, C. Bonfils, B. D. Santer, T. Das, G. Bala, A. W. Wood, T. Nozawa, A. A. Mirin, D. R. Cayan, and M. D. Dettinger. 2008. Human-induced changes in the hydrology of the western United States. Science 319:1080–1083.

Bartlett, M. G., D. S. Chapman, and R. N. Harris. 2004. Snow and the ground temperature record of climate change. Journal of Geophysical Research 109:14.

Bauerle, W. L., R. Oren, D. A. Way, S. S. Qian, P. C. Stoy, P. E. Thornton, J. D. Bowden, F. M. Hoffman, and R. F. Reynolds. 2012. Photoperiodic regulation of the seasonal pattern of photosynthetic capacity and the implications for carbon cycling. Proceedings of the National Academy of Sciences 109:8612–8617.

Beedlow, P. A., E. H. Lee, D. T. Tingey, R. S. Waschmann, and C. A. Burdick. 2013. The importance of seasonal temperature and moisture patterns on growth of douglas-fir in western Oregon, USA. Agricultural and Forest Meteorology 169:174–185.

Bellingham, K., and M. Fleming. (n.d.). Evaluation of the stevens hydra probe's temperature measurements from -30 to 40 degrees celsius. Technical paper. Stevens Water Monitoring Systems, Inc. Portland, OR, USA.

Biederman, J. A., P. D. Brooks, A. A. Harpold, D. J. Gochis, E. Gutmann, D. E. Reed, E. Pendall, and B. E. Ewers. 2012. Multiscale observations of snow accumulation and peak snowpack following widespread, insect-induced lodgepole pine mortality. Ecohydrology 7:150–162.

Bird, M. I., E. M. Veenendaal, and J. J. Lloyd. 2004. Soil carbon inventories and δ13C along a moisture gradient in botswana. Global Change Biology 10:342–349.

Birdsey, R. A. 1992. Carbon storage and accumulation in United States forest ecosystems. US Department of Agriculture, Forest Service Washington, DC.

Borken, W., and E. Matzner. 2009. Reappraisal of drying and wetting effects on c and n mineralization and fluxes in soils. Global Change Biology 15:808–824.

Boutin, R., and G. Robitaille. 1995. Increased soil nitrate losses under mature sugar maple trees affected by experimentally induced deep frost. Canadian Journal of Forest Research 25:588–602.

Bowling, D. R., and W. J. Massman. 2011. Persistent wind-induced enhancement of diffusive CO2 transport in a mountain forest snowpack. Journal of Geophysical Research 116.

Bowling, D. R., N. G. McDowell, B. J. Bond, B. E. Law, and J. R. Ehleringer. 2002. 13C content of ecosystem respiration is linked to precipitation and vapor pressure deficit. Oecologia 131:113–

124.

Bradford, J. B., R. A. Birdsey, L. A. Joyce, and M. G. Ryan. 2008. Tree age, disturbance history, and carbon stocks and fluxes in subalpine Rocky Mountain forests. Global Change Biology 14:2882–2897.

Brooks, P. D., and M. W. Williams. 1999. Snowpack controls on nitrogen cycling and export in seasonally snow-covered catchments. Hydrological Processes 13:2177–2190.

Brooks, P. D., P. Grogan, P. H. Templer, P. Groffman, M. G. Öquist, and J. Schimel. 2011. Carbon and nitrogen cycling in snow-covered environments. Geography Compass 5:682–699.

Brooks, P. D., D. McKnight, and K. Elder. 2005. Carbon limitation of soil respiration under winter snowpacks: potential feedbacks between growing season and winter carbon fluxes. Global Change Biology 11:231–238.

Brooks, P. D., S. K. Schmidt, and M. W. Williams. 1997. Winter production of CO2 and N2O from alpine tundra: environmental controls and relationship to inter-system c and n fluxes. Oecologia 110:403–413.

Brooks, P. D., M. W. Williams, and S. K. Schmidt. 1996. Microbial activity under alpine snowpacks, Niwot Ridge, Colorado. Biogeochemistry 32:93–113.

Brooks, P., M. Williams, and S. Schmidt. 1998. Inorganic nitrogen and microbial biomass dynamics before and during spring snowmelt. Biogeochemistry 43:1–15.

Brooks, P., M. Williams, D. Walker, and S. Schmidt. 1995. The Niwot Ridge snow fence experiment: biogeochemical responses to changes in the seasonal snowpack. Pages 293–302 *in* Biogeochemistry of seasonally snow-covered catchments.

Brown, R. D., and P. W. Mote. 2009. The response of northern hemisphere snow cover to a changing climate*. Journal of Climate 22:2124–2145.

Brown, T. J., B. L. Hall, and A. L. Westerling. 2004. The impact of twenty-first century climate change on wildland fire danger in the western United States: an applications perspective. Climatic Change 62:365–388.

Brown-Mitic, C., W. Shuttleworth, R. Chawn Harlow, J. Petti, E. Burke, and R. Bales. 2007. Seasonal water dynamics of a sky island subalpine forest in semi-arid southwestern United States. Journal of Arid Environments 69:237–258.

Callesen, I., J. Liski, K. Raulund-Rasmussen, M. T. Olsson, L. Tau-Strand, L. Vesterdal, and C. J. Westman. 2003. Soil carbon stores in nordic well-drained forest soils—relationships with climate and texture class. Global Change Biology 9:358–370.

Campbell, G. S., J. D. Jungbauer Jr, W. R. Bidlake, and R. D. Hungerford. 1994. Predicting the effect of temperature on soil thermal conductivity. Soil Science 158:307–313.

Campbell, J. L., O. J. Sun, and B. E. Law. 2004. Disturbance and net ecosystem production across three climatically distinct forest landscapes. Global Biogeochemical Cycles 18.

Case, M. J., and D. L. Peterson. 2005. Fine-scale variability in growth climate relationships of douglas-fir, north Cascade range, Washington. Canadian Journal of Forest Research 35:2743–2755.

Cayan, D. R., T. Das, D. W. Pierce, T. P. Barnett, M. Tyree, and A. Gershunov. 2010. Future dryness in the southwest US and the hydrology of the early 21st century drought. Proceedings of the National Academy of Sciences 107:21271–21276.

Clark, M. P., J. Hendrikx, A. G. Slater, D. Kavetski, B. Anderson, N. J. Cullen, T. Kerr, E. Örn Hreinsson, and R. A. Woods. 2011. Representing spatial variability of snow water equivalent in hydrologic and land-surface models: a review. Water Resources Research 47:W07539.

Clarke, A., and K. P. P. Fraser. 2004. Why does metabolism scale with temperature? Functional Ecology 18:243–251.

Clow, D. W. 2010. Changes in the timing of snowmelt and streamflow in Colorado: a response to recent warming. Journal of Climate 23:2293–2306.

Comerford, D. P., P. G. Schaberg, P. H. Templer, A. M. Socci, J. L. Campbell, and K. F. Wallin. 2013. Influence of experimental snow removal on root and canopy physiology of sugar maple trees in a northern hardwood forest. Oecologia 171:261–269.

Conant, R. T., J. M. Klopatek, and C. C. Klopatek. 2000. Environmental factors controlling soil respiration in three semiarid ecosystems. Soil Science Society of America Journal 64:383–390.

Conant, R. T., J. M. Klopatek, R. C. Malin, and C. C. Klopatek. 1998. Carbon pools and fluxes along an environmental gradient in northern Arizona. Biogeochemistry 43:43–61.

Conway, H., A. Gades, and C. F. Raymond. 1996. Albedo of dirty snow during conditions of melt. Water Resources Research 32:1713–1718.

Craine, J. M., A. J. Elmore, M. P. M. Aidar, M. Bustamante, T. E. Dawson, E. A. Hobbie, A. Kahmen, M. C. Mack, K. K. McLauchlan, A. Michelsen, G. B. Nardoto, L. H. Pardo, J. Peñuelas, P. B. Reich, E. A. G. Schuur, W. D. Stock, P. H. Templer, R. A. Virginia, J. M. Welker, and I. J. Wright. 2009. Global patterns of foliar nitrogen isotopes and their relationships with climate, mycorrhizal fungi, foliar nutrient concentrations, and nitrogen availability. New Phytologist 183:980–992.

Daly, C., M. Halbleib, J. I. Smith, W. P. Gibson, M. K. Doggett, G. H. Taylor, J. Curtis, and P. P. Pasteris. 2008. Physiographically sensitive mapping of climatological temperature and precipitation across the conterminous United States. International Journal of Climatology 28:2031–2064.

Daly, C., R. P. Neilson, and D. L. Phillips. 1994. A statistical-topographic model for mapping climatological precipitation over mountainous terrain. Journal of Applied Meteorology 33:140–158.

Davidson, E. A., E. Belk, and R. D. Boone. 1998. Soil water content and temperature as independent or confounded factors controlling soil respiration in a temperate mixed hardwood forest. Global Change Biology 4:217–227.

Davidson, E., and I. Janssens. 2006. Temperature sensitivity of soil carbon decomposition and feedbacks to climate change. Nature 440:165–173.

DeLuca, T. H., and G. H. Aplet. 2008. Charcoal and carbon storage in forest soils of the Rocky Mountain west. Frontiers in Ecology and the Environment 6:18–24.

DeLuca, T. H., D. R. Keeney, and G. W. McCarty. 1992. Effect of freeze-thaw events on mineralization of soil nitrogen. Biology and Fertility of Soils 14:116–120.

Dettinger, M. D., and D. R. Cayan. 1995. Large-scale atmospheric forcing of recent trends toward early snowmelt runoff in California. Journal of Climate 8:606–623.

Dixon, R. K., S. Brown, R. A. Houghton, A. M. Solomon, M. C. Trexler, and J. Wisniewski. 1994. Carbon pools and flux of global forest ecosystems. Science 263:185–190.

Djukic, I., F. Zehetner, M. Tatzber, and M. H. Gerzabek. 2010. Soil organic-matter stocks and characteristics along an alpine elevation gradient. Journal of Plant Nutrition and Soil Science 173:30–38.

Dyer, J. L., and T. L. Mote. 2007. Trends in snow ablation over North America. International Journal of Climatology 27:739–748.

Edwards, A. C., R. Scalenghe, and M. Freppaz. 2007. Changes in the seasonal snow cover of alpine regions and its effect on soil processes: a review. Quaternary International 162:172–181.

Ehleringer, J. R., and T. E. Cerling. 1995. Atmospheric CO2 and the ratio of intercellular to ambient CO2 concentrations in plants. Tree Physiology 15:105–111.

Ehleringer, J., D. Bowling, L. Flanagan, J. Fessenden, B. Helliker, L. Martinelli, and J. Ometto. 2002. Stable isotopes and carbon cycle processes in forests and grasslands. Plant Biology 4:181–189.

Eiriksson, D., M. Whitson, C. H. Luce, H. P. Marshall, J. Bradford, S. G. Benner, T. Black, H. Hetrick, and J. P. McNamara. 2013. An evaluation of the hydrologic relevance of lateral flow in snow at hillslope and catchment scales. Hydrological Processes 27:640–654.

Elberling, B., and K. K. Brandt. 2003. Uncoupling of microbial CO2 production and release in frozen soil and its implications for field studies of arctic c cycling. Soil Biology and Biochemistry 35:263–272.

Ellis, C. R., J. W. Pomeroy, R. L. Essery, and T. E. Link. 2011. Effects of needleleaf forest cover on radiation and snowmelt dynamics in the Canadian Rocky Mountains. Canadian Journal of Forest Research 41:608–620.

Ensminger, I., D. Sveshnikov, D. A. Campbell, C. Funk, S. Jansson, J. Lloyd, O. Shibistova, and G. Öquist. 2004. Intermittent low temperatures constrain spring recovery of photosynthesis in boreal scots pine forests. Global Change Biology 10:995–1008.

Fang, C., and J. B. Moncrieff. 2001. The dependence of soil CO2 efflux on temperature. Soil Biology & Biochemistry 33:155–165.

Farrell, R. E., P. J. Sandercock, D. J. Pennock, and C. Van Kessel. 1996. Landscape-scale variations in leached nitrate: relationship to denitrification and natural nitrogen-15 abundance. Soil Science Society of America Journal 60:1410.

Fassnacht, S., M. Williams, and M. Corrao. 2009. Changes in the surface roughness of snow from millimetre to metre scales. Ecological Complexity 6:221–229.

Feng, X., L. L. Nielsen, and M. J. Simpson. 2007. Responses of soil organic matter and microorganisms to freeze–thaw cycles. Soil Biology and Biochemistry 39:2027–2037.

Filippa, G., M. Freppaz, M. W. Williams, D. Helmig, D. Liptzin, B. Seok, B. Hall, and K. Chowanski. 2009. Winter and summer nitrous oxide and nitrogen oxides fluxes from a seasonally snow-covered subalpine meadow at Niwot Ridge, Colorado. Biogeochemistry 95:131–149.

Fitzhugh, R. D., C. T. Driscoll, P. M. Groffman, G. L. Tierney, T. J. Fahey, and J. P. Hardy. 2001. Effects of soil freezing disturbance on soil solution nitrogen, phosphorus, and carbon chemistry in a northern hardwood ecosystem. Biogeochemistry 56:215–238.

Flerchinger, G. N., K. R. Cooley, C. L. Hanson, and M. S. Seyfried. 1998. A uniform versus an aggregated water balance of a semi-arid watershed. Hydrological Processes 12:331–342.

Frazer, G. W., C. Canham, and K. Lertzman. 1999. Gap light analyzer (GLA), version 2.0: imaging software to extract canopy structure and gap light transmission indices from true-colour fisheye photographs, users manual and program documentation. Simon Fraser University, Burnaby, B.C.; Institute of Ecosystem Studies, Millbrook, New York.

Frei, A., and D. A. Robinson. 1999. Northern hemisphere snow extent: regional variability 1972–1994. International Journal of Climatology 19:1535–1560.

Gao, H., Q. Tang, X. Shi, C. Zhu, T. Bohn, F. Su, J. Sheffield, M. Pan, D. Lettenmaier, and E. Wood. 2010. Water budget record from variable infiltration capacity (VIC) model algorithm theoretical basis document. Algorithm Theoretical Basis Document for Terrestrial Water Cycle Data Records (in review).

Garten, C. T., and P. J. Hanson. 2006. Measured forest soil c stocks and estimated turnover times along an elevation gradient. Geoderma 136:342–352.

Garten Jr, C. T., W. M. P. Iii, P. J. Hanson, and L. W. Cooper. 1999. Forest soil carbon inventories and dynamics along an elevation gradient in the southern Appalachian Mountains. Biogeochemistry 45:115–145.

Gholz, H. L. 1982. Environmental limits on aboveground net primary production, leaf area, and biomass in vegetation zones of the Pacific Northwest. Ecology 63:469–481.

Gholz, H. L., D. A. Wedin, S. M. Smitherman, M. E. Harmon, and W. J. Parton. 2000. Long-term dynamics of pine and hardwood litter in contrasting environments: toward a global model of decomposition. Global Change Biology 6:751–765.

Gillies, R. R., S.-Y. Wang, and M. R. Booth. 2012. Observational and synoptic analyses of the winter precipitation regime change over Utah. Journal of Climate 25:4679–4698.

Gleason, K. E., A. W. Nolin, and T. R. Roth. 2013. Charred forests increase snowmelt: effects of burned woody debris and incoming solar radiation on snow ablation. Geophysical Research Letters 40:4654–4661.

Goulden, M. L., R. G. Anderson, R. C. Bales, A. E. Kelly, M. Meadows, and G. C. Winston. 2012. Evapotranspiration along an elevation gradient in California's Sierra Nevada. Journal of Geophysical Research 117:G03028.

Gower, S. T., R. E. McMurtrie, and D. Murty. 1996. Aboveground net primary production decline with stand age: potential causes. Trends in Ecology & Evolution 11:378–382.

Gower, S. T., K. A. Vogt, and C. C. Grier. 1992. Carbon dynamics of Rocky Mountain Douglas-fir: influence of water and nutrient availability. Ecological Monographs 62:43–65.

Grayson, R. B., A. W. Western, F. H. S. Chiew, and G. Blöschl. 1997. Preferred states in spatial soil moisture patterns: local and nonlocal controls. Water Resources Research 33:2897–2908.

Grier, C. G., and S. W. Running. 1977. Leaf area of mature northwestern coniferous forests: relation to site water balance. Ecology:893–899.

Groffman, P. M., C. T. Driscoll, T. J. Fahey, J. P. Hardy, R. D. Fitzhugh, and G. L. Tierney. 2001. Colder soils in a warmer world: a snow manipulation study in a northern hardwood forest ecosystem. Biogeochemistry 56:135–150.

Groffman, P. M., J. P. Hardy, C. T. Driscoll, and T. J. Fahey. 2006. Snow depth, soil freezing, and fluxes of carbon dioxide, nitrous oxide and methane in a northern hardwood forest. Global Change Biology 12:1748–1760.

Groffman, P., J. Hardy, S. Fashu-Kanu, C. Driscoll, N. Cleavitt, T. Fahey, and M. Fisk. 2011. Snow depth, soil freezing and nitrogen cycling in a northern hardwood forest landscape. Biogeochemistry 102:223–238.

Grogan, P., L. Illeris, A. Michelsen, and S. Jonasson. 2001. Respiration of recently-fixed plant carbon dominates mid-winter ecosystem CO2 production in sub-arctic heath tundra. Climatic Change 50:129–142.

Grogan, P., A. Michelsen, P. Ambus, and S. Jonasson. 2004. Freeze–thaw regime effects on carbon and nitrogen dynamics in sub-arctic heath tundra mesocosms. Soil Biology and Biochemistry 36:641–654.

Groisman, P. Y., T. R. Karl, R. W. Knight, and G. L. Stenchikov. 1994. Changes of snow cover, temperature, and radiative heat balance over the northern hemisphere. Journal of Climate 7:1633–1656.

Grundstein, A., P. Todhunter, and T. Mote. 2005. Snowpack control over the thermal offset of air and soil temperatures in eastern North Dakota. Geophysical Research Letters 32:4.

Guo, Y., P. Gong, R. Amundson, and Q. Yu. 2006. Analysis of factors controlling soil carbon in the conterminous United States. Soil Science Society of America Journal 70:601.

Haei, M., M. G. Öquist, I. Buffam, A. Ågren, P. Blomkvist, K. Bishop, M. Ottosson Löfvenius, and H. Laudon. 2010. Cold winter soils enhance dissolved organic carbon concentrations in soil and stream water. Geophysical Research Letters 37:L08501.

Hahnenberger, M., and K. Nicoll. 2012. Meteorological characteristics of dust storm events in the eastern Great Basin of Utah, U.S.A. Atmospheric Environment 60:601–612.

Hamlet, A. F., P. W. Mote, M. P. Clark, and D. P. Lettenmaier. 2005. Effects of temperature and precipitation variability on snowpack trends in the western United States. Journal of Climate 18:4545–4561.

Hamlet, A. F., P. W. Mote, M. P. Clark, and D. P. Lettenmaier. 2007. Twentieth-century trends in runoff, evapotranspiration, and soil moisture in the western United States. Journal of Climate 20:1468–1486.

Handley, L. L., A. T. Austin, G. R. Stewart, D. Robinson, C. M. Scrimgeour, J. A. Raven, T. H. E. Heaton, and S. Schmidt. 1999. The 15N natural abundance (δ15N) of ecosystem samples reflects measures of water availability. Functional Plant Biology 26:185–199.

Hansen, J., and L. Nazarenko. 2004. Soot climate forcing via snow and ice albedos. Proceedings of the National Academy of Sciences of the United States of America 101:423–428.

Hardy, J. P., R. E. Davis, R. Jordan, X. Li, C. Woodcock, W. Ni, and J. C. McKenzie. 1997. Snow ablation modeling at the stand scale in a boreal jack pine forest. Journal of Geophysical Research: Atmospheres 102:29397–29405.

Hardy, J. P., P. M. Groffman, R. D. Fitzhugh, K. S. Henry, A. T. Welman, J. D. Demers, T. J. Fahey, C. T. Driscoll, G. L. Tierney, and S. Nolan. 2001. Snow depth manipulation and its influence on soil frost and water dynamics in a northern hardwood forest. Biogeochemistry 56:151–174.

Hardy, J. P., R. Melloh, P. Robinson, and R. Jordan. 2000. Incorporating effects of forest litter in a snow process model. Hydrological Processes 14:3227–3237.

Hardy, J., R. Melloh, G. Koenig, D. Marks, A. Winstral, J. Pomeroy, and T. Link. 2004. Solar radiation transmission through conifer canopies. Agricultural and Forest Meteorology 126:257–270.

Harmon, M. E., W. L. Silver, B. Fasth, H. U. A. Chen, I. C. Burke, W. J. Parton, S. C. Hart, and W. S. Currie. 2009. Long-term patterns of mass loss during the decomposition of leaf and fine root litter: an intersite comparison. Global Change Biology 15:1320–1338.

Harmon, M. E., C. W. Woodall, B. Fasth, and J. Sexton. 2008. Woody detritus density and density reduction factors for tree species in the United States: a synthesis. US Department of Agriculture, Forest Service, Northern Research Station.

Harpold, A., P. Brooks, S. Rajagopal, I. Heidbuchel, A. Jardine, and C. Stielstra. 2012. Changes in snowpack accumulation and ablation in the intermountain west. Water Resources Research 48.

Haverkamp, R., F. J. Leij, C. Fuentes, A. Sciortino, and P. J. Ross. 2005. Soil water retention. Soil Science Society of America Journal 69:1881.

Havranek, W. M., and U. Benecke. 1978. The influence of soil moisture on water potential, transpiration and photosynthesis of conifer seedlings. Plant and Soil 49:91–103.

Hedstrom, N. R., and J. W. Pomeroy. 1998. Measurements and modelling of snow interception in the boreal forest. Hydrological Processes 12:1611–1625.

Hentschel, K., W. Borken, T. Zuber, C. Bogner, B. Huwe, and E. Matzner. 2009. Effects of soil frost on nitrogen net mineralization, soil solution chemistry and seepage losses in a temperate forest soil. Global Change Biology 15:825–836.

Higgins, R. W., Y. Yao, and X. L. Wang. 1997. Influence of the North American monsoon system on the US summer precipitation regime. Journal of Climate 10:2600–2622.

Hobbie, E. A., and A. P. Ouimette. 2009. Controls of nitrogen isotope patterns in soil profiles. Biogeochemistry 95:355–371.

Hobbie, S. E., and F. S. Chapin. 1996. Winter regulation of tundra litter carbon and nitrogen dynamics. Biogeochemistry 35:327–338.

Högberg, P., L. Högbom, H. Schinkel, M. Högberg, C. Johannisson, and H. Wallmark. 1996. 15N abundance of surface soils, roots and mycorrhizas in profiles of european forest soils. Oecologia 108:207–214.

Homann, P. S., J. S. Kapchinske, and A. Boyce. 2007. Relations of mineral-soil c and n to climate and texture: regional differences within the conterminous USA. Biogeochemistry 85:303–316.

Homann, P. S., P. Sollins, H. N. Chappell, and A. G. Stangenberger. 1995. Soil organic carbon in a mountainous, forested region: relation to site characteristics. Soil Science Society of America Journal 59:1468–1475.

Hood, E. W., M. W. Williams, and N. Caine. 2003. Landscape controls on organic and inorganic nitrogen leaching across an Alpine/Subalpine ecotone, Green Lakes Valley, Colorado Front Range. Ecosystems 6:0031–0045.

Houghton, R. A., and J. L. Hackler. 2000. Changes in terrestrial carbon storage in the United States. 1: the roles of agriculture and forestry. Global Ecology and Biogeography 9:125–144.

Hu, J., D. J. P. Moore, S. P. Burns, and R. K. Monson. 2010. Longer growing seasons lead to less carbon sequestration by a subalpine forest. Global Change Biology 16:771–783.

Hultine, K. R., and J. D. Marshall. 2000. Altitude trends in conifer leaf morphology and stable carbon isotope composition. Oecologia 123:32–40.

Jaeger III, C. H., R. K. Monson, M. C. Fisk, and S. K. Schmidt. 1999. Seasonal partitioning of nitrogen by plants and soil microorganisms in an alpine ecosystem. Ecology 80:1883–1891.

Jenkins, J. C., D. C. Chojnacky, L. S. Heath, and R. A. Birdsey. 2003. National-scale biomass estimators for United States tree species. Forest Science 49:12–35.

Jenny, H. 1941. Factors of soil formation: a system of quantitative pedology. Republished in 1994. Dover Publications, Inc.New York.

Jobbágy, E., and R. Jackson. 2000. The vertical distribution of soil organic carbon and its relation to climate and vegetation. Ecological Applications 10:423–436.

Kapnick, S., and A. Hall. 2012. Causes of recent changes in western North American snowpack. Climate Dynamics 38:1885–1899.

Kielland, K., K. Olson, R. W. Ruess, and R. D. Boone. 2006. Contribution of winter processes to soil nitrogen flux in taiga forest ecosystems. Biogeochemistry 81:349–360.

Kirschbaum, M. U. F. 1995. The temperature dependence of soil organic matter decomposition, and the effect of global warming on soil organic c storage. Soil Biology and Biochemistry 27:753–760.

Klopatek, J. M. 2002. Belowground carbon pools and processes in different age stands of douglas-fir. Tree Physiology 22:197–204.

Knowles, N., M. D. Dettinger, and D. R. Cayan. 2006. Trends in snowfall versus rainfall in the western United States. Journal of Climate 19:4545–4559.

Koh, S. C., B. Demmig-Adams, and W. W. Adams. 2009. Novel patterns of seasonal photosynthetic acclimation, including interspecific differences, in conifers over an altitudinal gradient. Arctic, Antarctic, and Alpine Research 41:317–322.

Koivusalo, H., and T. Kokkonen. 2002. Snow processes in a forest clearing and in a coniferous forest. Journal of Hydrology 262:145–164.

Körner, C. 1998. A re-assessment of high elevation treeline positions and their explanation. Oecologia 115:445–459.

Körner, C., and J. Paulsen. 2004. A world-wide study of high altitude treeline temperatures. Journal of Biogeography 31:713–732.

Körner, C., G. D. Farquhar, and S. C. Wong. 1991. Carbon isotope discrimination by plants follows latitudinal and altitudinal trends. Oecologia 88:30–40.

Kueppers, L. M., and J. Harte. 2005. Subalpine forest carbon cycling: short- and long-term influence of climate and species. Ecological Applications 15:1984–1999.

Kueppers, L. M., J. Southon, P. Baer, and J. Harte. 2004. Dead wood biomass and turnover time, measured by radiocarbon, along a subalpine elevation gradient. Oecologia 141:641–651.

Kunkel, M. L., A. N. Flores, T. J. Smith, J. P. McNamara, and S. G. Benner. 2011. A simplified approach for estimating soil carbon and nitrogen stocks in semi-arid complex terrain. Geoderma 165:1–11.

Lajtha, K., and J. Getz. 1993. Photosynthesis and water-use efficiency in pinyon-juniper communities along an elevation gradient in northern new mexico. Oecologia 94:95–101.

Law, B. E., O. J. Sun, J. Campbell, S. Van Tuyl, and P. E. Thornton. 2003. Changes in carbon storage and fluxes in a chronosequence of ponderosa pine. Global Change Biology 9:510–524.

Law, B. E., D. Turner, J. Campbell, O. J. Sun, S. Van Tuyl, W. D. Ritts, and W. B. Cohen. 2004. Disturbance and climate effects on carbon stocks and fluxes across western Oregon USA. Global Change Biology 10:1429–1444.

Lawler, R. R., and T. E. Link. 2011. Quantification of incoming all-wave radiation in discontinuous forest canopies with application to snowmelt prediction. Hydrological Processes 25:3322–3331.

Lawrence, C. R., and J. C. Neff. 2009. The contemporary physical and chemical flux of aeolian dust: a synthesis of direct measurements of dust deposition. Chemical Geology 267:46–63.

Lawrence, C. R., T. H. Painter, C. C. Landry, and J. C. Neff. 2010. Contemporary geochemical composition and flux of aeolian dust to the San Juan Mountains, Colorado, United States. Journal of Geophysical Research 115.

Leifeld, J., M. Zimmermann, J. Fuhrer, and F. Conen. 2009. Storage and turnover of carbon in grassland soils along an elevation gradient in the Swiss Alps. Global Change Biology 15:668–679.

Liang, X., D. P. Lettenmaier, E. F. Wood, and S. J. Burges. 1994. A simple hydrologically based model of land surface water and energy fluxes for general circulation models. Journal of Geophysical Research: Atmospheres 99:14415–14428.

Link, T. E., and D. Marks. 1999a. Point simulation of seasonal snow cover dynamics beneath boreal forest canopies. Journal of Geophysical Research: Atmospheres 104:27841–27857.

Link, T. E., and D. Marks. 1999b. Distributed simulation of snowcover mass- and energy-balance in the boreal forest. Hydrological Processes 13:2439–2452.

Link, T. E., D. Marks, and J. P. Hardy. 2004. A deterministic method to characterize canopy radiative transfer properties. Hydrological Processes 18:3583–3594.

Lipson, D. A., C. W. Schadt, and S. K. Schmidt. 2002. Changes in soil microbial community structure and function in an alpine dry meadow following spring snow melt. Microbial Ecology 43:307–314.

Lipson, D. A., S. K. Schmidt, and R. K. Monson. 1999. Links between microbial population dynamics and nitrogen availability in an alpine ecosystem. Ecology 80:1623–1631.

Lipson, D. A., S. K. Schmidt, and R. K. Monson. 2000. Carbon availability and temperature control the post-snowmelt decline in alpine soil microbial biomass. Soil Biology & Biochemistry 32:441–448.

Liptzin, D., M. W. Williams, D. Helmig, B. Seok, G. Filippa, K. Chowanski, and J. Hueber. 2009. Process-level controls on CO2 fluxes from a seasonally snow-covered subalpine meadow soil, Niwot Ridge, Colorado. Biogeochemistry 95:151–166.

Liski, J., and J. Westman. 1997. Carbon storage in forest soil of finland. 1. effect of thermoclimate. Biogeochemistry 36:239–260.

Litaor, M. I., M. Williams, and T. R. Seastedt. 2008. Topographic controls on snow distribution, soil moisture, and species diversity of herbaceous alpine vegetation, Niwot Ridge, Colorado. Journal of Geophysical Research-Biogeosciences 113:10.

Littell, J. S., D. L. Peterson, and M. Tjoelker. 2008. Douglas-fir growth in mountain ecosystems: water limits tree growth from stand to region. Ecological Monographs 78:349–368.

Lloyd, J., and J. Taylor. 1994. On the temperature dependence of soil respiration. Functional Ecology 8:315–323.

Logan, J. A., W. W. Macfarlane, and L. Willcox. 2010. Whitebark pine vulnerability to climate-driven mountain pine beetle disturbance in the greater yellowstone ecosystem. Ecological Applications 20:895–902.

Loik, M. E., D. D. Breshears, W. K. Lauenroth, and J. Belnap. 2004. A multi-scale perspective of water pulses in dryland ecosystems: climatology and ecohydrology of the western USA. Oecologia

141:269–281.

Lundquist, J. D., and D. R. Cayan. 2007. Surface temperature patterns in complex terrain: daily variations and long-term change in the central Sierra Nevada, California. Journal of Geophysical Research-Atmospheres 112.

Lundquist, J. D., and F. Lott. 2008. Using inexpensive temperature sensors to monitor the duration and heterogeneity of snow-covered areas. Water Resources Research 44.

Manzoni, S., J. P. Schimel, and A. Porporato. 2011. Responses of soil microbial communities to water stress: results from a meta-analysis. Ecology 93:930–938.

Marks, D., and J. Dozier. 1992. Climate and energy exchange at the snow surface in the alpine region of the Sierra Nevada: 2. snow cover energy balance. Water Resources Research 28:3043–3054.

Marks, D., and A. Winstral. 2001. Comparison of snow deposition, the snow cover energy balance, and snowmelt at two sites in a semiarid mountain basin. Journal of Hydrometeorology 2:213–227.

Marshall, J. D., and J. Zhang. 1994. Carbon isotope discrimination and water-use efficiency in native plants of the north-central rockies. Ecology 75:1887–1895.

Masbruch, M. D., D. S. Chapman, and D. K. Solomon. 2012. Air, ground, and groundwater recharge temperatures in an alpine setting, Brighton Basin, Utah. Water Resources Research 48:W10530.

Massman, W. 1998. A review of the molecular diffusivities of H2O, CO2, CH4, CO, O3, SO2, NH3, N2O, NO, and NO2 in air, O2 and N2 near STP. Atmospheric Environment 32:1111–1127.

Mast, M. A., K. Wickland, R. Striegl, and D. Clow. 1998. Winter fluxes of CO2 and CH4 from subalpine soils in Rocky Mountain National Park, Colorado. Global Biogeochemical Cycles 12:607–620.

Matzner, E., and W. Borken. 2008. Do freeze-thaw events enhance c and n losses from soils of different ecosystems? a review. European Journal of Soil Science 59:274–284.

McCabe, G. J., and M. P. Clark. 2005. Trends and variability in snowmelt runoff in the western United States. Journal of Hydrometeorology 6:476–482.

McDowell, N., H. Barnard, B. Bond, T. Hinckley, R. Hubbard, H. Ishii, B. Köstner, F. Magnani, J. Marshall, F. Meinzer, N. Phillips, M. Ryan, and D. Whitehead. 2002. The relationship between tree height and leaf area: sapwood area ratio. Oecologia 132:12–20.

McNamara, J. P., D. Chandler, M. Seyfried, and S. Achet. 2005. Soil moisture states, lateral flow, and streamflow generation in a semi-arid, snowmelt-driven catchment. Hydrological Processes 19:4023–4038.

Melloh, R. A., J. P. Hardy, R. N. Bailey, and T. J. Hall. 2002. An efficient snow albedo model for the open and sub-canopy. Hydrological Processes 16:3571–3584.

Melloh, R. A., J. P. Hardy, R. E. Davis, and P. B. Robinson. 2001. Spectral albedo/reflectance of littered forest snow during the melt season. Hydrological Processes 15:3409–3422.

Mikan, C. J., J. P. Schimel, and A. P. Doyle. 2002. Temperature controls of microbial respiration in arctic tundra soils above and below freezing. Soil Biology and Biochemistry 34:1785–1795.

Miller, M. E., M. A. Bowker, R. L. Reynolds, and H. L. Goldstein. 2012. Post-fire land treatments and wind erosion – lessons from the Milford Flat fire, UT, USA. Aeolian Research 7:29–44.

Milly, P. C. D., K. A. Dunne, and A. V. Vecchia. 2005. Global pattern of trends in streamflow and water availability in a changing climate. Nature 438:347–350.

Mock, C. J. 1996. Climatic controls and spatial variations of precipitation in the western United States. Journal of Climate 9:1111–1125.

Molotch, N., P. Brooks, S. Burns, M. Litvak, R. Monson, J. McConnell, and K. Musselman. 2009. Ecohydrological controls on snowmelt partitioning in mixed-conifer sub-alpine forests. Ecohydrology 2:129–142.

Monson, R. K., S. P. Burns, M. W. Williams, A. C. Delany, M. Weintraub, and D. A. Lipson. 2006a. The contribution of beneath-snow soil respiration to total ecosystem respiration in a high-elevation, subalpine forest. Global Biogeochemical Cycles 20:GB3030, doi:10.1029/2005GB002684, 2006.

Monson, R. K., D. L. Lipson, S. P. Burns, A. A. Turnipseed, A. C. Delany, M. W. Williams, and S. K. Schmidt. 2006b. Winter forest soil respiration controlled by climate and microbial community composition. Nature 439:711–714.

Monson, R. K., J. P. Sparks, T. N. Rosenstiel, L. E. Scott-Denton, T. E. Huxman, P. C. Harley, A. A. Turnipseed, S. P. Burns, B. Backlund, and J. Hu. 2005. Climatic influences on net ecosystem CO2 exchange during the transition from wintertime carbon source to springtime carbon sink in a high-elevation, subalpine forest. Oecologia 146:130–147.

Monson, R. K., A. A. Turnipseed, J. P. Sparks, P. C. Harley, L. E. Scott-Denton, K. Sparks, and T. E. Huxman. 2002. Carbon sequestration in a high-elevation, subalpine forest. Global Change Biology 8:459–478.

Moore, B., and B. H. Braswell. 1994. Planetary metabolism: understanding the carbon cycle. Ambio 23:4–12.

Mote, P. W. 2006. Climate-driven variability and trends in mountain snowpack in western North America. Journal of Climate 19:6209–6220.

Mote, P. W., A. F. Hamlet, M. P. Clark, and D. P. Lettenmaier. 2005. Declining mountain snowpack in western North America. Bulletin of the American Meteorological Society 86:39–49.

Moyes, A. B., A. J. Schauer, R. T. W. Siegwolf, and D. R. Bowling. 2010. An injection method for measuring the carbon isotope content of soil carbon dioxide and soil respiration with a tunable diode laser absorption spectrometer. Rapid Communications in Mass Spectrometry 24:894–900.

Muhr, J., W. Borken, and E. Matzner. 2009. Effects of soil frost on soil respiration and its radiocarbon signature in a Norway spruce forest soil. Global Change Biology 15:782–793.

Munson, S. M., J. Belnap, and G. S. Okin. 2011. Responses of wind erosion to climate-induced vegetation changes on the Colorado Plateau. Proceedings of the National Academy of Sciences 108:3854–3859.

Murphy, K. L., J. M. Klopatek, and C. C. Klopatek. 1998. The effects of litter quality and climate on decomposition along an elevational gradient. Ecological Applications 8:1061–1071.

Musselman, K. N., N. P. Molotch, and P. D. Brooks. 2008. Effects of vegetation on snow accumulation and ablation in a mid-latitude sub-alpine forest. Hydrological Processes 22:2767–2776.

Musselman, K. N., N. P. Molotch, S. A. Margulis, P. B. Kirchner, and R. C. Bales. 2012a. Influence of canopy structure and direct beam solar irradiance on snowmelt rates in a mixed conifer forest. Agricultural and Forest Meteorology 161:46–56.

Musselman, K. N., N. P. Molotch, S. A. Margulis, M. Lehning, and D. Gustafsson. 2012b. Improved

snowmelt simulations with a canopy model forced with photo-derived direct beam canopy transmissivity. Water Resources Research 48.

Myneni, R., R. Ramakrishna, R. Nemani, and S. Running. 1997. Estimation of global leaf area index and absorbed par using radiative transfer models. IEEE Transactions on Geoscience and Remote Sensing 35:1380–1393.

Natural Resources Conservation Service. 2010. Snow survey and water supply forecasting. *in* National Engineering Handbook. U.S. Department of Agriculture.

Nayak, A., D. Marks, D. G. Chandler, and M. Seyfried. 2010. Long-term snow, climate, and streamflow trends at the Reynolds Creek Experimental Watershed, Owyhee Mountains, Idaho, United states. Water Resources Research 46:W06519.

Neff, J. C., A. P. Ballantyne, G. L. Farmer, N. M. Mahowald, J. L. Conroy, C. C. Landry, J. T. Overpeck, T. H. Painter, C. R. Lawrence, and R. L. Reynolds. 2008. Increasing eolian dust deposition in the western United States linked to human activity. Nature Geoscience 1:189–195.

Nobrega, S., and P. Grogan. 2007. Deeper snow enhances winter respiration from both plant-associated and bulk soil carbon pools in birch hummock tundra. Ecosystems 10:419–431.

Nowinski, N. S., L. Taneva, S. E. Trumbore, and J. M. Welker. 2010. Decomposition of old organic matter as a result of deeper active layers in a snow depth manipulation experiment. Oecologia 163:785–792.

Ohara, N., M. Kavvas, D. Easton, E. Dogrul, J. Yoon, and Z. Chen. 2011. Role of snow in runoff processes in a subalpine hillslope: field study in the Ward Creek Watershed, Lake Tahoe, California, during 2000 and 2001 water years. Journal of Hydrologic Engineering 16:521–533.

Oliver, C. D. 1980. Forest development in North America following major disturbances. Forest Ecology and Management 3:153–168.

Öquist, G., and N. P. Huner. 2003. Photosynthesis of overwintering evergreen plants. Annual Review of Plant Biology 54:329–355.

Öquist, M. G., T. Sparrman, L. Klemedtsson, S. H. Drotz, H. Grip, J. Schleucher, and M. Nilsson. 2009. Water availability controls microbial temperature responses in frozen soil CO2 production. Global Change Biology 15:2715–2722.

Orchard, V., and F. Cook. 1983. Relationship between soil respiration and soil moisture. Soil Biology and Biochemistry 15:447–453.

Oren, R., and D. E. Pataki. 2001. Transpiration in response to variation in microclimate and soil moisture in southeastern deciduous forests. Oecologia 127:549–559.

Painter, T. H., A. P. Barrett, C. C. Landry, J. C. Neff, M. P. Cassidy, C. R. Lawrence, K. E. McBride, and G. L. Farmer. 2007. Impact of disturbed desert soils on duration of mountain snow cover. Geophysical Research Letters 34.

Painter, T. H., J. S. Deems, J. Belnap, A. F. Hamlet, C. C. Landry, and B. Udall. 2010. Response of Colorado River runoff to dust radiative forcing in snow. Proceedings of the National Academy of Sciences 107:17125–17130.

Pataki, D. E., R. Oren, and W. K. Smith. 2000. Sap flux of co-occurring species in a western subalpine forest during seasonal soil drought. Ecology 81:2557–2566.

Pearson, J. A., T. J. Fahey, and D. H. Knight. 1984. Biomass and leaf area in contrasting lodgepole pine

forests. Canadian Journal of Forest Research 14:259–265.

Pederson, G. T., J. L. Betancourt, and G. J. McCabe. 2013. Regional patterns and proximal causes of the recent snowpack decline in the Rocky Mountains, U.S. Geophysical Research Letters 40:1811–1816.

Pederson, G. T., S. T. Gray, C. A. Woodhouse, J. L. Betancourt, D. B. Fagre, J. S. Littell, E. Watson, B. H. Luckman, and L. J. Graumlich. 2011. The unusual nature of recent snowpack declines in the North American cordillera. Science 333:332–335.

Pierce, D. W., T. P. Barnett, H. G. Hidalgo, T. Das, C. Bonfils, B. D. Santer, G. Bala, M. D. Dettinger, D. R. Cayan, A. Mirin, A. W. Wood, and T. Nozawa. 2008. Attribution of declining western US snowpack to human effects. Journal of Climate 21:6425–6444.

Pomeroy, J. W., and K. Dion. 1996. Winter radiation extinction and reflection in a boreal pine canopy: measurements and modelling. Hydrological Processes 10:1591–1608.

Pomeroy, J. W., D. Marks, T. Link, C. Ellis, J. Hardy, A. Rowlands, and R. Granger. 2009. The impact of coniferous forest temperature on incoming longwave radiation to melting snow. Hydrological Processes 23:2513–2525.

Pomeroy, J., A. Rowlands, J. Hardy, T. Link, D. Marks, R. Essery, J. Sicart, and C. Ellis. 2008. Spatial variability of short wave irradiance for snowmelt in forests. Journal of Hydrometeorology 9:1482–1490.

Post, W. M., W. R. Emanuel, P. J. Zinke, and A. G. Stangenberger. 1982. Soil carbon pools and world life zones. Nature 298:156–159.

Pugh, E., and E. Small. 2012. The impact of pine beetle infestation on snow accumulation and melt in the headwaters of the Colorado River. Ecohydrology 5:467–477.

Raich, J. W., and W. H. Schlesinger. 1992. The global carbon dioxide flux in soil respiration and its relationship to vegetation and climate. Tellus B 44:81–99.

Raleigh, M. S., K. Rittger, C. E. Moore, B. Henn, J. A. Lutz, and J. D. Lundquist. 2013. Ground-based testing of MODIS fractional snow cover in subalpine meadows and forests of the Sierra Nevada. Remote Sensing of Environment 128:44–57.

Read, J., and G. Farquhar. 1991. Comparative studies in nothofagus (fagaceae). i. leaf carbon isotope discrimination. Functional Ecology 5:684–695.

Regonda, S. K., B. Rajagopalan, M. Clark, and J. Pitlick. 2005. Seasonal cycle shifts in hydroclimatology over the western United States. Journal of Climate 18:372–384.

Riveros-Iregui, D. A., and B. L. McGlynn. 2009. Landscape structure control on soil CO2 efflux variability in complex terrain: scaling from point observations to watershed scale fluxes. Journal of Geophysical Research 114:G02010–G02010.

Running, S. W. 1994. Testing forest-BGC ecosystem process simulations across a climatic gradient in Oregon. Ecological Applications 4:238–247.

Ryan, M., D. Binkley, and J. Fownes. 1997. Age-related decline in forest productivity: pattern and process. Pages 213–262 *in* M. Begon and A.H. Fitter, editor. Advances in ecological research. Academic Press.

Savitch, L. V., E. D. Leonardos, M. Krol, S. Jansson, B. Grodzinski, N. P. A. Huner, and G. Öquist. 2002. Two different strategies for light utilization in photosynthesis in relation to growth and

cold acclimation. Plant, Cell & Environment 25:761–771.

Schadt, C. W., A. P. Martin, D. A. Lipson, and S. K. Schmidt. 2003. Seasonal dynamics of previously unknown fungal lineages in tundra soils. Science 301:1359–1361.

Scherrer, D., and C. Körner. 2010. Infra-red thermometry of alpine landscapes challenges climatic warming projections. Global Change Biology 16:2602–2613.

Schimel, D. S., B. H. Braswell, E. A. Holland, R. McKeown, D. S. Ojima, T. H. Painter, W. J. Parton, and A. R. Townsend. 1994. Climatic, edaphic, and biotic controls over storage and turnover of carbon in soils. Global Biogeochemical Cycles 8:279–293.

Schimel, D. T., G. F. Kittel, S. Running, R. Monson, A. Turnispeed, and D. Anderson. 2002. Carbon sequestration studied in western U.S. mountains. Eos Trans. AGU 83:445, 449.

Schimel, J. P., and J. S. Clein. 1996. Microbial response to freeze-thaw cycles in tundra and taiga soils. Soil Biology and Biochemistry 28:1061–1066.

Schimel, J. P., and C. Mikan. 2005. Changing microbial substrate use in arctic tundra soils through a freeze-thaw cycle. Soil Biology and Biochemistry 37:1411–1418.

Schimel, J. P., C. Bilbrough, and J. M. Welker. 2004. Increased snow depth affects microbial activity and nitrogen mineralization in two arctic tundra communities. Soil Biology and Biochemistry 36:217–227.

Schlesinger, W. H. 1977. Carbon balance in terrestrial detritus. Annual Review of Ecology and Systematics 8:51–81.

Schlesinger, W. H. 1997. Biogeochemistry: an analysis of global change. 2nd ed. Academic PressSan Diego.

Schmid, M.-O., S. Gubler, J. Fiddes, and S. Gruber. 2012. Inferring snowpack ripening and melt-out from distributed measurements of near-surface ground temperatures. The Cryosphere 6:1127–1139.

Schmidt, S. K., and D. A. Lipson. 2004. Microbial growth under the snow: implications for nutrient and allelochemical availability in temperate soils. Plant and Soil 259:1–7.

Schmidt, S., K. Wilson, R. Monson, and D. Lipson. 2009. Exponential growth of "snow molds" at sub-zero temperatures: an explanation for high beneath-snow respiration rates and q 10 values. Biogeochemistry 95:13–21.

Schneider, G. W., and N. F. Childers. 1941. Influence of soil moisture on photosynthesis, respiration, and transpiration of apple leaves. Plant Physiology 16:565–583.

Schulze, E.-D., R. Williams, G. Farquhar, W. Schulze, J. Langridge, J. Miller, and B. Walker. 1998. Carbon and nitrogen isotope discrimination and nitrogen nutrition of trees along a rainfall gradient in northern Australia. Functional Plant Biology 25:413–425.

Schurmann, A., J. Mohn, and R. Bachofen. 2002. N2O emissions from snow-covered soils in the Swiss Alps. Tellus B 54:134–142.

Schuur, E. A., and P. A. Matson. 2001. Net primary productivity and nutrient cycling across a mesic to wet precipitation gradient in Hawaiian montane forest. Oecologia 128:431–442.

Seager, R., and G. A. Vecchi. 2010. Greenhouse warming and the 21st century hydroclimate of southwestern North America. Proceedings of the National Academy of Sciences 107:21277–21282.

Seager, R., M. F. Ting, I. Held, Y. Kushnir, J. Lu, G. Vecchi, H. P. Huang, N. Harnik, A. Leetmaa, N. C. Lau, C. H. Li, J. Velez, and N. Naik. 2007. Model projections of an imminent transition to a more arid climate in southwestern North America. Science 316:1181–1184.

Seneviratne, G. 2000. Litter quality and nitrogen release in tropical agriculture: a synthesis. Biology and Fertility of Soils 31:60–64.

Serreze, M. C., M. P. Clark, R. L. Armstrong, D. A. McGinnis, and R. S. Pulwarty. 1999. Characteristics of the western United States snowpack from snowpack telemetry (SNOTEL) data. Water Resources Research 35:2145–2160.

Seyfried, M. 1998. Spatial variability constraints to modeling soil water at different scales. Geoderma 85:231–254.

Seyfried, M. S., G. N. Flerchinger, M. D. Murdock, C. L. Hanson, and S. Van Vactor. 2001. Long-term soil temperature database, Reynolds Creek Experimental Watershed, Idaho, United States. Water Resources Research 37:2843–2846.

Seyfried, M. S., L. E. Grant, E. Du, and K. Humes. 2005. Dielectric loss and calibration of the hydra probe soil water sensor. Vadose Zone J. 4:1070–1079.

Seyfried, M. S., L. E. Grant, D. Marks, A. Winstral, and J. McNamara. 2009. Simulated soil water storage effects on streamflow generation in a mountainous snowmelt environment, Idaho, USA. Hydrological Processes 23:858–873.

Sheppard, P. R., A. C. Comrie, G. D. Packin, K. Angersbach, and M. K. Hughes. 2002. The climate of the US southwest. Climate Research 21:219–238.

Sicart, J. E., R. L. H. Essery, J. W. Pomeroy, J. Hardy, T. Link, and D. Marks. 2004. A sensitivity study of daytime net radiation during snowmelt to forest canopy and atmospheric conditions. Journal of Hydrometeorology 5:774–784.

Six, J., R. T. Conant, E. A. Paul, and K. Paustian. 2002. Stabilization mechanisms of soil organic matter: implications for c-saturation of soils. Plant and Soil 241:155–176.

Skiles, S. M., T. H. Painter, J. S. Deems, A. C. Bryant, and C. C. Landry. 2012. Dust radiative forcing in snow of the Upper Colorado River Basin: 2. interannual variability in radiative forcing and snowmelt rates. Water Resources Research 48:W07522.

Skopp, J., M. D. Jawson, and J. W. Doran. 1990. Steady-state aerobic microbial activity as a function of soil water content. Soil Science Society of America Journal 54:1619.

Smith, T. J., J. P. McNamara, A. N. Flores, M. M. Gribb, P. S. Aishlin, and S. G. Benner. 2011. Small soil storage capacity limits benefit of winter snowpack to upland vegetation. Hydrological Processes 25:3858–3865.

Sommerfeld, R. A., W. J. Massman, R. C. Musselman, and A. R. Mosier. 1996. Diffusional flux of CO2 through snow: spatial and temporal variability among alpine-subalpine sites. Global Biogeochemical Cycles 10:473–482.

Sommerfeld, R. A., A. R. Mosier, and R. C. Musselman. 1993. CO2, CH4 and N2O flux through a Wyoming snowpack and implications for global budgets. Nature 361:140–142.

Spaans, E. J. A., and J. M. Baker. 1996. The soil freezing characteristic: its measurement and similarity to the soil moisture characteristic. Soil Science Society of America Journal 60:13.

Sparks, J. P., and J. R. Ehleringer. 1997. Leaf carbon isotope discrimination and nitrogen content for

riparian trees along elevational transects. Oecologia 109:362–367.

Steenburgh, W. J., J. D. Massey, and T. H. Painter. 2012. Episodic dust events of Utah's Wasatch Front and adjoining region. Journal of Applied Meteorology and Climatology 51:1654–1669.

Steltzer, H., C. Landry, T. Painter, J. Anderson, and E. Ayres. 2009. Biological consequences of earlier snowmelt from desert dust deposition in alpine landscapes. Proceedings of the National Academy of Sciences of the United States of America 106:11629–11634.

Stewart, G., M. Turnbull, S. Schmidt, and P. Erskine. 1995. 13C natural abundance in plant communities along a rainfall gradient: a biological integrator of water availability. Functional Plant Biology 22:51–55.

Stewart, I. T. 2009. Changes in snowpack and snowmelt runoff for key mountain regions. Hydrological Processes 23:78–94.

Stewart, I. T., D. R. Cayan, and M. D. Dettinger. 2004. Changes in snowmelt runoff timing in western North America under a 'business as usual' climate change scenario. Climatic Change 62:217–232.

Stewart, I. T., D. R. Cayan, and M. D. Dettinger. 2005. Changes toward earlier streamflow timing across western North America. Journal of Climate 18:1136–1155.

Sturm, M., J. Holmgren, M. König, and K. Morris. 1997. The thermal conductivity of seasonal snow. Journal of Glaciology 43:26–41.

Sun, O. J., J. Campbell, B. E. Law, and V. Wolf. 2004. Dynamics of carbon stocks in soils and detritus across chronosequences of different forest types in the Pacific Northwest, USA. Global Change Biology 10:1470–1481.

Sun, Z. J., N. J. Livingston, R. D. Guy, and G. J. Ethier. 1996. Stable carbon isotopes as indicators of increased water use efficiency and productivity in white spruce (picea glauca (moench) voss) seedlings. Plant, Cell & Environment 19:887–894.

Sutinen, M.-L., T. Holappa, and K. Kujala. 1999. Seasonal changes in soil temperature and in the frost hardiness of scots pine roots under subarctic conditions: comparison with soil temperature and snow-cover under different simulated winter conditions. Phyton (Horn) 39:213–218.

Sutinen, R., A. Vajda, P. Hänninen, and M.-L. Sutinen. 2009. Significance of snowpack for root-zone water and temperature cycles in subarctic lapland. Arctic, Antarctic, and Alpine Research 41:373–380.

Tague, C., and H. Peng. 2013. The sensitivity of forest water use to the timing of precipitation and snowmelt recharge in the California Sierra: implications for a warming climate. Journal of Geophysical Research: Biogeosciences 118:875–887.

Tague, C., K. Heyn, and L. Christensen. 2009. Topographic controls on spatial patterns of conifer transpiration and net primary productivity under climate warming in mountain ecosystems. Ecohydrology 2:541–554.

Taylor, B. R., and H. G. Jones. 1990. Litter decomposition under snow cover in a balsam fir forest. Canadian Journal of Botany 68:112–120.

Tewksbury, C., and H. Van Miegroet. 2007. Soil organic carbon dynamics along a climatic gradient in a southern Appalachian spruce–fir forest. Canadian Journal of Forest Research 37:1161–1172.

Thomas, C. K., B. E. Law, J. Irvine, J. G. Martin, J. C. Pettijohn, and K. J. Davis. 2009. Seasonal hydrol-

ogy explains interannual and seasonal variation in carbon and water exchange in a semiarid mature ponderosa pine forest in central Oregon. Journal of Geophysical Research: Biogeosciences 114.

Townsend, A. R., P. M. Vitousek, and S. E. Trumbore. 1995. Soil organic matter dynamics along gradients in temperature and land use on the island of Hawaii. Ecology 76:721–733.

Trofymow, J. A., H. J. Barclay, and K. M. McCullough. 1991. Annual rates and elemental concentrations of litter fall in thinned and fertilized douglas-fir. Canadian Journal of Forest Research 21:1601–1615.

Trumbore, S., O. Chadwick, and R. Amundson. 1996. Rapid exchange between soil carbon and atmospheric carbon dioxide driven by temperature change. Science 272:393–396.

Van Miegroet, H., M. T. Hysell, and A. D. Johnson. 2000. Soil microclimate and chemistry of spruce-fir tree islands in northern Utah. Soil Science Society of America Journal 64:1515–1525.

Villalba, R., T. T. Veblen, and J. Ogden. 1994. Climatic influences on the growth of subalpine trees in the Colorado Front Range. Ecology 75:1450–1462.

Vitousek, P. M., C. B. Field, and P. A. Matson. 1990. Variation in foliar δ 13C in Hawaiian metrosideros polymorpha: a case of internal resistance? Oecologia 84:362–370.

Vitousek, P. M., P. A. Matson, and D. R. Turner. 1988. Elevational and age gradients in Hawaiian montane rainforest: foliar and soil nutrients. Oecologia 77:565–570.

Vogt, K. A., D. J. Vogt, E. E. Moore, B. A. Fatuga, M. R. Redlin, and R. L. Edmonds. 1987. Conifer and angiosperm fine-root biomass in relation to stand age and site productivity in douglas-fir forests. Journal of Ecology 75:857–870.

Vucetich, J., D. Reed, A. Breymeyer, M. Degórski, G. Mroz, J. Solon, E. Roo-Zielinska, and R. Noble. 2000. Carbon pools and ecosystem properties along a latitudinal gradient in northern scots pine (pinus sylvestris) forests. Forest Ecology and Management 136:135–145.

Waddell, K. L. 2002. Sampling coarse woody debris for multiple attributes in extensive resource inventories. Ecological Indicators 1:139–153.

Wang, Y., R. Amundson, and X.-F. Niu. 2000. Seasonal and altitudinal variation in decomposition of soil organic matter inferred from radiocarbon measurements of soil CO2 flux. Global Biogeochemical Cycles 14:199–211.

Waring, R. H., P. E. Schroeder, and R. Oren. 1982. Application of the pipe model theory to predict canopy leaf area. Canadian Journal of Forest Research 12:556–560.

Warren, C. R., J. F. McGrath, and M. A. Adams. 2001. Water availability and carbon isotope discrimination in conifers. Oecologia 127:476–486.

Warren, S. G., and W. J. Wiscombe. 1980. A model for the spectral albedo of snow. II: snow containing atmospheric aerosols. Journal of the Atmospheric Sciences 37:2734–2745.

Wei, K., and G. Jia. 2009. Soil n-alkane δ13C along a mountain slope as an integrator of altitude effect on plant species δ13C. Geophysical Research Letters 36.

Westerling, A. L., H. G. Hidalgo, D. R. Cayan, and T. W. Swetnam. 2006. Warming and earlier spring increase western US forest wildfire activity. Science 313:940–943.

Western, A. W., S.-L. Zhou, R. B. Grayson, T. A. McMahon, G. Blöschl, and D. J. Wilson. 2004. Spatial correlation of soil moisture in small catchments and its relationship to dominant spatial

hydrological processes. Journal of Hydrology 286:113–134.

Whiteman, C. D. 2000. Mountain meteorology: fundamentals and applications. Oxford University Press, USA.

Williams, C. J., J. P. McNamara, and D. G. Chandler. 2009. Controls on the temporal and spatial variability of soil moisture in a mountainous landscape: the signature of snow and complex terrain. Hydrol. Earth Syst. Sci. 13:1325–1336.

Williams, M. W., P. D. Brooks, and T. Seastedt. 1998. Nitrogen and carbon soil dynamics in response to climate change in a high-elevation ecosystem in the Rocky Mountains, U.S.A. Arctic and Alpine Research 30:26–30.

Winkler, R., S. Boon, B. Zimonick, and K. Baleshta. 2010. Assessing the effects of post-pine beetle forest litter on snow albedo. Hydrological Processes 24:803–812.

Woodall, C., B. Walters, S. Oswalt, G. Domke, C. Toney, and A. Gray. 2013. Biomass and carbon attributes of downed woody materials in forests of the United States. Forest Ecology and Management 305:48–59.

Yoo, K., R. Amundson, A. M. Heimsath, and W. E. Dietrich. 2006. Spatial patterns of soil organic carbon on hillslopes: integrating geomorphic processes and the biological c cycle. Geoderma 130:47–65.

Zarter, C. R., W. W. Adams, V. Ebbert, D. J. Cuthbertson, I. Adamska, and B. Demmig-Adams. 2006a. Winter down-regulation of intrinsic photosynthetic capacity coupled with up-regulation of elip-like proteins and persistent energy dissipation in a subalpine forest. New Phytologist 172:272–282.

Zarter, C. R., B. Demmig-Adams, V. Ebbert, I. Adamska, and W. W. Adams. 2006b. Photosynthetic capacity and light harvesting efficiency during the winter-to-spring transition in subalpine conifers. New Phytologist 172:283–292.

Zhang, T. 2005. Influence of the seasonal snow cover on the ground thermal regime: an overview. Reviews of Geophysics 43:23.